THE UNIVERSITY OF MICHIGAN

COLLEGE OF LITERATURE, SCIENCE, AND THE ARTS
Department of Chemistry

Technical Report

DIFLUOROPHOSPHINE LIGANDS, THEIR PREPARATION, PROPERTIES, AND CHEMISTRY

Ralph William Rudolph

ORA Project 06785

supported by:

PETROLEUM RESEARCH FUND
OF THE
AMERICAN CHEMICAL SOCIETY
GRANT NO. PRF 2089-A3

administrated through:

OFFICE OF RESEARCH ADMINISTRATION ANN ARBOR

May 1966

This report was also a dissertation submitted in partial fulfillment of the requirements for the degree of Doctor of Philosophy in the University of Michigan, 1966.

To

My Wife, Margaret,

and

Our Parents

Acknowledgements

The author wishes to express special thanks to the graduate and postdoctoral students in the research groups of Messrs. Parry and Taylor. Their advice and assistance helped in many aspects of this research. Worthy of particular thanks are C. F. Farran, for his help with portions of the vibrational studies, and Frank Parker, for the determination of several nmr spectra.

I also wish to express my gratitude to Professor R. C. Taylor for many stimulating and constructive discussions.

My deepest expression of gratitude is reserved for Professor R. W. Parry. One cannot imagine working for a more patient and understanding person. Without his apt suggestions and expert guidance this research would not have come to fruition. It is indeed a reward to work for such an inspired and dedicated teacher. I can only emulate the high professional standards which he exemplifies.

The generous financial support of Union Carbide, Tecumseh Products Company, The Lotta B. Backus Fellowship Fund, The National Science Foundation, and The Horace H. Rackham School of Graduate Studies is gratefully acknowledged.

Table of Contents

List of Tables

List of Figures

Abstract

DIFLUOROPHOSPHINE LIGANDS, THEIR PREPARATION, PROPERTIES, AND CHEMISTRY

by Ralph William Rudolph

The nature of the P-B coordinate bond in various phosphine-borane systems is presently the subject of considerable controversy. This study was concerned with the preparation, properties, and chemistry of a series of ligands, the difluorophosphines, PF_2X, which should in theory be closely related to PF_3 in bonding properties.

The routes leading to known difluorophosphines were summarized. The preparation and characterization of the new mixed phosphorus halide, PF_2I, led to two new synthetic methods for the preparation of difluorophosphine ligands. The new species PF_2CN and F_2POPF_2 were prepared by a metathetic reaction between PF_2I and the appropriate copper(I) salt according to the equation:

$$nPF_2I + Cu_nX \rightarrow (PF_2)_nX + nCuI$$

(x = valence of anion X^{n-}).

A coupling reaction effected the preparation of F_2PPF_2 and PHF_2 according to the following equation:

$$PF_2I + RI + 2Hg \rightarrow Hg_2I_2 + PF_2R \quad (R = H, PF_2).$$

The new species, difluoroiodophosphine, cyanodifluorophosphine, μ-oxo-bisdifluorophosphine, tetrafluorodiphosphine, and difluorophosphine were characterized and

compared with similar known compounds such as PF_2Cl, $P(CN)_3$, $F_2P(O)\text{-}O\text{-}P(O)F_2$, N_2F_4, PF_3, PH_3, and NHF_2. In most cases, infrared, Raman, and nmr spectroscopy were used to obtain information concerning structure and bonding. Preliminary investigations explored the hydrolysis and aminolysis of PHF_2. The new ligand, PHF_2, was also found to form adducts with BH_3 and HI, and effect the displacement of CO from $Ni(CO)_4$ to form difluorophosphine-nickel-carbonyl-derivatives. Base displacement reactions and other evidence demonstrated that the relative base strength towards borane decreases in the order $PHF_2 > PF_3 > PH_3$. NMR spectroscopic studies showed that the unexpected stability of $PHF_2 \cdot BH_3$ cannot be attributed to an unusual structure. The nmr data for the series $PH_XF_{3-X} \cdot BH_3$ ($x = 0,1,3$) were discussed and compared to data for the series $PH_XMe_{3-X} \cdot BH_3$ ($x = 0 \rightarrow 3$) in relationship to structure and bonding.

The unexpected stability of $PHF_2 \cdot BH_3$ demands at least a two-parameter model to rationalize the behavior. Some schools of thought will use a synergistic balancing of sigma- and pi-bonding to explain the trend. However, it is postulated that an F--H--F interaction may exist in PHF_2. Such an interaction is "pictured" as resulting in a marked loosening of the phosphorus lone-pair electrons and a concommitant increase in the base strength of PHF_2 towards BH_3 when compared with PF_3 and PH_3. The latter model also implies a pyramidal geometry for PHF_2 with short F--F and H--F non-bonded distances.

Historical Background

When Chatt and Williams prepared $(PF_3)_2PtCl_2$ and $[(PF_3)PtCl_2]_2$ they noted their close physical and chemical similarity to the corresponding carbonyl complexes.[1,2] It had been suggested by Pauling[3] that bonding in the metal carbonyls involves the filled d-orbitals of the transition metal in double bonding. Thus, it is not surprising that the similar coordinating ability of PF_3 and CO led Chatt to postulate that filled d-orbitals on the acceptor metal atom were essential for coordination with PF_3. He felt that the electronegative nature of the fluorines attached to phosphorus would markedly reduce the ability of PF_3 to coordinate via a classical dative bond. Thus, the existence of a second type of bonding was postulated to explain the nature of the chemical bond in trifluorophosphine complexes, i.e., a double bond which involved a weak σ-bond as well as a π-bond utilizing the filled d-orbitals of the metal and the vacant 3d-orbitals in PF_3. Since boron and aluminum do not have filled d-orbitals, Chatt did not expect them to form stable complexes with PF_3. He was unable to prepare trifluorophosphine complexes of aluminum chloride or aluminum bromide and observed that Booth and Walkup could not effect the formation of $PF_3 \cdot BF_3$[4].

Subsequently, in direct conflict with the predictions

of Chatt, Parry and Bissot prepared $PF_3 \cdot BH_3$[5] and found it to be similar in many respects to $BH_3 \cdot CO$[6]. To explain the existence of $PF_3 \cdot BH_3$, Graham and Stone[7] expanded the arguments which Bauer[8] and Burg[9] had forwarded to explain the existence of $BH_3 \cdot CO$ and the stability of phosphinoborane polymers. They argued that $PF_3 \cdot BH_3$ and $BH_3 \cdot CO$ might owe their existence to supplementary π-bonding which involved the overlap of the vacant 3d-orbitals of phosphorus and a pseudo π-orbital formed by the hydrogen atoms of the borane group. In this light, Graham and Stone thought that it was significant that PF_3 did not bond to other Group-III acceptor molecules, like BF_3, yet does form stable complexes with subgroup elements, e.g., $Ni(PF_3)_4$[10], where bonding is believed to be multiple in character.

Surprised at the existence of $PF_3 \cdot BH_3$ and $BH_3 \cdot CO$, the arguments of Chatt were subsequently modified[11] so as to be similar to the "hyperconjugation" effect[12] of organic chemistry and to be more in line with the ideas of Burg, Graham, and Stone.

Although Chatt[1,2] originally reported that aluminum chloride does not form a complex with PF_3, under different conditions Alton[13] has been able to characterize $PF_3 \cdot AlCl_3$. Thus, the predictive value of the π-bonding arguments has been reduced and a modification of assumptions is demanded. In fact, about the time of Alton's work[13], Stone[14] conceded that "by using a strong

enough acceptor atom (boron is rather weak in this respect compared with aluminum or gallium) it might well be possible to make a PF_3 adduct of a Group III acceptor molecule in which the dative bonding could be described in terms of a classical σ-bond."

Alton[13] offered an alternative rationalization to correlate the difference in behavior of PF_3 toward various acids. It was noted that bonding to phosphorus is strongly field-dependent.[15] Since phosphorus is a relatively large nucleus, a considerable gain in energy may result if a phosphine ligand is able to closely approach the reference acid where the field strength would be greater. Phosphorus also should form stronger bonds to a given reference acid as the polarizability of the lone-pair on the phosphorus increases. Thus, the alkyl phosphines with polarizable lone-pair electrons are strong bases towards most reference acids, but in the case of PF_3 even though the electron pair is still available, its bonding propensity is reduced by its lower polarizability and bonding will result only in the case of close approach by the reference acid. Alton estimated that the reorganization energy required to deform BH_3 into a bonding configuration (sp^2 to ~sp^3) was significantly smaller than for the corresponding change in BF_3. Thus, a closer approach of borane is possible and bond formation is possible, whereas, the energy required to deform BF_3 and allow close approach precludes bond formation.

Apparently the deformation energy of aluminum chloride is also small enough to be overcome by coordinate bond formation. The ability of aluminum chloride to dimerize to Al_2Cl_6 (like borane to B_2H_6) is probably an indication of its low reorganization energy.

Although some of Alton's ideas are presented in the more recent literature[16], most authors still appear to favor a supplementary $d\pi - p\pi$ back-bonding to explain the existence of $PF_3 \cdot BH_3$. Likewise, the ability of BH_3 to reverse the "normal" order of coordinating ability (N > P; O > S) has been explained by Graham, Stone, Coyle and Burg[7,17-19] in terms of similar π-bonding arguments. It should be noted however, that in these cases the "reversal" can be explained in terms of a change in size of the donor atom and a change in the nature of the donor electron pair so that the polarizability of the pair and the field strength of the reference acid are of basic importance. Shore and co-workers have recently shown that this apparent "reversal" of coordinating ability is a function of the strength of the reference acid[20]. Thus, the nature of the chemical bond between phosphines and Main-Group-III acceptors, in particular borane, is still subject to considerable disagreement.

Since the original work of Chatt and Wilkinson[1,2,10] on the PF_3 complexes of platinum and nickel, interest in the similarity of PF_3 and CO as ligands in transition metal chemistry has grown considerably. Subsequent work

on such systems has been conducted by Clark, Kruck and others[21-23]. Among the transition metal complexes of PF_3, where there are filled d-orbitals on the metal to participate in a $d\pi$ - $p\pi$ interaction with the vacant 3d-orbitals on phosphorus, there appears to be no serious disagreement with the existence of double-bonding which supplements the dative P-metal bond in a synergistic manner. There is some debate, however, as to the influence which such double bonds have on compound properties. For example, the Ni-P stretching force constant, in a recent Raman-spectroscopic investigation[24] of $Ni(PF_3)_4$, was found quite clearly in the range for single bonds.

Since difluorophosphine ligands are closely related to PF_3, their synthesis and coordination chemistry have been of recent interest; Schmutzler[25] has recently published a comprehensive review on the fluorides of phosphorus including a summary of the chemistry of difluorophosphine ligands.

Statement of the Problem

Since the nature of the coordinate bond in various phosphine-borane systems has been the subject of considerable controversy, it was desired to study a series of phosphines in which the π-bonding propensity, theoretically, should be relatively large. The difluorophosphines should prove ideal for such a test of theory because the electronegative fluorines lower the energy of the 3d-orbitals on phosphorus and thus make them more readily available as acceptor orbitals. Therefore, a study involving the synthesis, characterization, and chemistry of several difluorophosphines, PF_2X, was undertaken. As a result, the interesting ligand difluorophosphine, PHF_2, was discovered and subjected to further study. In particular, the stable species $PHF_2 \cdot BH_3$ was compared with $PH_3 \cdot BH_3$ and $PF_3 \cdot BH_3$ in an attempt to gain a greater understanding of the nature of the P-B bond.

Results and Discussion

I. Synthetic Methods for the Preparation of Difluorophosphine Ligands.

A portion of the present study was spent in the development of new preparations for difluorophosphine ligands. Section I of the discussion is an attempt to classify the known and newly developed preparations into various "type-reactions"; however, two novel syntheses of dimethylaminodifluorophosphine which could not be adequately classified have also been reported[26,27]. One involves the reaction of boron trifluoride with trisdimethylaminophosphine[26]

$$2BF_3 + P(NMe_2)_3 \rightarrow F_2PNMe_2 + 2Me_2NBF_2.$$

The other is the aminolysis of trichloromethyldifluorophosphine[27]

$$Cl_3CPF_2 + Me_2NH \rightarrow CCl_3H + F_2PNMe_2.$$

The remaining routes to difluorophosphines have been classified as A) Fluorination of the Corresponding Halophosphine, B) Deamination of Dimethylaminodifluorophosphine, C) Aminolysis, D) Metathesis, and E) Coupling. Several new difluorophosphines have been prepared during the course of this research - difluoroiodophosphine (PF_2I), μ-oxo-bisdifluorophosphine (F_2POPF_2), cyanodifluorophosphine (PF_2CN), tetrafluorodiphosphine (F_2PPF_2), and difluorophosphine (PHF_2). The characterization of these new

species is discussed in Section II.

A. Fluorination of the Corresponding Halophosphine.

$$RPX_2 \xrightarrow[\text{agent}]{\text{fluorinating}^*} RPF_2;\ X = Cl,\ Br,\ I \qquad \text{(Eqn. 8-1)}$$

The early patent literature[28] (1936-39) describes this method for the preparation of difluorophosphines, however, the description of $F_2PN(C_2H_5)_2$ differs considerably from that mentioned in subsequent research[29].

More recently, Martin[30,31] and co-workers used the method of equation 8-1 for the preparation of difluorophosphites, $ROPF_2$. Other studies indicate that the fluorination of alkyldihalophosphines[32,33] does not proceed smoothly but is accompanied by oxidation-reduction and the formation of fluorophosphoranes, RPF_4. When more electronegative substituents are placed on the phosphorus, or in the case of dichlorophosphites ($ROPCl_2$) and dialkylaminodichlorophosphines (R_2NPCl_2), the fluorination occurs more smoothly without appreciable oxidation-reduction[26,29-31,34-37].

Booth[38,39] used a similar type-reaction

$$PX_3 \xrightarrow[\text{agent}]{\text{fluorinating}^*} PF_2X;\ X = Cl,\ Br$$

for the preparation of mixed phosphorus halides. Among those prepared were PF_2Cl and PF_2Br from PCl_3 and PBr_3, respectively. More recently, Holmes and Gallagher[40]

* Typical fluorinating agents used are SbF_3, AsF_3, and NaF.

simplified Booth's procedure, but an even more convenient preparation of halodifluorophosphines will be discussed in Section I-B.

The fluorination of $P(NCO)_3$ and $P(NCS)_3$ with SbF_3 to give $PF_2(NCO)$ and $PF_2(NCS)$[41], respectively, might also be classified with the above reactions since isocyanates and isothiocyanates are considered to be halogenoids.

For the present work the general synthetic method of equation 8-1 was used for the preparation of dimethylaminodifluorophosphine, a starting material; however, the procedure was not used for other syntheses since, as the above discussion indicates, the fluorination of halophosphines has been rather exhaustively studied[25].

B. Deamination of Dimethylaminodifluorophosphine.

$$F_2PNMe_2 + 2HX \rightarrow PF_2X + Me_2NH\cdot HX; \quad X = Cl, Br, I$$

This route to halodifluorophosphines was developed by Fleming[42] and Moyé[43] in our laboratories. Subsequently, it was reported independently[44,45]. Halodifluorophosphines have been prepared previously by the partial fluorination of the appropriate phosphorus trihalide[38-40]. However, these methods yield mixtures which are difficult to separate. The action of a hydrogen halide on dimethylaminodifluorophosphine provides a unique route for the preparation of pure PF_2X ligands.

Of special interest in this study was difluoroiodophosphine which had been implied by Cavell[44] but never

characterized. During this work it was found to be stable enough for a complete characterization and was used as a reactive intermediate for the introduction of the PF_2- moiety into new molecules. A discussion of the synthetic methods which utilize the lability of the P-I bond can be found in Sections I-D,E.

C. Aminolysis.

$$PF_2X + 2HNR_2 \rightarrow F_2PNR_2 + R_2NH\cdot HX; \quad X = F, Cl$$

The interaction of an amine and a phosphorus halide is a general method for the preparation of aminohalophosphines[46,47] which has not been applied extensively to phosphorus trifluorides. Fleming[42] developed this route to F_2PNMe_2, but Van Doorne[37] found that PF_3 and N-methylaniline do not undergo this type-reaction. This method has been independently reported by Cavell[44] who found that, in addition to PF_3, PF_2Cl also yields F_2PNMe_2 on aminolysis with dimethylamine.

These studies indicate that this may be a convenient route to selected aminodifluorophosphines, and that aminolysis will probably proceed more smoothly as the halogen substituent is varied from Cl through I, the order of increasing P-X bond lability; however, this postulate was not tested during the present work.

D. Metathesis.

$$PF_2I + CuX \rightarrow PF_2X + CuI$$

This route to difluorophosphines was discovered during the course of this study when small amounts of F_2POPF_2 were isolated from the reaction mixture after PF_2I had been treated with powdered copper metal in an attempt to prepare P_2F_4. As subsequent investigation showed the F_2POPF_2 must have resulted from small amounts of Cu_2O in the copper metal since treatment of PF_2I with Cu_2O gave F_2POPF_2 in good yields.

Apparently this metathetic reaction with cuprous salts may be extended to some degree since when PF_2I was treated with cuprous cyanide, PF_2CN was isolated and characterized.

E. Coupling.

$$PF_2I + RI + 2Hg \rightarrow PF_2R + Hg_2I_2$$

The preparation of the parent member of the difluorophosphine homologous series, PHF_2, was effected by this route with HI as the source of hydrogen. The reaction is similar to that used by Burg and Mahler[48] for the preparation of $(CF_3)_2PH$ from $(CF_3)_2PI$ and a proton source in the presence of mercury.

Previously, Bennet et al.[49] had isolated tetrakistrifluoromethyldiphosphine, $(CF_3)_2PP(CF_3)_2$, from a similar coupling-reaction by treating $(CF_3)_2PI$ with mercury. It is not surprising then that tetrafluorodiphosphine, F_2PPF_2, has also been isolated in this study from an analogous reaction between PF_2I and mercury. It

is felt that a wide variety of compounds containing the PF_2-moiety might be made by analogous coupling-reactions. In fact, preliminary results indicate that $F_2P\text{-}CH_2\text{-}CH{=}CH_2$ is produced when PF_2I and allyl iodide are shaken with mercury[50].

II. Characterization of New Difluorophosphines.

The characterization of the new difluorophosphine ligands prepared in this study is described below. Techniques such as nmr, infrared, and mass spectroscopy, as well as more classical methods were used to obtain a complete characterization. A typical experiment describing the preparation of each new species is described in the Experimental Section.

A. Characterization of Difluoroiodophosphine, PF_2I.

Difluoroiodophosphine was obtained in 94% yields from the reaction of HI and F_2PNMe_2 according to the equation

$$F_2PNMe_2 + 2HI \rightarrow PF_2I + Me_2NH\cdot HI.$$

Although Cavell[44] indicated that PF_2I was too unstable for characterization, it was found that at 25° in the gas phase, in a pyrex container, after 1 day, and with p(initial) = 37 mm, PF_2I was ca. 1% decomposed; after 9 days it was 19% decomposed. However, the rate of disproportionation according to the equation

$$3PF_2I \rightarrow 2PF_3 + PI_3$$

was pressure dependent since with p(initial) = 280 mm,

after 1 day the PF_2I vapor was 6% decomposed, and after 8 days 87% decomposition had occurred.

An unequivocal characterization of PF_2I is obtained fron the elemental analysis, vapor density molecular weight, and mass spectrum, tabulated in Table 1 A, B, and C, respectively. The mass spectrum confirms the vapor density molecular weight for the monomer PF_2I and displays the expected fragmentation pattern. In the mass spectrum observed experimentally there were a number of additional minor peaks. These extraneous peaks were ascribed to small amounts of impurities which resulted from the reaction of PF_2I with traces of water in the vacuum system or to traces of unreacted F_2PNMe_2 in the PF_2I sample.

The vapor pressure data for difluoroiodophosphine are compared in Table 2 with those calculated from the vapor pressure equation. Also included in Table 2 are the freezing point, boiling point, and Trouton constant for PF_2I.

The phosphorus and fluorine nmr spectra of PF_2I (Figure 1) display the expected spin-spin splitting patterns with P-F coupling somewhat smaller than in PF_3.[51] The 1:2:1 triplet (J_{PF} = 1337 cps) centered 242.2 ppm downfield from OPA in the ^{31}P nmr spectrum of PF_2I (Figure 1) shows that two equivalent fluorines (2I + 1 = 3) are directly bonded to phosphorus; the doublet (J_{PF} = 1340 cps) displayed 31.9 ppm downfield from TFA

Table 1

Characterization

of

Difluoroiodophosphine

A. Elemental analysis.

	P	F	I
found:	15.37	18.09	64.34
calcd:	15.81	19.39	64.78

B. Vapor density molecular weight.

obsvd: 192.9 g./mole calcd: 195.9 g./mole

C. Mass spectrum.

m/e	relative peak height	assignment
196	100	PF_2I^+
177	15	PFI^+
158	6	PI^+
127	71	I^+
88	1	PF_3^+
69	60	PF_2^+
63.5	4	I^{2+}
50	29	PF^+
31	11	P^+
19	3	F^+

Table 2

Physical Constants of PF_2I

A. Vapor pressure data.

°C	mm (obsvd)	mm (calcd)
-63.5	5.0	5.0
-45.6	19.8	18.9
-30.6	48.2	48.7
-22.9	74.5	75.8
0.0	240.1	244.4

B. Equation.

$$\log p(\text{mm}) = \frac{-1514}{T} + 7.929$$

C. Trouton constant: 23.09 cal./ deg. mole

b.p. (extrapolated): 26.7°C

m.p.: -93.8 to -93.3°C

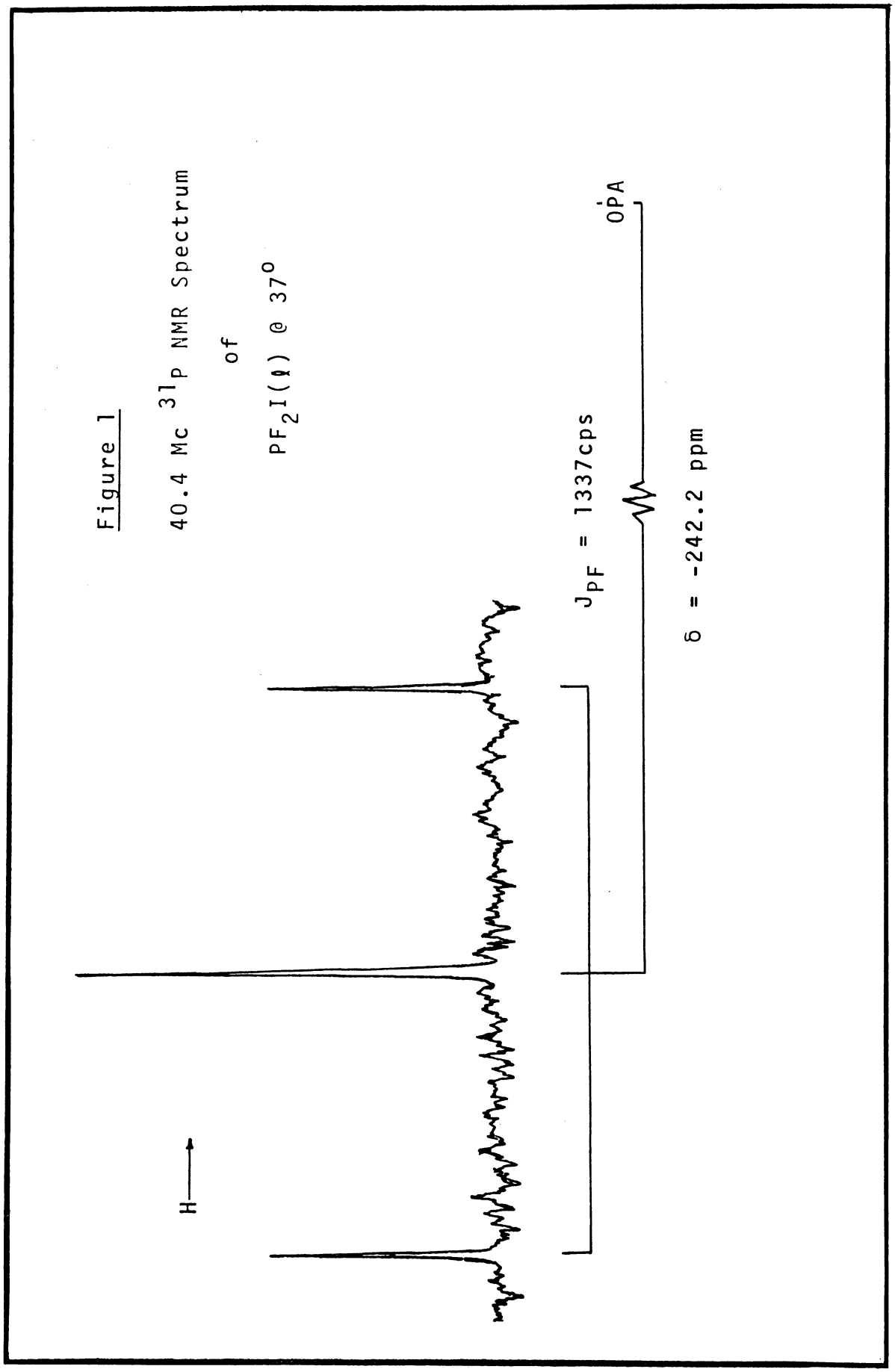
Figure 1
40.4 Mc ^{31}P NMR Spectrum
of
$PF_2I(\ell)$ @ 37°
H
J_{PF} = 1337cps
OPA
δ = -242.2 ppm

in the ^{19}F nmr spectrum (Figure 2) further indicates that the fluorine nuclei are bonded to a single atom ($I = \frac{1}{2}$). It has been noted that P-F spin-spin coupling constants correlate qualitatively with the s-character of the σ-bonding hybrid of phosphorus[51]. When compared with $J_{PF}(PF_3) = 1441$ cps[51], the $J_{PF}(PF_2I) = 1340$ cps indicated that the P-F bonds in difluoroiodophosphine have less "s-character" than those in PF_3 which is usually considered to be close to an sp^3 hybrid. Couched in more fundamental terms, the F-P-F bond angle in PF_2I is probably less than that in PF_3 (104°)[52].

The infrared and Raman spectra of difluoroiodophosphine are displayed in Figures 3 and 4, respectively. The observed frequencies and tentative assignments are tabulated in Table 3. Since both planar (C_{2v}) and pyramidal (C_s) geometries for PF_2I would be expected to display six fundamental vibrations, the geometry of the molecule cannot be confirmed from the number of observed vibrational frequencies. Five of the fundamentals were assigned from the infrared and the sixth was observed in the Raman effect at 202 cm^{-1}, apparently too close to the cut off of the infrared spectrometer for observation. Polarization studies were precluded by the rapid decomposition of PF_2I under the influence of the mercury arc light even at -40°. The resolution in the Raman spectra was apparently insufficient to resolve the two P-F vibrations expected near 830 cm^{-1} and the two other motions near

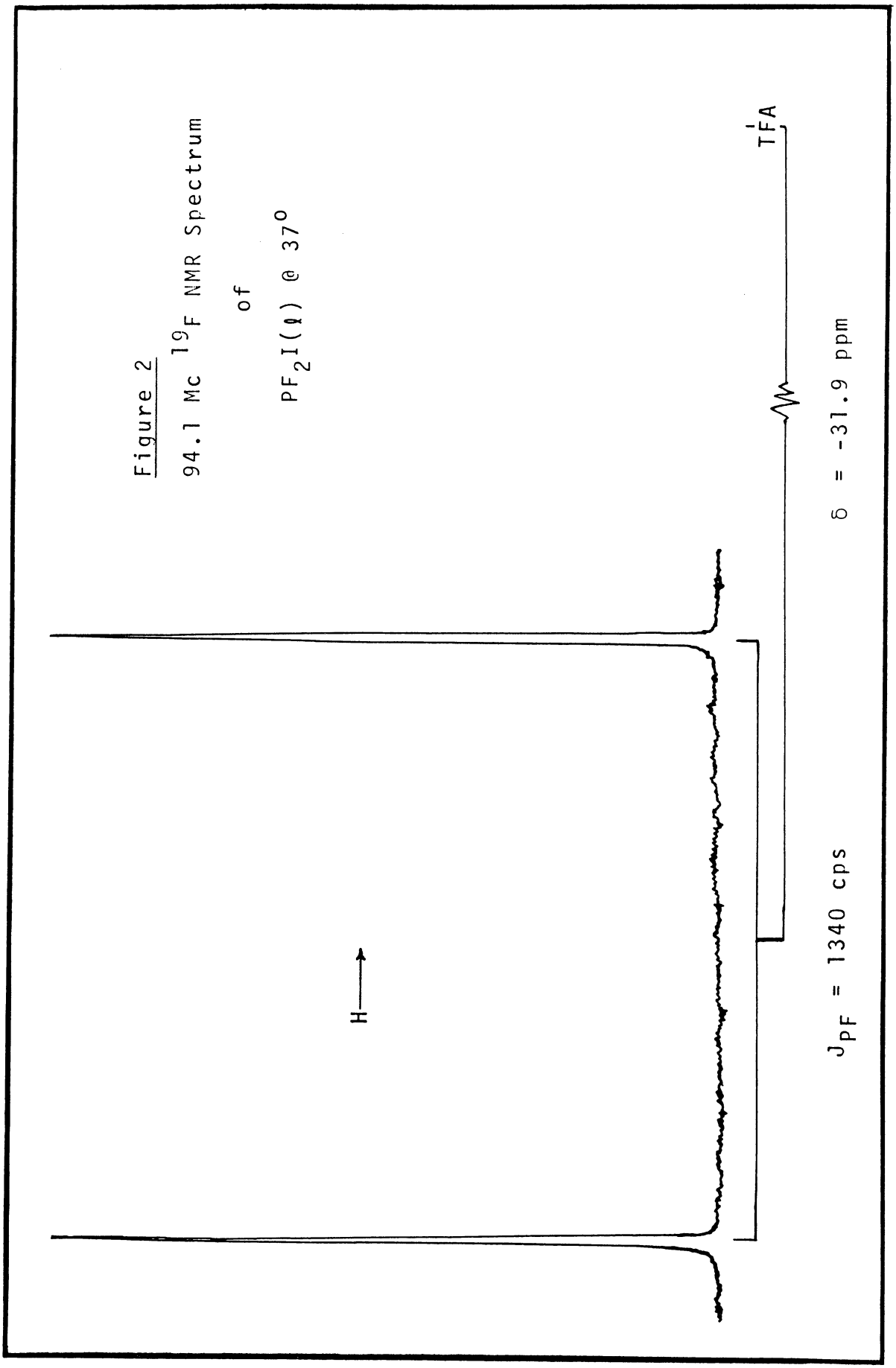
Figure 2
94.1 Mc ^{19}F NMR Spectrum
of
$PF_2I(\ell)$ @ 37°
TFA
δ = -31.9 ppm
J_{PF} = 1340 cps
H

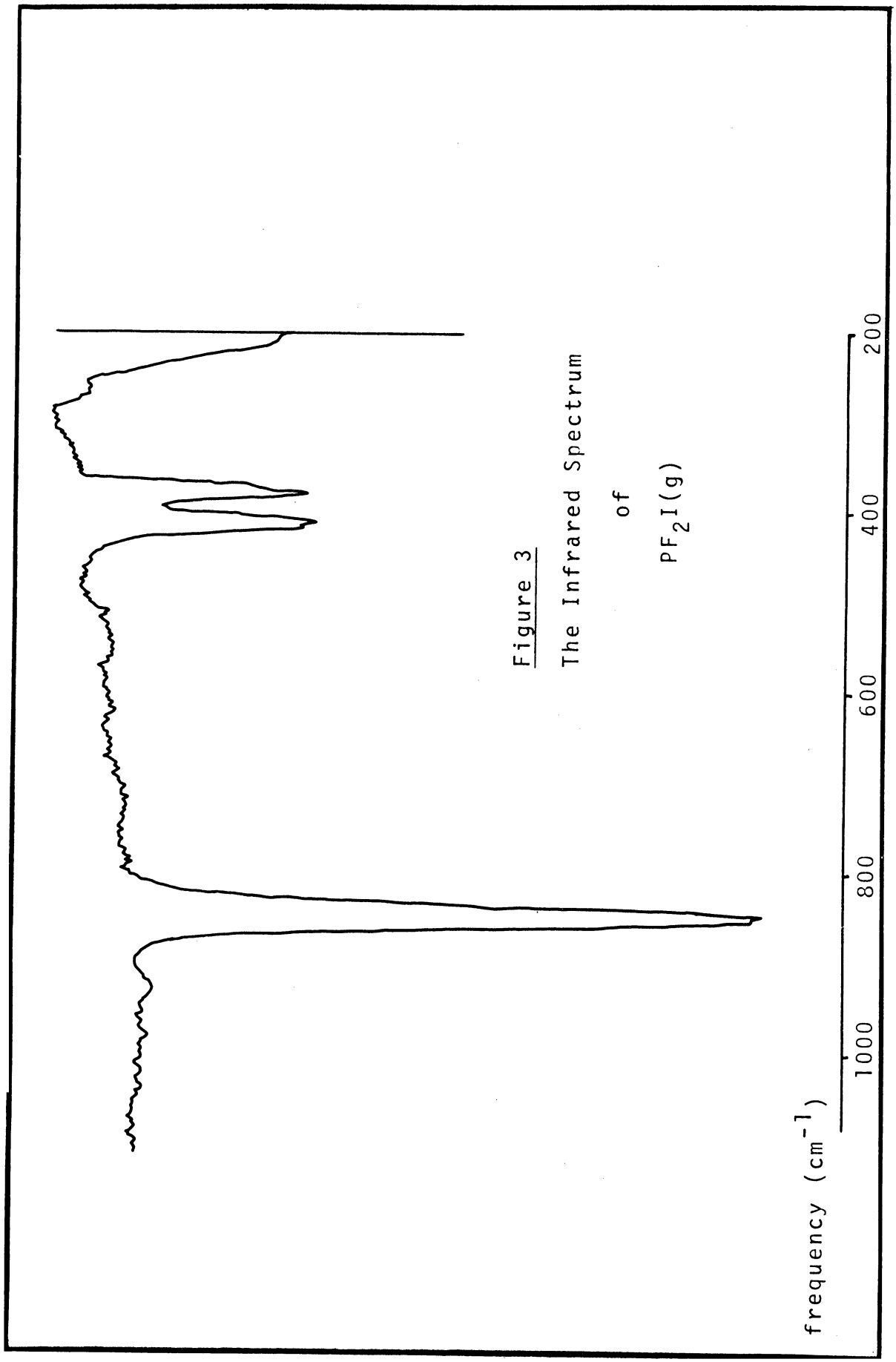

Figure 3

The Infrared Spectrum of $PF_2I(g)$

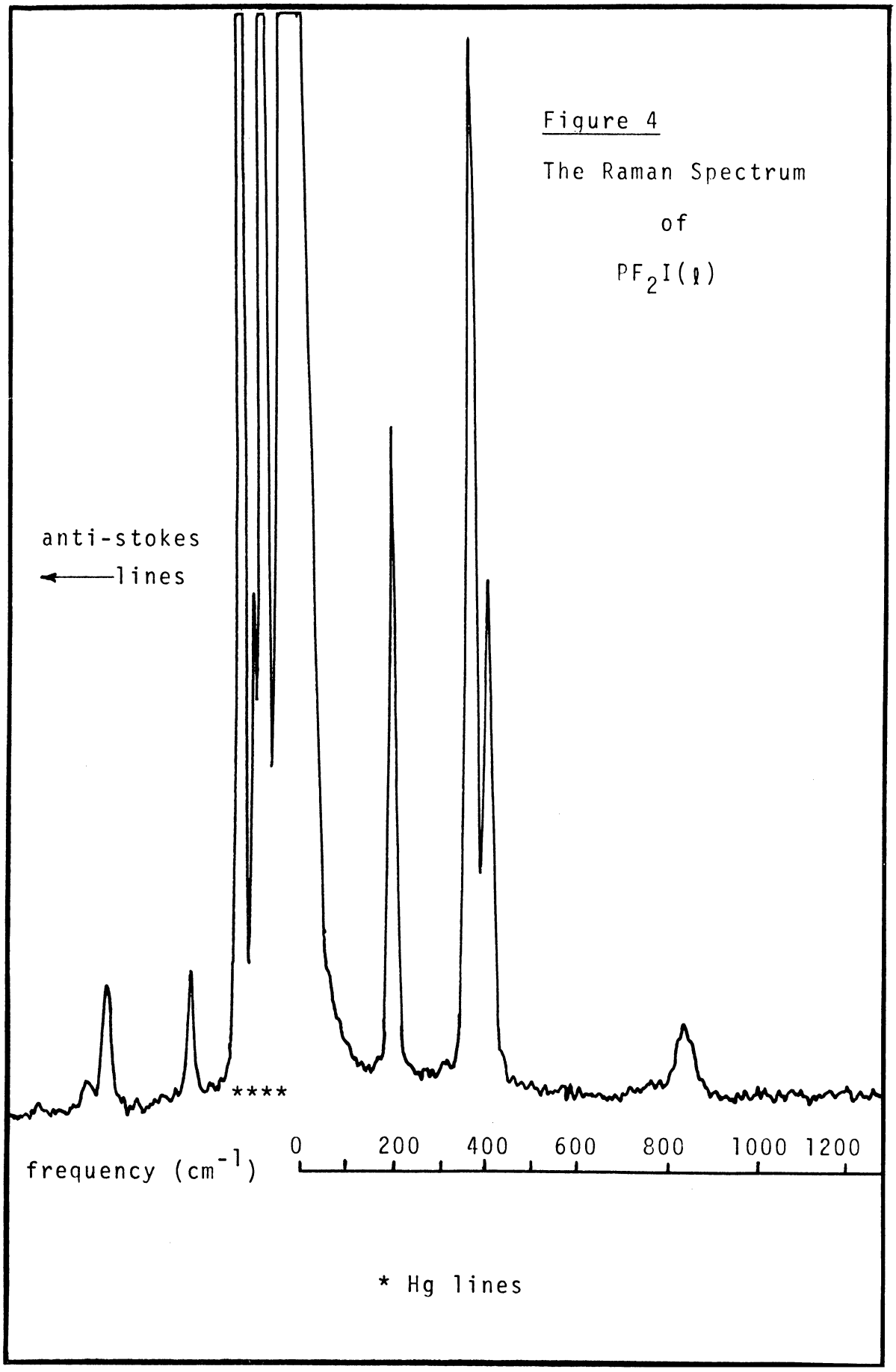

Figure 4

The Raman Spectrum

of

PF_2I(ℓ)

368cm^{-1}, thus only four bands were observed. The P-F motions in the infrared were assigned on the basis of their similarity, both in vibrational-frequency and band-shape, to those of molecules like PF_2Cl, PF_2Br, and PF_3.

Table 3

Infrared & Raman Spectra* of PF_2I

Infrared (g)			Raman (ℓ)(-40°)
freq. (cm^{-1}) & intensity	note	assgn.	freq. (cm^{-1}) & intensity
850.4 s		$\nu_s PF$	828 w
845.3 vs		$\nu_{as} PF$	
417.5 m	R		
411.8 m	Q	$\delta_s FPF$	404 s
407.0 m	P		
378.5 m		$\nu_s PI$	368 vs
372 w	sh	$\omega_{as} PF_2$	
		$\delta_s PF_2I$	202 s

* For an explanation of notation see Appendix A.

B. Characterization of Cyanodifluorophosphine, PF_2CN.

Cyanodifluorophosphine was prepared by treating CuCN with difluoroiodophosphine as represented in the equation

$$PF_2I + CuCN \rightarrow PF_2CN + CuI.$$

In contrast to $P(CN)_3$[53], a colorless, slightly volatile solid, PF_2CN is a colorless volatile liquid which is characteristically similar to the halogenoid-halides of

phosphorus[54]. Although, at this time the characterization of PF_2CN is not extensive, the vapor density molecular weight, and mass spectrum shown in Table 4 offer good evidence for the formulation PF_2CN. Experimentally, a separation of PF_2CN from small amounts of impurities like HCN, PF_2I, F_2PNMe_2 in the PF_2I, and PO-containing species, was difficult because of the similarity in volatility among the compounds; minor peaks attributable to these species, although not all noted in Table 4, did appear in the observed mass spectrum. The intensity of the HCN peak, as noted in Table 4, is appreciable; however, the spectrometer is very sensitive to HCN, and the slight leak in the inlet system of the instrument may have led to partial hydrolysis of PF_2CN and production of HCN. Nevertheless, the salient feature of the mass spectrum is a fragmentation pattern consistent with the formulation PF_2CN. In fact the presence of a peak at m/e = 43(PC^+) is good evidence that PF_2CN is a true cyanide as opposed to an isocyanide which would be expected to give a peak at m/e = 45(PN^+).

The ^{19}F nmr spectrum of liquid cyanodifluorophosphine at -20° (Figure 5) consists of a simple doublet centered 11.7 ppm upfield from TFA (external std). The doublet splitting of 1267 cps is attributed to spin-spin coupling of the fluorine nuclei with the single phosphorus nucleus. While the fluorine spectrum shows that one phosphorus is present in the molecule, the ^{31}P spectrum (Figure 6)

Table 4

Characterization

of

Cyanodifluorophosphine

A. Vapor density molecular weight.

obsvd: 97.5 g./mole calcd: 95.0 g./mole

B. Mass spectrum.

m/e	relative peak height	assignment
95	27.1	PF_2CN^+
88	2.0	PF_3^+
76	14.2	$PFCN^+$
69	100.0	PF_2^+
57	1.9	PCN^+
50	17.6	PF^+
43	1.8	PC^+
38	1.4	$PFCN^{2+}$
31	13.3	P^+
27	12.6	HCN^+
26	9.6	CN^+
19	1.6	F^+
14	2.5	N^+

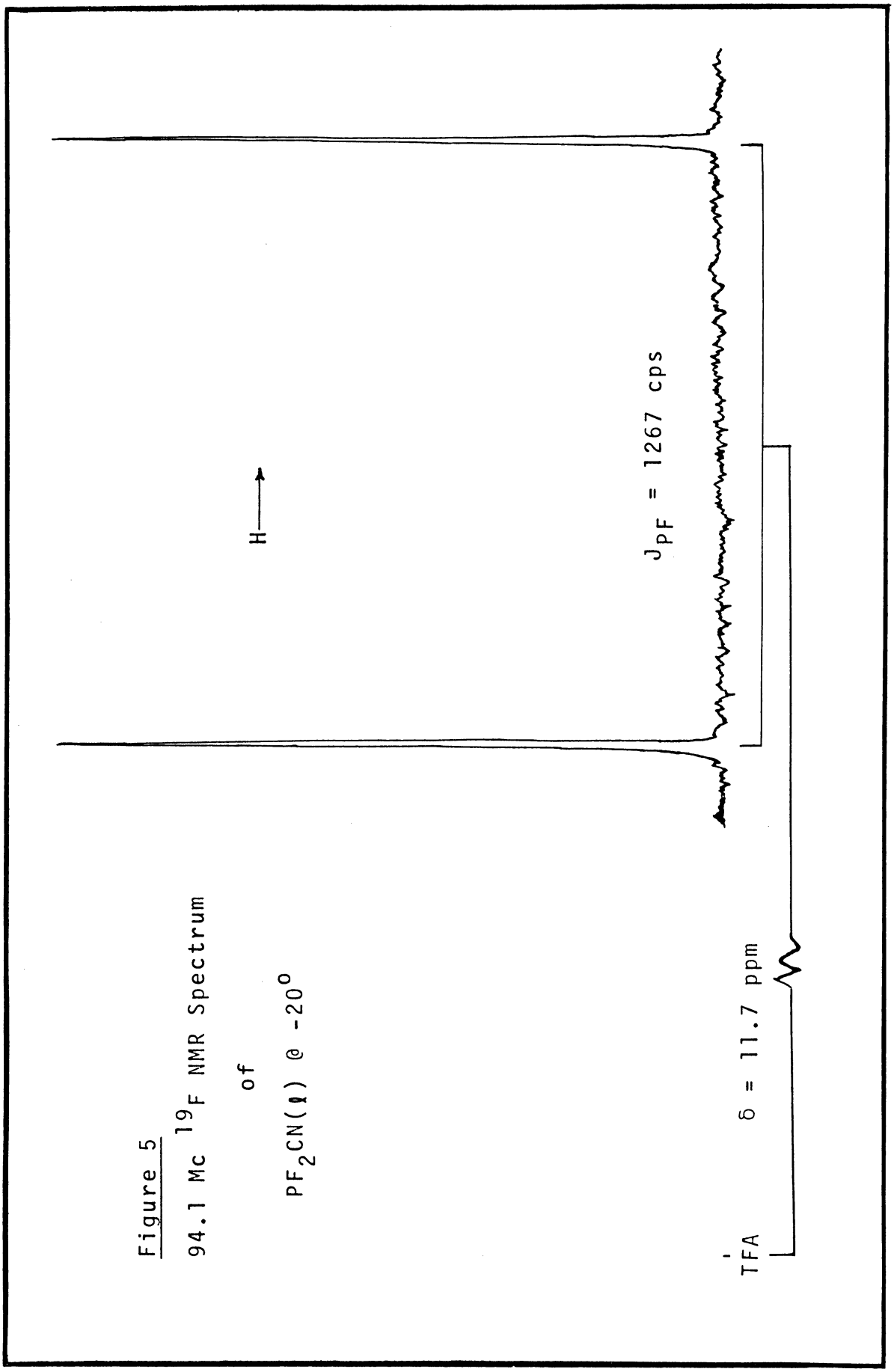

Figure 5

94.1 Mc ^{19}F NMR Spectrum

of

PF_2CN(ℓ) @ -20°

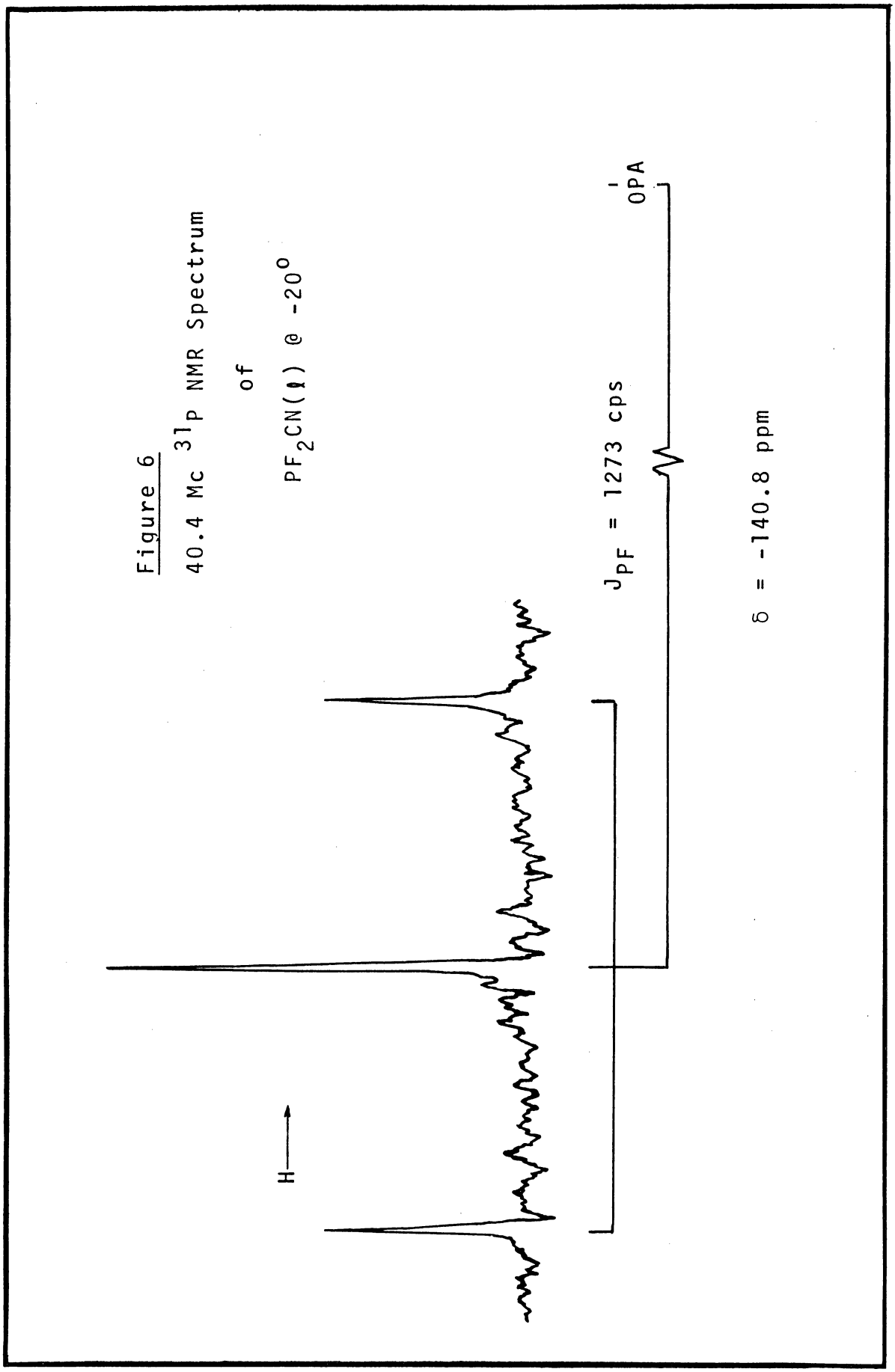
Figure 6
40.4 Mc ^{31}P NMR Spectrum
of
$PF_2CN(I)$ @ -20°
H
J_{PF} = 1273 cps
OPA
δ = -140.8 ppm

clearly establishes the presence of two equivalent fluorines bonded to the phosphorus. The 1:2:1 triplet (J_{PF} = 1273 cps) in the ^{31}P nmr is centered 140.8 ppm downfield from OPA. Even at -20° there was significant disproportionation of PF_2CN (ℓ) as evidenced by the formation of white solids [probably $P(CN)_3$] in the nmr tube and the appearance of PF_3 in the nmr spectrum. The equation probably is

$$3PF_2CN \rightarrow 2PF_3 + P(CN)_3.$$

The infrared spectrum of PF_2CN gas is shown in Figure 7; in Table 5, the vibrational frequencies derived from the spectrum are compared with those for $P(CN)_3$ and PF_2Cl in order to aid in making tentative assignments.

If the cyanide moiety is considered as a point mass, i.e., if the motions due to cyanide [$\nu_s CN$, $\omega_{as} PCN$, $\delta_s PCN$] are neglected, the spectra of PF_2Cl and PF_2CN would be expected to be very similar; under these limiting conditions they are similar as can be seen in Table 5. In fact, the band shapes in the P-F and P-X stretching regions are also very similar. Notably, the P-Cl bending and wagging motions could not be detected under the conditions used to determine the gas phase spectrum of PF_2Cl. Likewise, under similar experimental conditions, for gaseous PF_2CN the corresponding P-CN wagging and bending motions did not appear in the expected region (250 - 320 cm^{-1})[55, 56a]. However, according to the

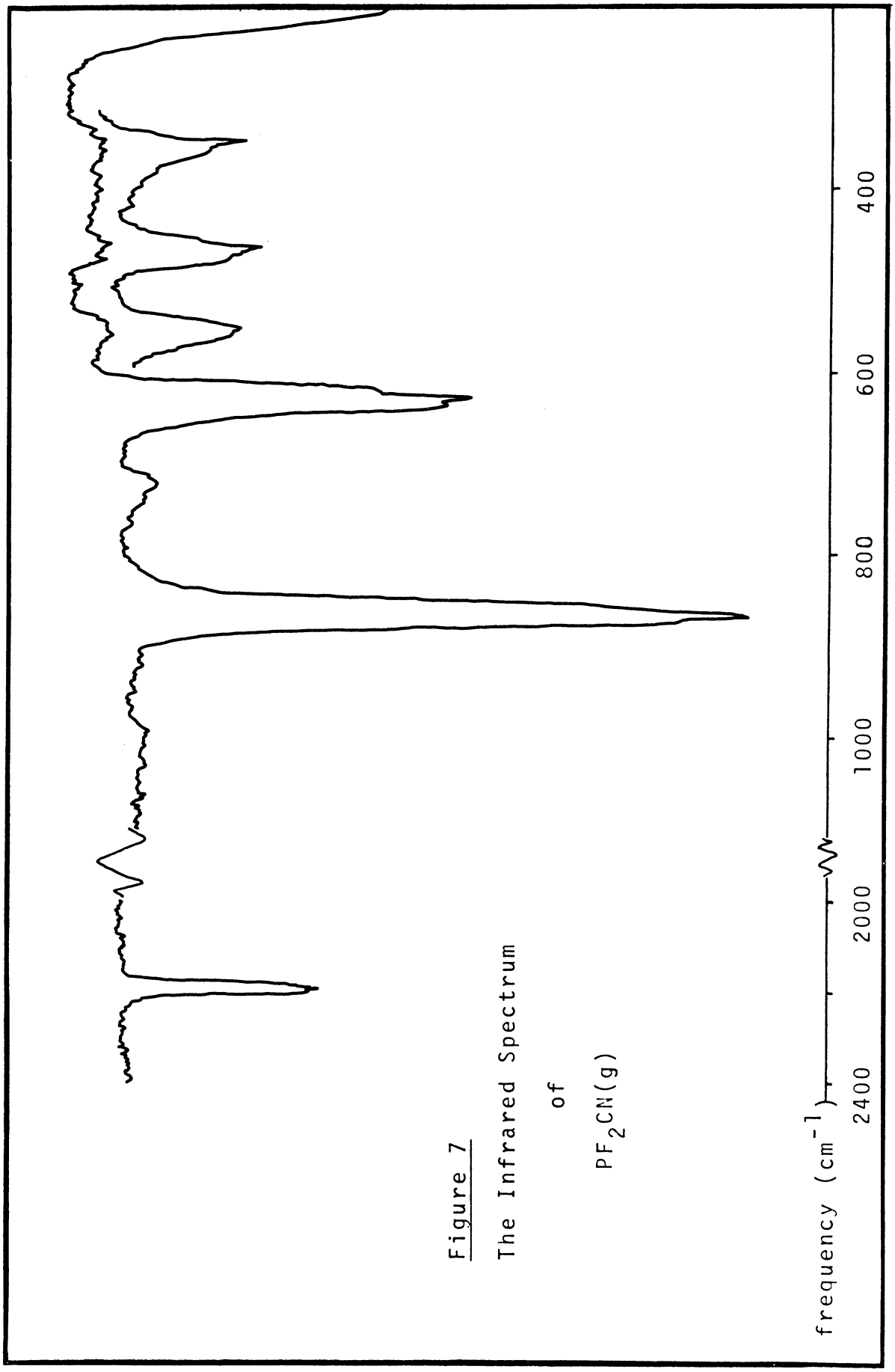

Figure 7

The Infrared Spectrum

of

$PF_2CN(g)$

Table 5

The Infrared Spectra* of PF_2CN, PF_2Cl, and $P(CN)_3$

PF_2CN(g)			PF_2Cl(g)			$P(CN)_3$ (56a)	
freq. (cm^{-1}) & intensity	note	assgn.	freq. (cm^{-1}) & intensity	note	assgn.	freq. (cm^{-1}) & intensity	assgn.
2193.9 vs		ν_sCN				2204 vs	νCN
869.4 s		ν_sPF	864.5 s		ν_sPF		
866.6 vvs		ν_{as}PF	853.5 vvs		ν_{as}PF		
						633 s	$2\cdot\delta_s PC_3$
636.4	R		550.3	R		605 vs	$\nu_{as}PC_3$
629.0 vs	Q	ν_sPC	543.7 vs	Q	ν_sPCl		
622.1	P		538	P		585 s	$\nu_s PC_3$
549 w		δ_sPCN					
						464 w	δPCN
460.5 w	†	ω_{as}PCN				451 w	
			421	R			
344.6 w	†	δ_sFPF	412.2 m	Q	δ_sFPF		
			404	P			
			302‡		δ_sPCl‡	312 m	$\delta_s PC_3$
						276 w	$\delta_{as}PC_3$
			259‡		ω_{as}PCl‡	267 m-w	

* For an explanation of notation see Appendix A.
† Indication of P and R branches.
‡ Not observed in spectra determined on PF_2Cl vapor in this study. Taken from Delwaulle and Francois.(55)

assignments of Miller[56b] for $P(CN)_3$ the latter motions would fall below 200 cm^{-1}, the limit of our instrument. Unless the two "missing" frequencies are accidentally degenerate with those noted in Table 5, only seven of the expected nine fundamental vibrations for PF_2CN have been observed. The expected pyramidal geometry (C_s symmetry) for PF_2CN cannot be ascertained from the number of observed fundamentals in the infrared since the planar model (C_{2v} symmetry) would also have nine fundamentals.

Under high resolution the C-N stretching in PF_2CN appeared to be composed of a number of lines spaced by 2.3 cm^{-1}. The surprising number of lines observed in the C-N stretching region is probably attributable to "hot" bands as explained in Appendix C.

Due to the lack of model compounds, and since the cyanide and isocyanide stretching frequencies fall close together[57], it is not felt that the infrared spectrum of PF_2CN can be used to differentiate between the cyanide and isocyanide structure.

C. The Characterization of μ-Oxo-bisdifluorophosphine, F_2POPF_2.

The interesting new species μ-oxo-bisdifluorophosphine was isolated in 73% yield from the reaction of PF_2I and Cu_2O according to the equation

$$2PF_2I + Cu_2O \rightarrow F_2POPF_2 + 2CuI.$$

This new species is the first highly volatile compound containing a P-O-P link. One closely related compound

described in the literature[58,59] is diphosphoryltetrafluoride, $F_2P(O)-O-P(O)F_2$, which boils at 71° as compared to -18.3° (extrapolated from vapor pressure equation) for F_2POPF_2.

Although some difficulty was encountered in obtaining a satisfactory elemental analysis for F_2POPF_2 by classical techniques, it is felt that a good characterization of the new species has been obtained on the basis of other evidence.

The low resolution ^{31}P and ^{19}F nmr spectra of F_2POPF_2 (*l*) consist of a 1:2:1 triplet and a simple doublet, respectively; the coupling constants derived from both the ^{19}F and ^{31}P spectra agree closely and are comparable to P-F couplings observed in related compounds. Although a more complete discussion of nmr spectra will follow, the 1:2:1 triplet of the ^{31}P nmr spectrum indicates that each phosphorus is bound directly to two fluorine nuclei. This "elemental analysis" by nmr, when considered with other data presented below, offers no reasonable alternative to the formulation F_2POPF_2.

The mass spectrum of F_2POPF_2 (Table 6) has the expected fragmentation pattern. Since no peaks appeared at higher than m/e = 154, the parent peak for F_2POPF_2, the spectrum affords a confirmation of the vapor density molecular weight of 154.2 g./mole.

The vapor pressure data for F_2POPF_2 were obtained and are summarized in Table 7 where they are compared

Table 6

Characterization

of

μ-Oxo-bisdifluorophosphine

A. Vapor density molecular weight.

obsvd: 154.2 g./mole calcd: 154.0 g./mole

B. Mass spectrum.

m/e	relative peak height	assignment
154	20.0	$F_2POPF_2^+$
135	2.6	F_2POPF^+
88	2.5	PF_3^+
85	3.3	PF_2O^+
69	100.0	PF_2^+
66	4.3	PFO^+
50	16.8	PF^+
47	27.7	PO^+
31	5.9	P^+
25	0.4	PF^{2+}
19	1.2	F^+
16	0.4	O^+
15.5	0.3	P^{2+}

Table 7

Physical Constants of F_2POPF_2

A. Vapor pressure data.

°C	mm (obsvd)	mm (calcd)
-83.6	13.1	13.3
-78.5	19.5	20.0
-63.0	61.0	60.4
-50.0	141.6	143.1
-45.0	190.5	189.5

B. Equation.

$$\log p(\text{mm}) = \frac{-1300}{T} + 7.981$$

C. Trouton constant

23.33 cal./deg. mole

b.p.(extrapolated)

-18.3°C

m.p.

-132.1 to -131.8°C

with values calculated from the vapor pressure equation. Also included in Table 7 are the freezing point, boiling point, and Trouton constant for F_2POPF_2.

Samples of F_2POPF_2 have been stored in clean glass tubes at 25°C and saturation pressure for one day with less that 1% decomposition. At lower pressures and temperatures the compound is even more stable; however, adsorbant surfaces like asbestos accelerate the disproportionation, i.e., a sample of F_2POPF_2 placed in contact with asbestos paper at 25° was nearly 100% decomposed after one day according to the equation

$$F_2POPF_2 \rightarrow PF_3 + (POF)_n.$$

The infrared spectrum of gaseous μ-oxo-bisdifluorophosphine is displayed in Figure 8. The comparison of the infrared spectrum of F_2POPF_2 with the Raman spectrum of $F_2P(O)\text{-}O\text{-}P(O)F_2$[59] shown in Table 8 indicates the presence of a P-O-P oxygen bridge bond in F_2POPF_2. The salient difference between F_2POPF_2 and $F_2P(O)\text{-}O\text{-}P(O)F_2$ is the absence of the terminal P-O bonds in the former. Thus, the very intense absorption characteristic of P-O (the 1400 - 1200 cm^{-1} region)[59,60] is absent in the infrared of F_2POPF_2; however, absorption bands characteristic of a P-O-P bridged linkage are observed at 976.1 and 682 cm^{-1}. The latter assignment of P-O-P vibrations agrees closely with that made by Corbridge[60] who observed that many species containing a P-O-P link absorb in the 970 - 870 and ~ 700 cm^{-1} regions. On the other

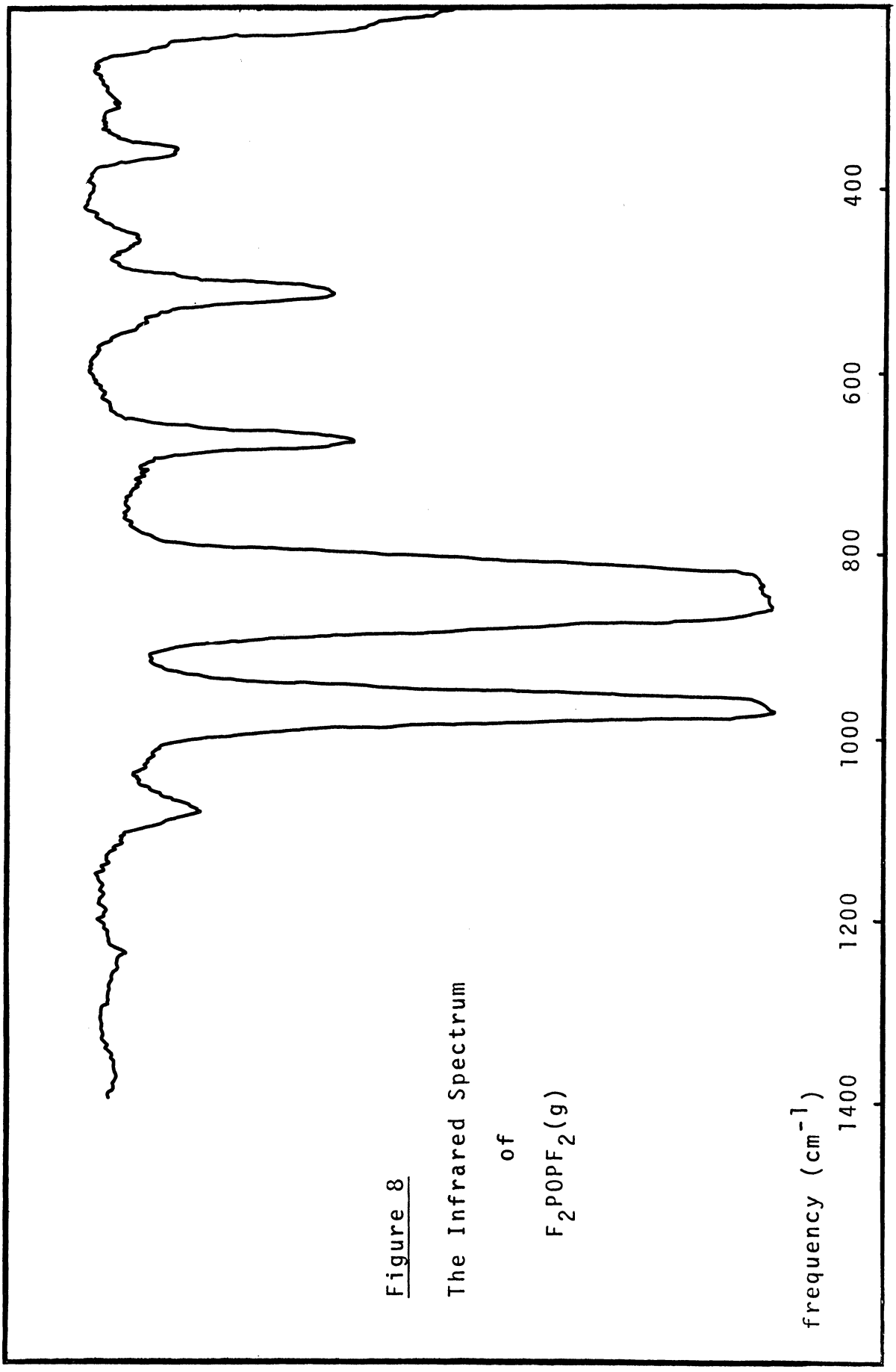

Figure 8

The Infrared Spectrum of $F_2POPF_2(g)$

Table 8

A Comparison of the Vibrational Spectra*

of F_2POPF_2 and $F_2P(O)-O-P(O)F_2$

Infrared $F_2POPF_2(g)$				Raman $F_2P(O)-O-P(O)F_2(\ell)$ (59)		
freq. (cm^{-1}) & intensity		note	assgn.	freq. (cm^{-1}) & polarization		assgn.
				1390	p	νPO
				1370		νPO
				1270	dp	overtone
1077	w		overtone	1083	dp	overtone
976.1	vvs	br	ν_{as}POP	987	dp	ν_{as}POP
863.1	vvs	br	νPF	951	dp	νPF
853	vvs			890	p	
842	vvs			855		
682	m		ν_sPOP	721	p	ωPO
				700		
				518		PF_2 scissors
519	m	sh	PF_2 scissors			
515	m			480	p	ν_sPOP
				440	p	PF_2 scissors
460	w		ρPF_2	395		ρPF_2, ωPO, and torsional modes
359	w		τPF_2	362		
				352		
				340		
				295		
				273	dp	
				205		
				160	p	POP scissors

* For an explanation of notation see Appendix A.

hand, Robinson[59] assigned absorptions around 700 cm^{-1} in $Cl_2P(O)-O-P(O)Cl_2$ and $F_2P(O)-O-P(O)F_2$ to P-O wagging motions. Such P-O wagging motions are precluded in F_2POPF_2, and since the absorption at 682 cm^{-1} seems too low to be assigned to a P-F stretch and too high to be attributed to any PF_2 deformation, it has been assigned to the assymetric P-O-P stretch. Also in accord with the assignments made here Griffiths[61] has made the following assignments for $(CF_3)_2POP(CF_3)_2$: $\nu_{as}POP$ = 925 and ν_s = 715 cm^{-1}.

The high resolution ^{19}F nmr spectrum of $F_2POPF_2(\ell)$ is shown in Figure 9. The spectrum remained unchanged from -80 to 37°, and therefore, it seems unlikely that the "unusual" splitting pattern can be attributed to temperature dependent phenomena like exchange or internal rotation. The spectrum is probably best described as a "second-order" A_2X_4 type. An analysis of this spectrum in terms of an $X_2AA'X'_2$ system is found in Appendix D. The phosphorus spectrum (Figure 10) also appears to be consistent with an $X_2AA'X'_2$ type, however, analysis is incomplete at this time.

The ^{31}P (δ = -111 ppm, OPA std) and ^{19}F chemical shifts (δ = -39.9 ppm, TFA std) of F_2POPF_2 are both in good agreement with the corresponding values for PF_3 [$\delta(P)$ = -105 ppm; $\delta(F)$ = -42.3 ppm]; this agreement is not surprising if F_2POPF_2 is considered as two PF_3 molecules with a bridging oxygen, fluorine's neighbor

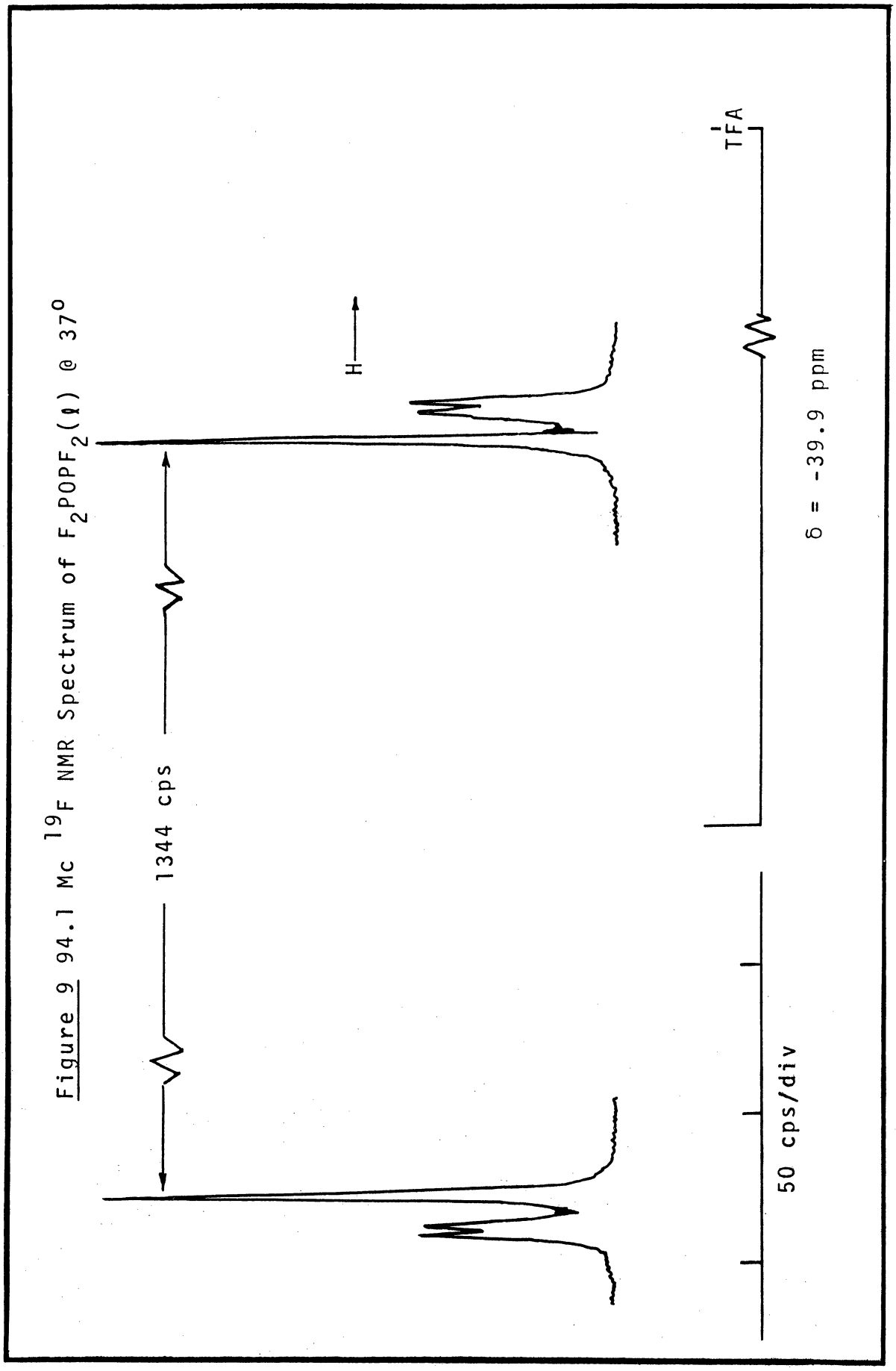

Figure 9 94.1 Mc ^{19}F NMR Spectrum of $F_2POPF_2(\ell)$ @ 37°

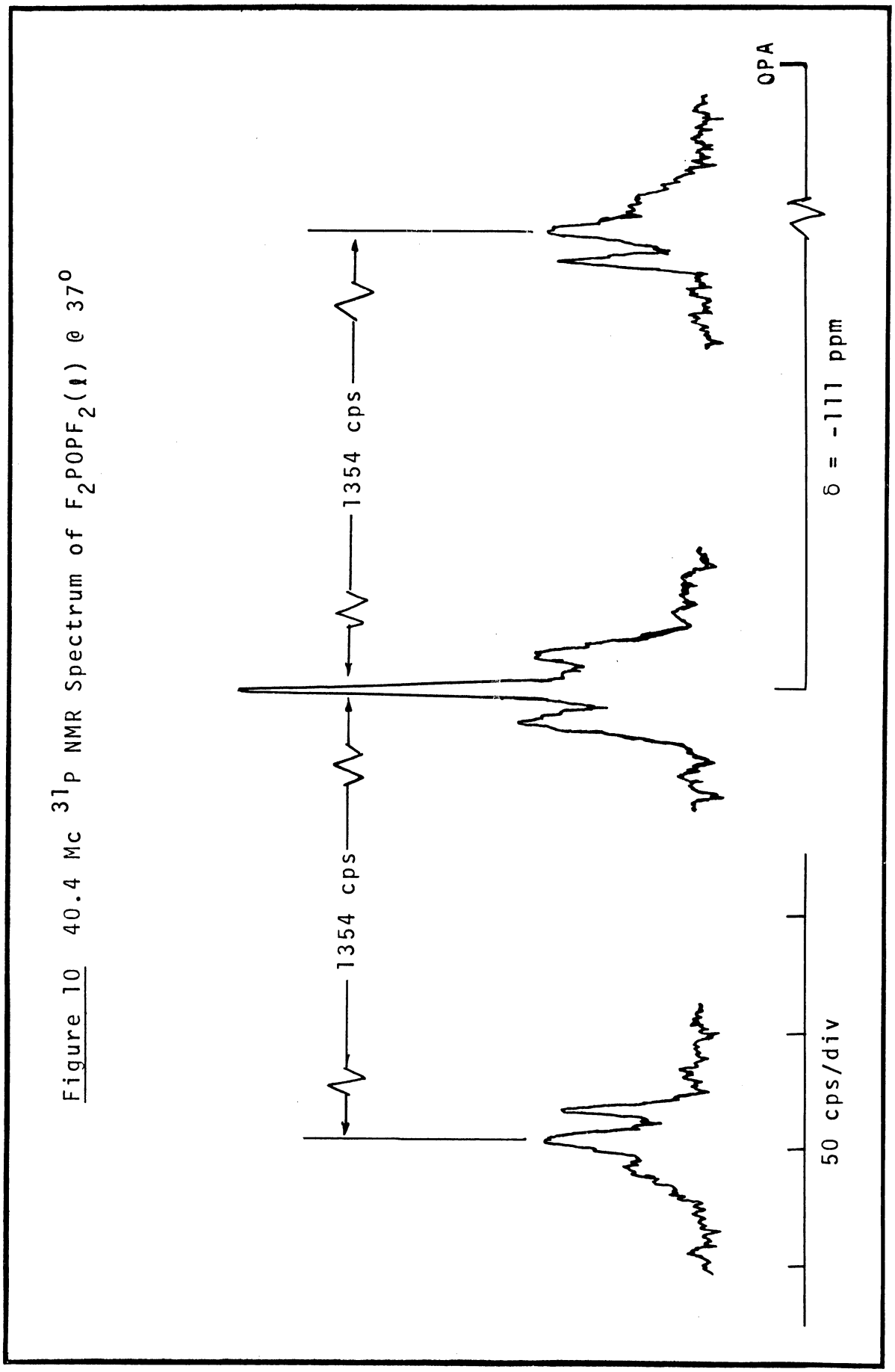

Figure 10 40.4 Mc ^{31}P NMR Spectrum of F_2POPF_2(ℓ) @ 37°

in the periodic chart, replacing a fluorine atom in each PF_3 unit.

D. Characterization of Tetrafluorodiphosphine, P_2F_4.

The literature[62-64] mentions several attempted preparations of tetrafluorodiphosphine via the fluorination of a tetrahalodiphosphine, P_2X_4. In the course of this study, P_2F_4 was isolated in 94% yield when PF_2I was shaken with mercury. The equation for the reaction is

$$2PF_2I + 2Hg \rightarrow P_2F_4 + Hg_2I_2.$$

High yields were obtained when the initial pressure of PF_2I was around 50 mm; however, in another experiment when the initial pressure of PF_2I was raised ca. 450 mm, the main reaction was disproportionation of the PF_2I according to

$$3PF_2I \rightarrow 2PF_3 + PI_3.$$

When the P_2F_4 was separated from the unreacted PF_2I (see Experimental), a small amount of F_2PNMe_2 was detected in the unreacted PF_2I. Perhaps the presence of F_2PNMe_2 in the PF_2I was a factor which promoted the formation of P_2F_4 since others[45] have unsuccessfully tried to prepare P_2F_4 from the reaction of PF_2I and Hg.

Although the characterization of tetrafluorodiphosphine is not extensive, several pieces of evidence confirm the formula P_2F_4. A mass balance of products and reactants (see Experimental) shows that two moles of PF_2I react with mercury to form one mole of a species having a vapor

density molecular weight of 140.1 g./mole; theory for the monomer P_2F_4 is 138.0 g./mole. The principal ions which appear in the mass spectrum (Table 9) correspond to the fragmentation pattern anticipated for P_2F_4; the m/e = 138 peak, which corresponds to the $P_2F_4^+$ parent ion, confirms the vapor density molecular weight. Other minor peaks attributed to fragments from F_2POPF_2 and PHF_2 were also observed in the spectrum but were not mentioned in Table 9. Since after P_2F_4 has been transferred a number of times in the vacuum system the sample is found to contain F_2POPF_2 and PHF_2, it is not surprising that the latter species appear in the mass spectrum. It is felt that the PHF_2 and F_2POPF_2 result from hydrolysis of the P_2F_4 by trace amounts of water adsorbed on the stopcock grease. Perhaps the equation is

$$2P_2F_4 + H_2O \rightarrow 2PHF_2 + F_2POPF_2.$$

Tetrafluorodiphosphine and diphosphine are probably essentially isostructural and in both cases all nuclei are magnetically active with $I = \frac{1}{2}$. Since P_2H_4 has been observed to give "complex" nmr spectra which can be interpreted in terms of an $X_2AA'X'_2$ system[65], it is to be expected that P_2F_4 should also have $X_2AA'X'_2$ nmr spectra. The ^{19}F nmr spectrum of $P_2F_4(\ell)$ has been determined at -20°, and as shown in Figure 11, it is indeed complex as is the ^{31}P spectrum (Figure 12). Although analyses of these "second-order" spectra are not complete at this time, it is felt that they will be consistent

Table 9

Characterization

of

Tetrafluorodiphosphine

A. Vapor density molecular weight.

obsvd: 140.1 g./mole calcd: 138.0 g./mole

B. Mass spectrum.

m/e	relative peak height	assignment
138	29.5	$P_2F_4^+$
119	10.3	$P_2F_3^+$
88	7.8	PF_3^+
69	100.0	PF_2^+
50	26.5	PF^+
31	12.4	P^+
25	2.2	PF^{2+}
19	3.3	F^+
15.5	1.2	P^{2+}

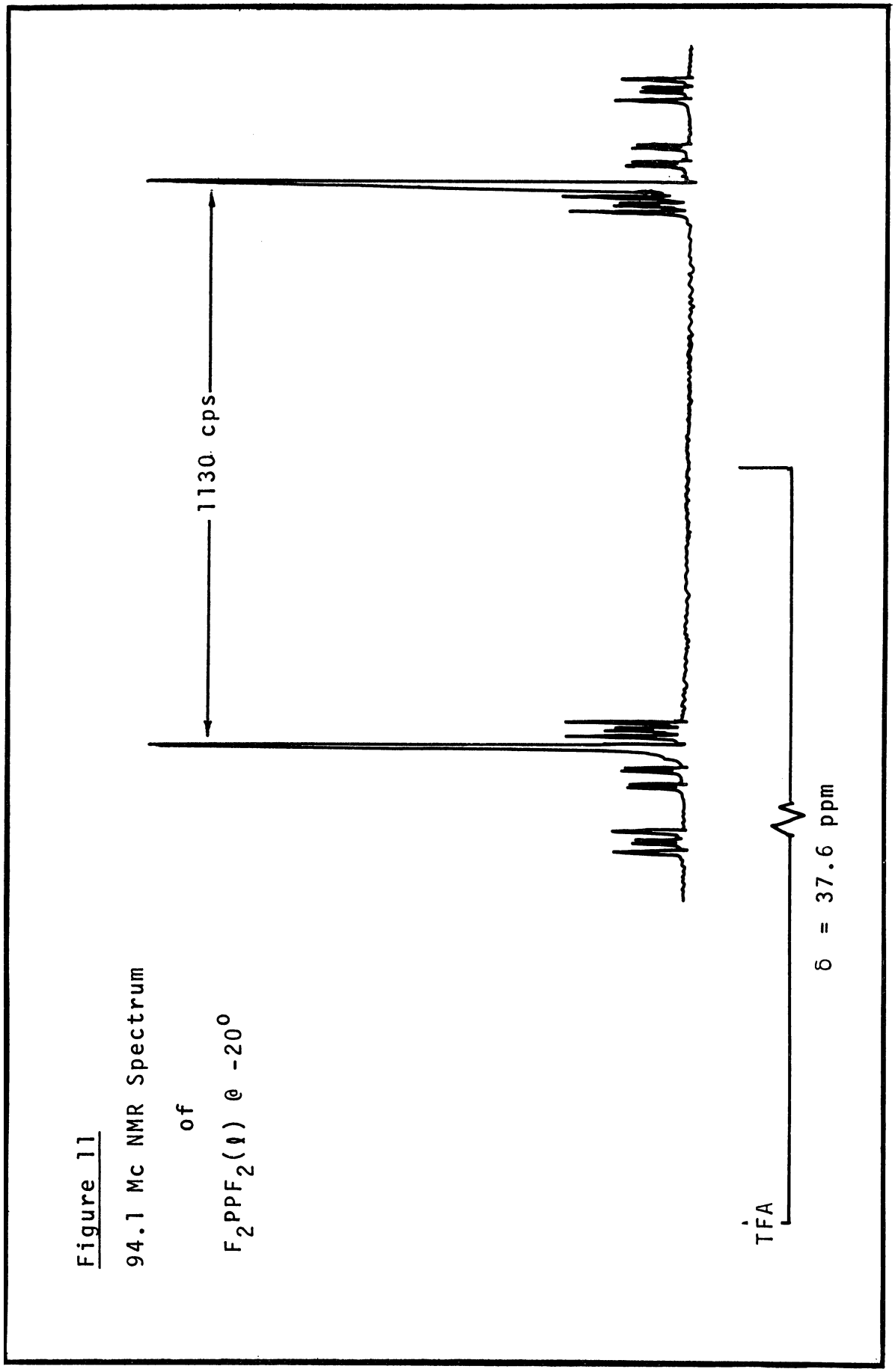

Figure 11

94.1 Mc NMR Spectrum

of

F_2PPF_2(ℓ) @ -20°

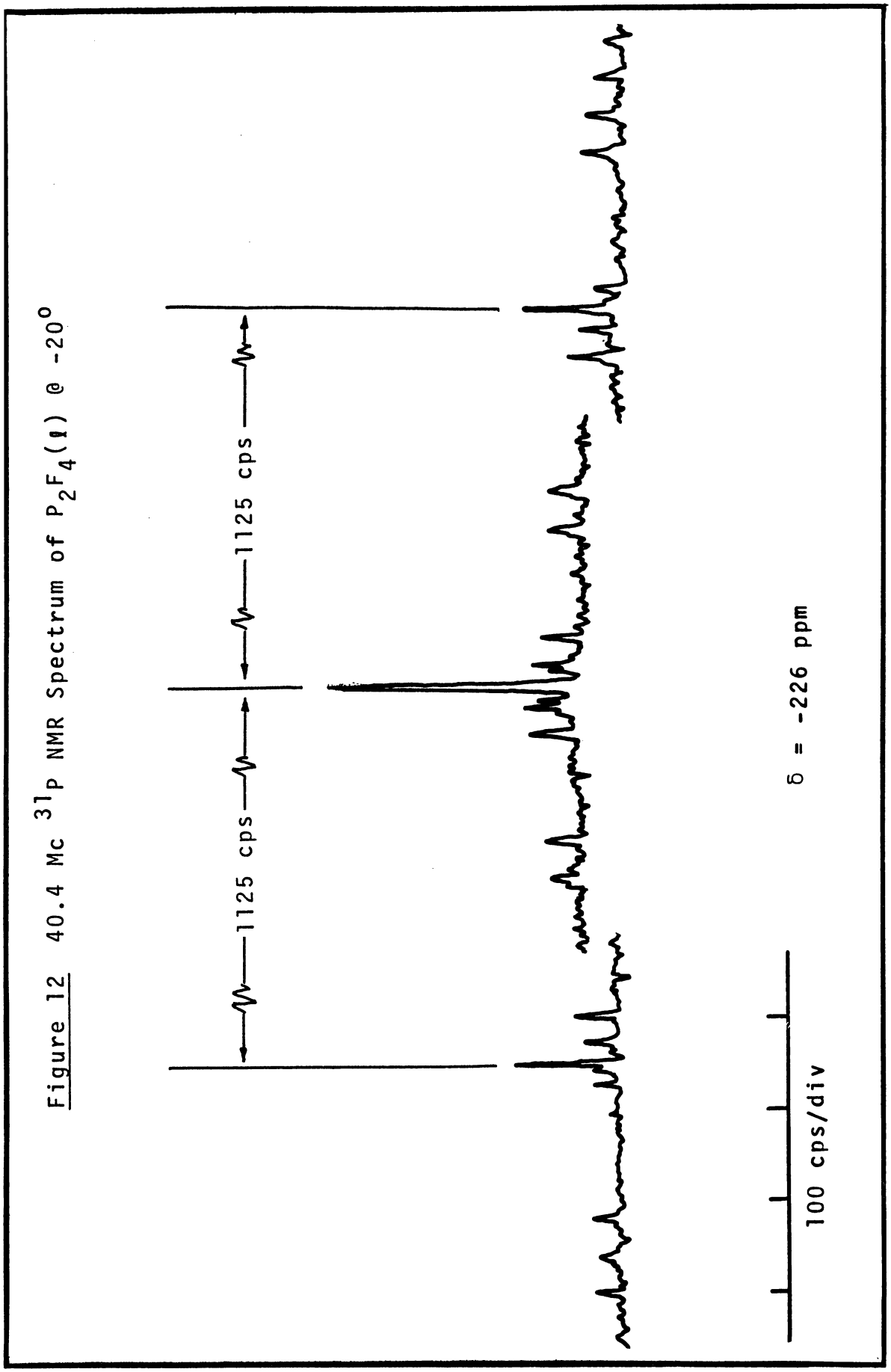

Figure 12 40.4 Mc ^{31}P NMR Spectrum of $P_2F_4(g)$ @ -20°

with an $X_2AA'X'_2$ system. The problem of analysis is discussed in more detail in Appendix D.

A number of configurations may be proposed for the F_2PPF_2 molecule. Some reasonable configurations for F_2PPF_2 and their respective symmetries are illustrated in Figure 13 along with the infrared and Raman activity predicted for each symmetry. The infrared and Raman spectra of F_2PPF_2 are displayed in Figures 14 and 15, respectively; the vibrational frequencies and tentative assignments derived from these spectra are shown in Table 10. A comparison of the vibrational spectra predicted for each form of F_2PPF_2 (Figure 13) with those actually observed indicates that tetrafluorodiphosphine probably exists in the trans conformation. The latter conclusion was reached as discussed below.

The mutual exclusion rule[66] states that in molecules containing a center of symmetry no coincidences should occur between transitions allowed in the infrared and those allowed in the Raman. The near overlap of a few frequencies in the infrared and Raman spectra of P_2F_4 determined in this study is probably accidental. This accidental overlap may be due to frequency shifts caused by the different physical states of P_2F_4 used in determining the respective vibrational spectra. Thus, the mutual exclusion rule apparently holds, pointing to either a trans or planar form for the molecule. The appearance of only seven bands in the Raman spectrum, one of which

Figure 13

Some Possible Configurations for F_2PPF_2

Planar (D_{2h}) Trans (C_{2h}) Cis (C_{2v}) Semi-Eclipsed (C_2) Gauche (C_2)

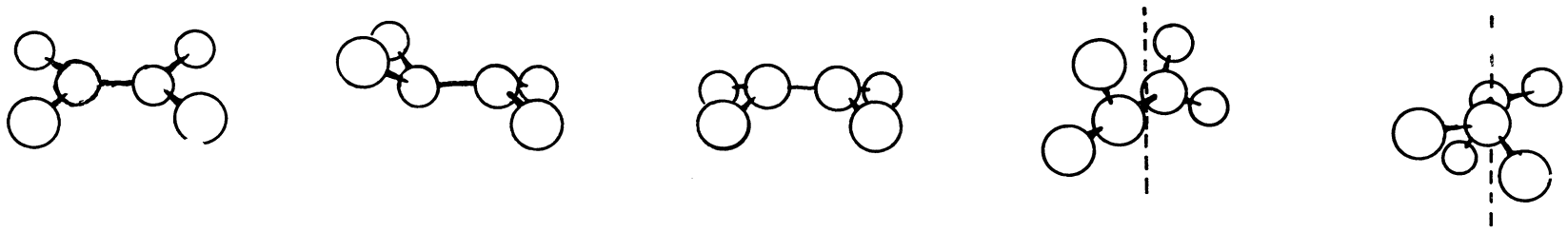

Symmetry Modes of Vibrational Spectra

IR	Raman	IR	Raman	IR	Raman	IR	Raman
1 B_{1u}	3 A_g	3 A_u	4 A_g	4 A_1	4 A_1	12 B	12 B
2 B_{2u}	2 B_{1g}	3 B_u	2 B_g	3 B_1	3 A_2		
2 B_{3u}	1 B_{2g}			2 B_2	3 B_1		
1 inactive A_u					2 B_2		

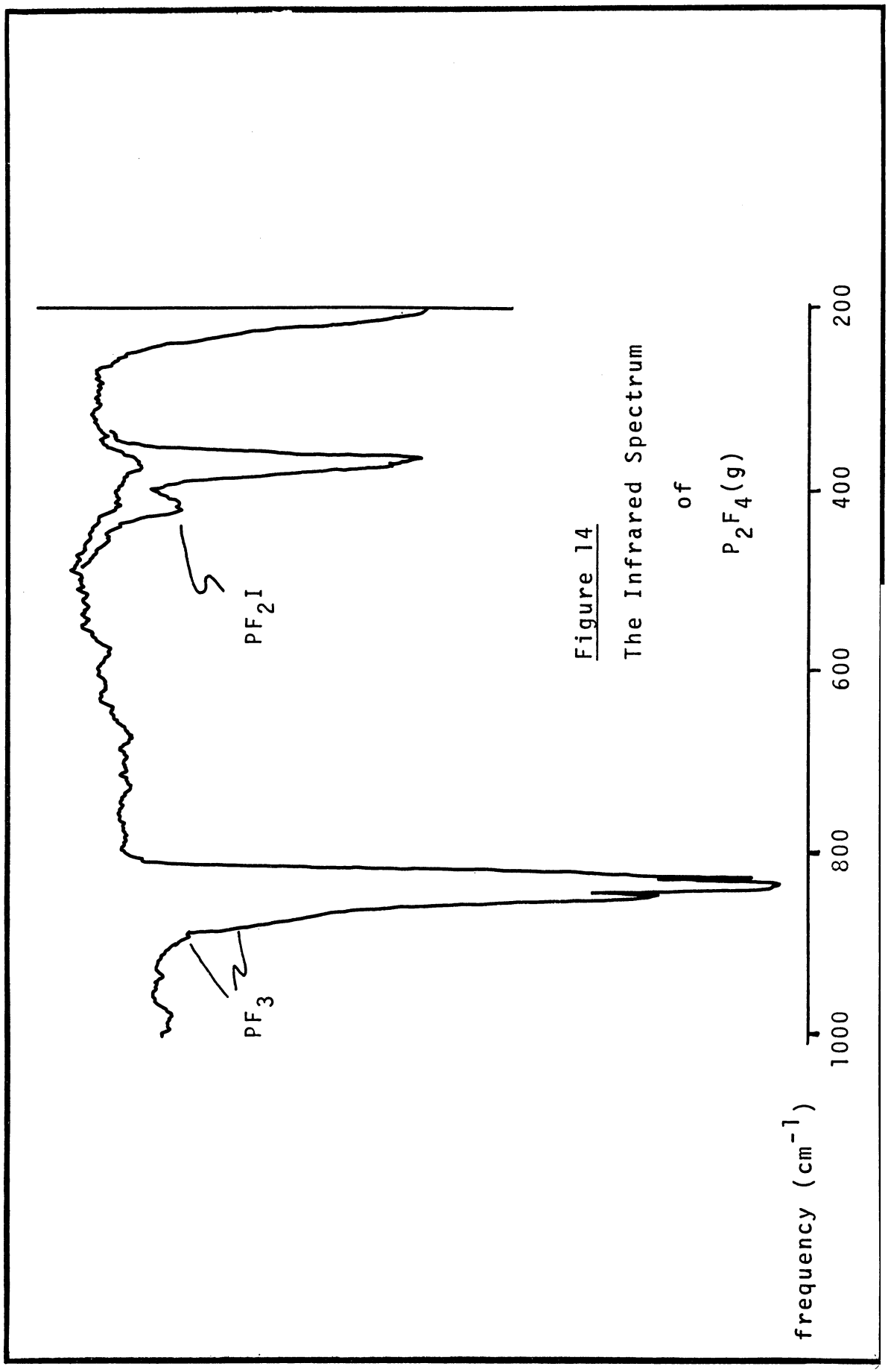

Figure 14

The Infrared Spectrum of $P_2F_4(g)$

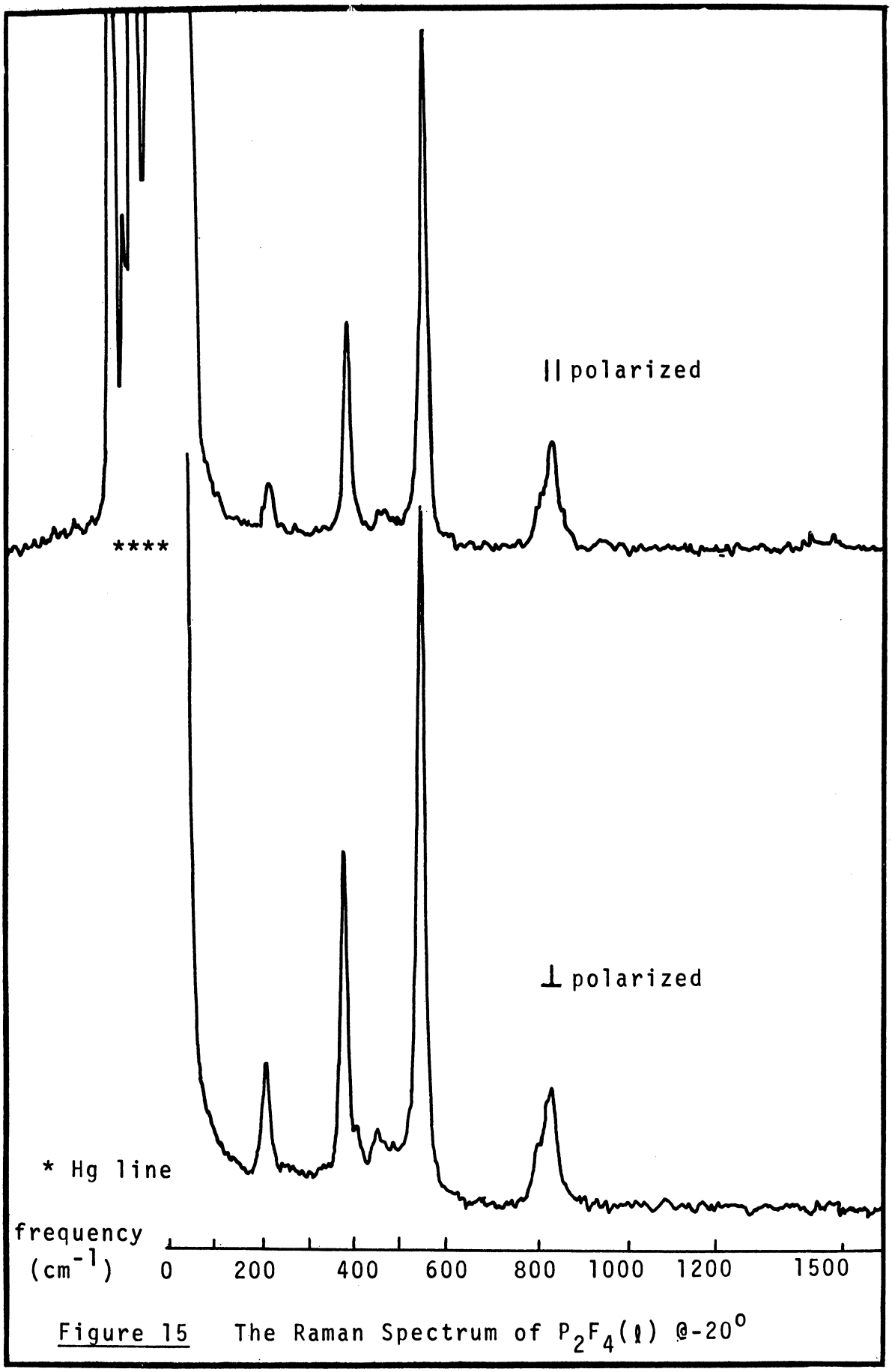

Figure 15 The Raman Spectrum of P_2F_4(ℓ) @-20°

Table 10

Vibrational Spectra of P_2F_4*

Infrared P_2F_4 (g) freq. (cm^{-1}) & intensity	note	assignment	Raman $P_2F_4(\ell)$ at -20° freq. (cm^{-1}) & intensity	note
		$\rho_s PF_2$	214 m	p
361 m		$\rho_{as} PF_2$		
365 m		$\delta_{as} PF_2$		
		$\delta_s PF_2$	377 s	p
378.7 vw	PF_2I	impurity		
		$2 \cdot \rho_s PF_2$	403 vw, sh	p
417.8 412.2 406.8 } vw	PF_2I	impurity		
		$\delta_{s-as} PF_2$?	453 w	dp?
		$\nu_s PP$	541 vs	p
		$\nu_{s-as} PF$	803 w, sh	dp?
827.8 vvs	P	$\nu_{as} PF$		
833.9 vvs	R			
		$\nu_s PF$	825 m	p?
839 vvs	P	$\nu_{as} PF$		
846.9 vvs	R			

* For an explanation of notation see Appendix A.

is probably an overtone, is evidence against the cis, gauche, and semi-eclipsed conformations as possible structures since all twelve vibrations should be active in these cases. Futhermore, the observation of a P-P stretching vibration at 541 cm^{-1} in the Raman and absence of the corresponding motion in the infrared spectrum would not be expected if the cis, gauche, or semi-eclipsed forms of P_2F_4 were correct. Finally, a consideration of the number and distribution of polarized Raman lines offers good evidence for the elimination of the planar form of P_2F_4 from further consideration. Although polarization is possible only in the case of totally symmetric lines, it is not always necessarily observed[66]. Since no polarization was apparent in the P-F stretching region, the totally symmetric P-F stretch must not display a polarization effect. In addition to a P-F stretch, two totally symmetric vibrations are expected for planar P_2F_4 and three for trans molecule. The observation of three <u>definitely</u> polarized lines in the Raman effect, well outside the P-F stretching region, therefore strongly indicates that the trans form represents the correct structure for P_2F_4.

Since N_2F_4 is known to yield NF_2 free radicals[67-69], it is of interest to investigate the epr spectrum of P_2F_4. A broad signal was indeed found for all the samples of P_2F_4 investigated (Figure 16). In the case of the single line observed for neat $P_2F_4(\ell)$ the g-value was determined

Figure 16

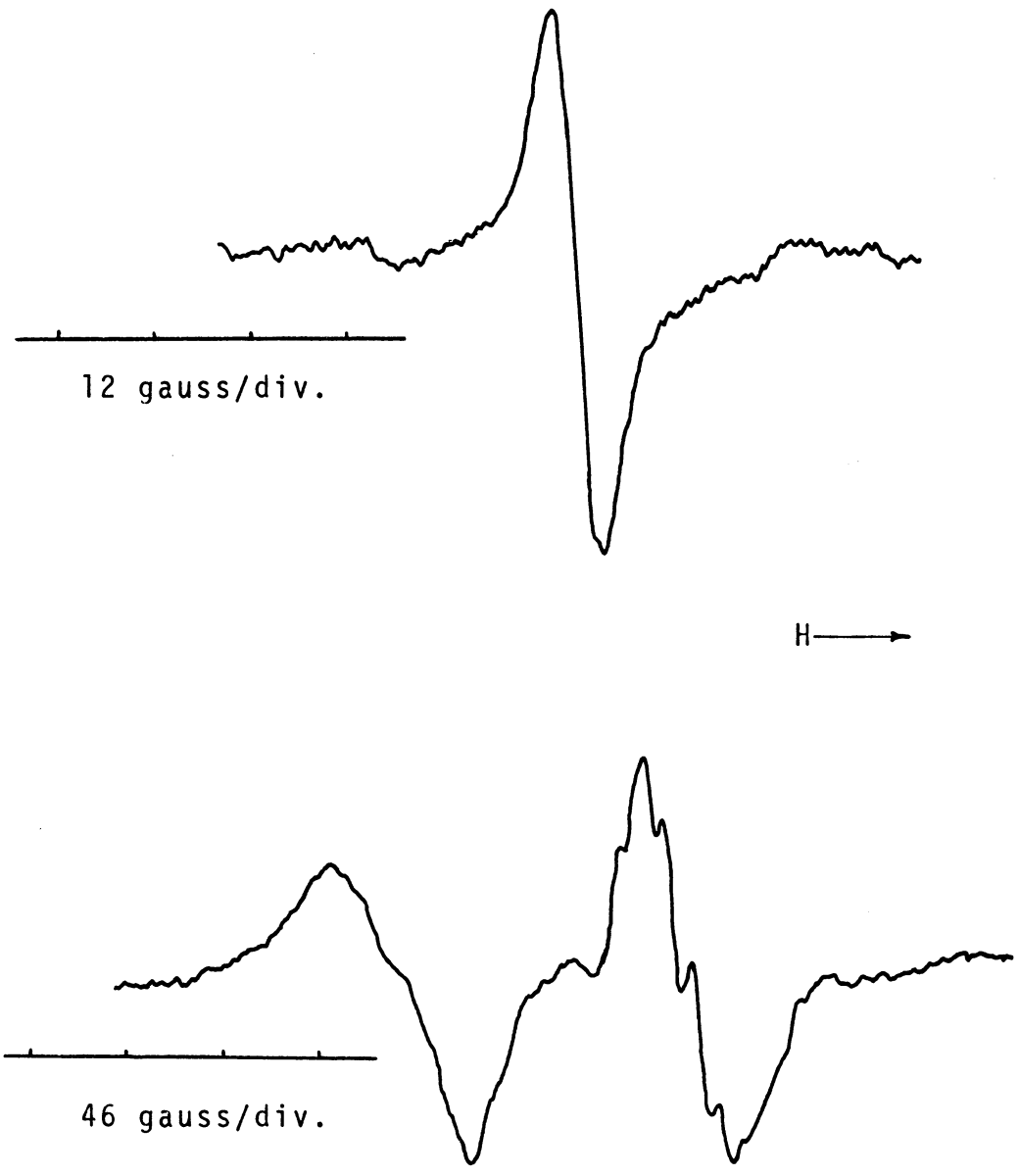
A. EPR Spectrum of P_2F_4(ℓ) @ 20°
12 gauss/div.
H
46 gauss/div.
B. EPR Spectrum of P_2F_4(g) or P_2F_4 in CCl_4 @ 20°

to be 2.00129(Figure 16A). More complex spectra were observed for neat P_2F_4(g) and P_2F_4 in CCl_4; the spectra appeared to be the same for the gas and solution and fine structure was noted on the high-field line (Figure 16B). It should be noted that the signals observed for P_2F_4 were weak; because of the high sensitivity of the epr spectrometer, the observed signals may be due to impurities.

E. Characterization of Difluorophosphine, PHF_2.

The parent member of the difluorophosphine homologous series, PHF_2, was prepared by the "coupling-reaction" represented in the equation

$$PF_2I + HI + 2Hg \rightarrow PHF_2 + Hg_2I_2.$$

Nitrogen has been known to form haloamines for some time[70-72]. The literature also mentions the attempted characterization of halophosphines, but no real halophosphines were ever isolated[73,74]. Therefore, PHF_2 is the first fully characterized halophosphine. Recently, however, Blaser and Worms[75,76] reported the isolation of an halide of hypophosphorus acid; when hypophosphorus acid was dissolved in excess liquid HF at -78° and the solution then allowed to warm slowly to room temperature, they obtained PH_2F_3. From a similar reaction between HF and phosphorus acid they isolated PHF_4 which is not as stable as PH_2F_3 and decomposes at room temperature to give HF and PF_3, irreversibly. The recent Russian literature[77] also reports a new class of hydrogen-containing

aryl phosphorus fluorides which were isolated during attempts to prepare fluorophosphines from aryldichlorophosphines and potassium bifluoride:

$$ArPCl_2 + 2KHF_2 \rightarrow 2KCl + HF + ArPF_3H.$$

In contrast to difluoroamine, NHF_2, difluorophosphine never underwent violent disproportionation during the course of the present investigation. It is a stable, colorless gas which can be maintained at 25° and saturation pressure for 5 hr. with less that 5% decomposition. At lower pressures and temperatures it is even more stable.

Although some difficulty was encountered in obtaining a complete elemental analysis, the formula PHF_2 is supported unequivocally by other data such as the hydrogen analysis, the vapor density molecular weight, and the mass spectrum, which are shown in Table 11. The proton, fluorine, and phosphorus spectra (Figures 17, 18, and 19, respectively) alone unequivocally confirm the PHF_2 formula.

The vapor density molecular weight is consistent with that for the monomer PHF_2 and is confirmed by the mass spectrum (Table 11) which had no peaks at higher m/e values than 70 and displayed the fragmentation pattern anticipated for PHF_2.

The proton nmr spectrum (Figure 17) shows a doublet, due to P-H spin-spin coupling, with each member of the doublet split into a 1:2:1 triplet by spin-spin coupling

Table 11

Characterization

of

Difluorophosphine

A. Hydrogen analysis.

obsvd: 1.46 calcd for PHF_2: 1.43

B. Vapor density molecular weight.

obsvd: 70.8 g./mole calcd: 70.0 g./mole

C. Mass spectrum.

m/e	relative peak height	assignment
70	100.0	PHF_2^+
69	52.4	PF_2^+
51	84.3	PHF^+
50	27.5	PF^+
34.5	0.8	PF_2^{2+}
32	3.9	PH^+
31	16.0	P^+
25.5	1.0	PHF^{2+}
25	3.0	PF^{2+}
20	0.6	HF^+
19	4.6	F^+
16	1.2	PH^{2+}
16.5	2.3	P^{2+}

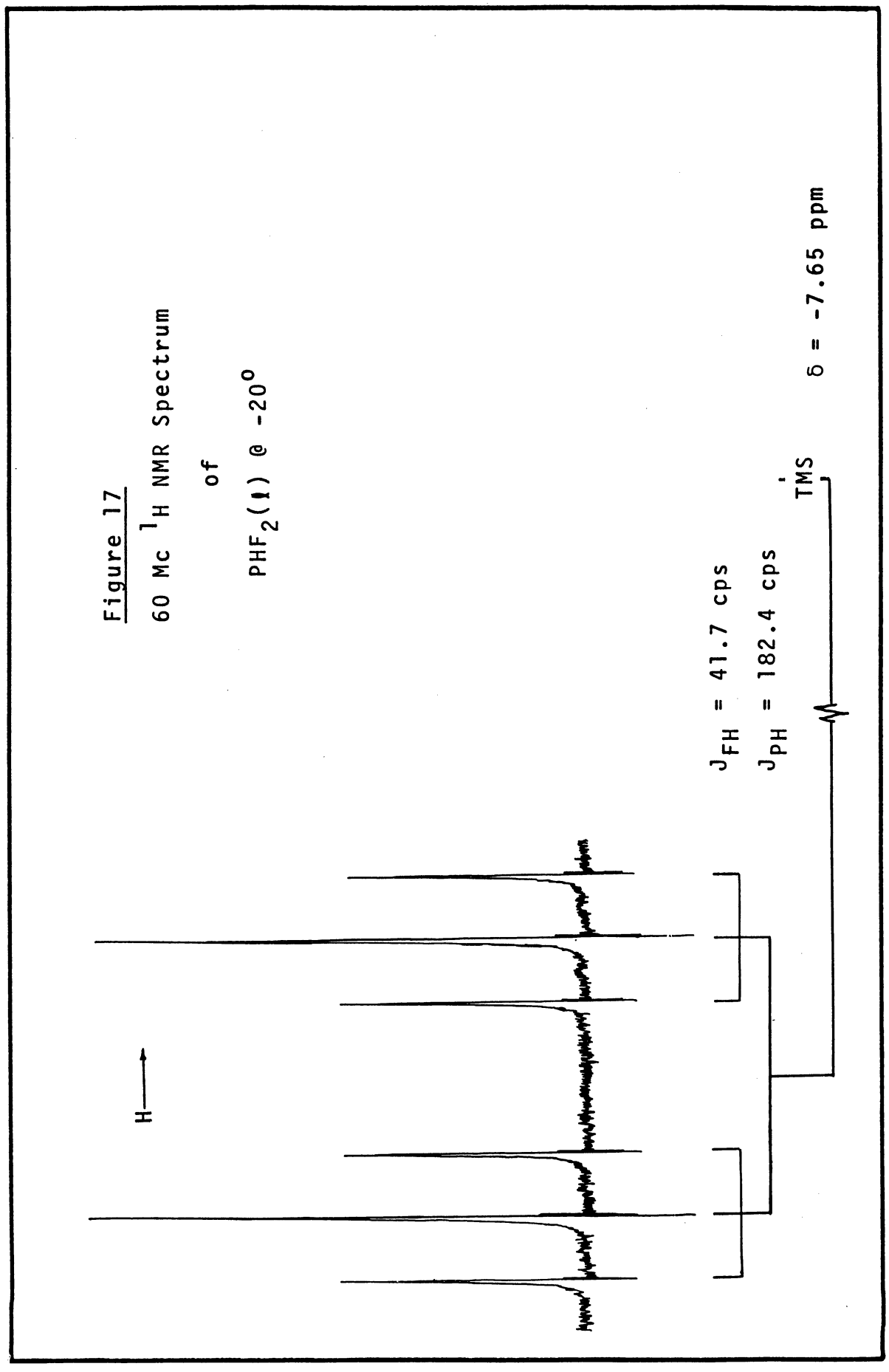
Figure 17
60 Mc ^{1}H NMR Spectrum
of
PHF_2(▮) @ -20°
H
J_{FH} = 41.7 cps
J_{PH} = 182.4 cps
TMS
δ = -7.65 ppm

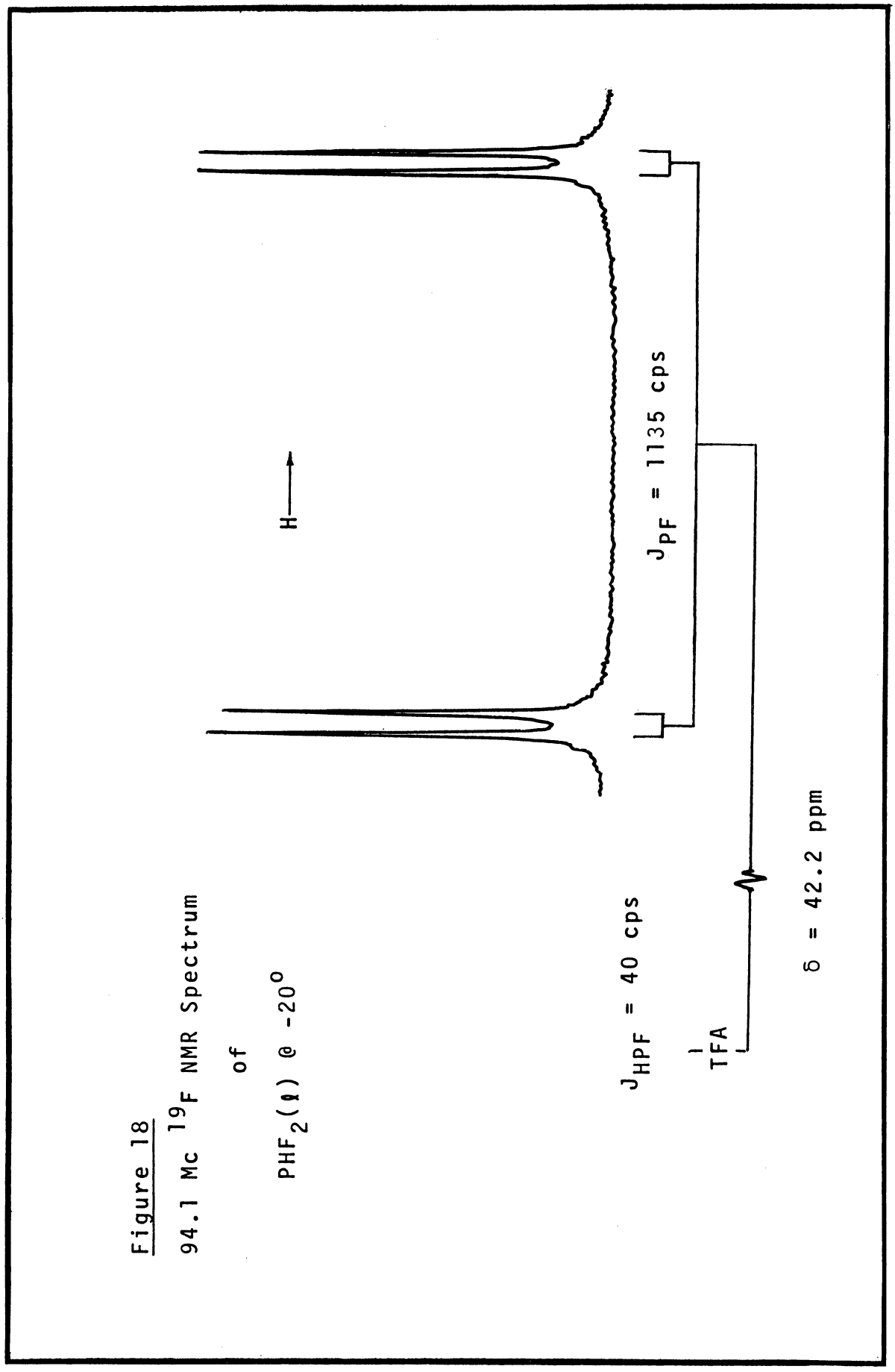

Figure 18

94.1 Mc ^{19}F NMR Spectrum

of

PHF_2(ℓ) @ -20°

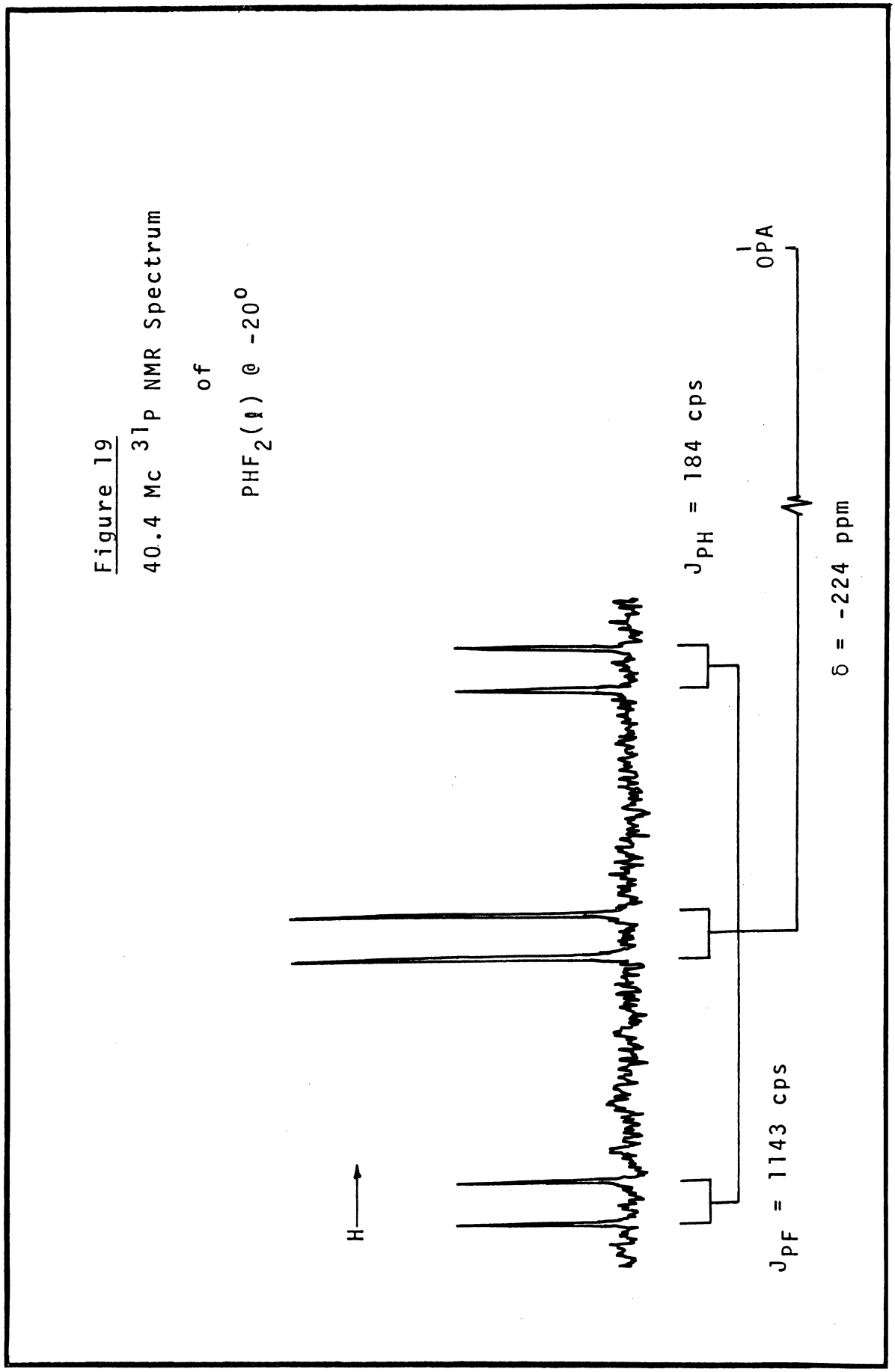

Figure 19

40.4 Mc ^{31}P NMR Spectrum

of

PHF_2(ℓ) @ -20°

of the hydrogen with two equivalent fluorine nuclei. The P-H coupling constant is 182.4 cps and the F-H coupling constant is 41.7 cps. The P-H coupling constant is discussed further below. The fluorine nmr signal (Figure 18) is also split into a doublet by coupling with a single phosphorus nucleus, and each member of the original doublet is again split into a doublet by coupling with the proton attached to phosphorus. The P-F coupling constant was determined to be 1135 cps. The J_{FH} value of 40 cps is consistent with the value of 41.7 cps found in the proton nmr spectrum. The fluorine nmr signal for PHF_2 occurs 42.2 ppm upfield from TFA. The phosphorus nmr spectrum (Figure 19) shows the expected 1:2:1 triplet (J_{PF} = 1143 cps) of doublets (J_{PH} = 184 cps) centered 224 ppm downfield from OPA.

It is interesting to compare the coupling constants derived from the nmr spectra of difluorophosphine with those of related compounds for which the molecular geometry is known as shown in Table 12. Examination of the

Table 12

Comparison of Coupling Constants and Geometry

	PHF_2	PH_3	PF_3	F_2PNMe_2
J_{PF}(cps)	1135	—	1441[51]	1194[42]
J_{PH}(cps)	182.4	182.2[65a]	—	—
∠ FPF	?	—	104°[52]	92.5°[79]
∠ XPH	?	93.3°[78]	—	—

table reveals that J_{PH} for phosphine and difluorophosphine are almost identical. Also, the J_{PF} value for difluorophosphine is closer to that found for dimethylaminodifluorophosphine than that found for trifluorophosphine. Since PH[80] and PF[51] coupling constants correlate qualitatively with molecular geometry, it would appear that PHF_2 is pyramidal with the P-substituent bond angles close to 90°. Stated in terms of the σ-bonding hybridization of phosphorus, difluorophosphine apparently exhibits p^3- hybridization with the lone-pair electrons on phosphorus having a high degree of "s-character".

The vapor pressure data for PHF_2, tabulated in Table 14, indicated that it is less volatile than either PH_3 or PF_3. A comparison of freezing points, boiling points, and Trouton constants for PHF_2, PH_3, and PF_3 as shown in Table 13, further substantiates the difference in volatility. Since difluorophosphine freezes and boils

Table 13

Comparison of Physical Properties

	b.p. (°C)	f.p. (°C)	Trouton Const. (cal./deg.mole)
PF_3[47]	-101.8	-151.5	23.1
PH_3[47]	-87.8	-133.8	18.8
PHF_2	-64.6	-124.2 to -123.6	24.7

Table 14

Physical Constants for PHF_2

A. Vapor pressure data.

°C	mm (obsvd)	mm (calcd)
-129.4	2.7	2.8
-112.0	20.6	19.7
-100.9	56.4	55.5
-84.4	206.0	206.7
-78.5	308.2	313.7

B. Equation.

$$\log p(mm) = \frac{-1126}{T} + 8.280$$

C. Trouton constant

24.70 cal./deg. mole

b.p.(extrapolated)

-64.6°C

m.p.

-124.2 to -123.6°C

at higher temperatures than either PH_3 or PF_3, and likewise, displays a higher entropy of vaporization (Trouton constant), it would appear that difluorophosphine is associated in the condensed states. It is yet to be determined whether association occurs through a $\rangle P\text{-}F\text{---}H\text{---}P\langle$ or a $\rangle P\text{---}H\text{---}P\langle$ type interaction. The difference in the proton chemical shifts for liquid PHF_2 (-7.65 ppm) and gaseous PHF_2(-1.3 ppm)* seems to corroborate the presence of association in the liquid[77]. The corresponding difference in the chemical shifts of liquid PH_3 (-1.76 ppm) and gaseous PH_3 (-1.3 ppm)[78] is even smaller. The larger difference for PHF_2 probably points to a stronger association in liquid PHF_2 than is present in liquid PH_3. This implies that the P-H linkage is less protonic in PH_3 than in PHF_2.

The infrared spectrum of gaseous PHF_2 (Figure 20) shows the six fundamentals expected for either the planar (C_{2v} symmetry) or the pyramidal (C_s symmetry) PHF_2 molecule. Examination of the spectrum, however, reveals that several of the absorption bands have definite shapes

---

* While discussing chemical shift of PHF_2 vapor, it should be noted that the spectrum was very different from that of the liquid. It was very complex and the exact nature of the spectrum was difficult to determine since the low proton concentration presented difficulties with saturation of the signal by the radiofrequency field. Nevertheless, the center of the multiplet was determined to be 1.3 ppm downfield from TMS (internal), and when cooled and liquified, the sample displayed the simple doublet of triplets observed previously for $PHF_2(\ell)$.

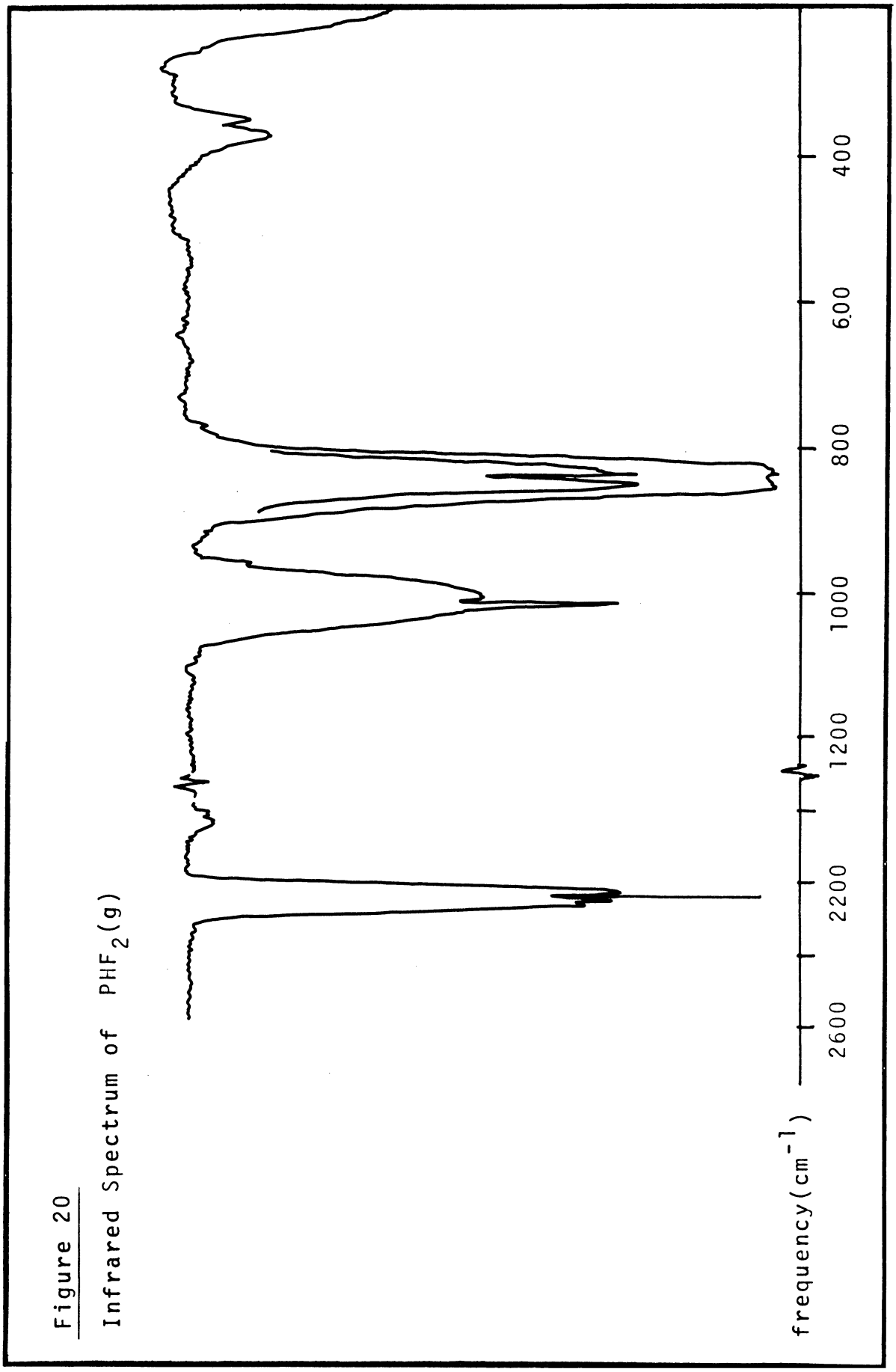

Figure 20

Infrared Spectrum of $PHF_2(g)$

characteristic of vibration-rotation interaction. These band-outlines were used as an aid in making tentative vibrational assignments (Table 15). Since the P-H stretching motion and F-P-F deformation motion are separated from other absorptions which might complicate the interpretation of their band-outlines, their band-outlines were compared with those predicted for the planar or pyramidal geometries for PHF_2. The analysis, which is discussed in detail an Appendix B, is consistent with a pyramidal geometry for PHF_2 and inconsistent with a planar configuration, thus confirming the same conclusion drawn from the nmr coupling constants observed for liquid PHF_2.

When compared with the P-H stretching frequencies of phosphine ($\nu_s PH$ = 2327, $\nu_{as} PH$ = 2421 cm^{-1})[83], the P-H stretching frequency observed for difluorophosphine (2240.5 cm^{-1}) indicated that the P-H bond is probably more labile in difluorophosphine.

The infrared spectrum of solid PHF_2 was also determined and is displayed in Figure 21. The tentative vibrational assignments for both solid and gaseous PHF_2 are given in Table 15. When comparing the infrared spectra of solid and gaseous difluorophosphine, it is interesting to note the pronounced shift of the P-H stretching motion to a higher frequency in the solid, contrary to what would be expected if hydrogen bonding occurred in the solid. The lowering of the P-F stretching

Table 15

Infrared Spectra* of PHF_2

PHF_2(g) freq. (cm^{-1}) & intensity		note	assignment	PHF_2(s) freq. (cm^{-1}) & intensity		note
2251	s	R, br				
2240.5	vs	Q	$\nu_s PH$	2317.0	vs	
2233	s	P, br				
1015.7	vs		$\delta_s PH$	1008.5	vs	
			?	980	w	
1008	s	br	$\omega_{as} PH$	968.0	s	
957.7	vw		?			
838.3	vs		$\nu_{as} PF$	825.7	s	
851.4	vvs	R	$\nu_s PF$	794	m	sh
825.3	vvs	P		782.8	vvs	br
367	w	R, br	$\delta_s FPF$	371.3	vs	
348	w	P, br				

* For an explanation of notation see Appendix A.

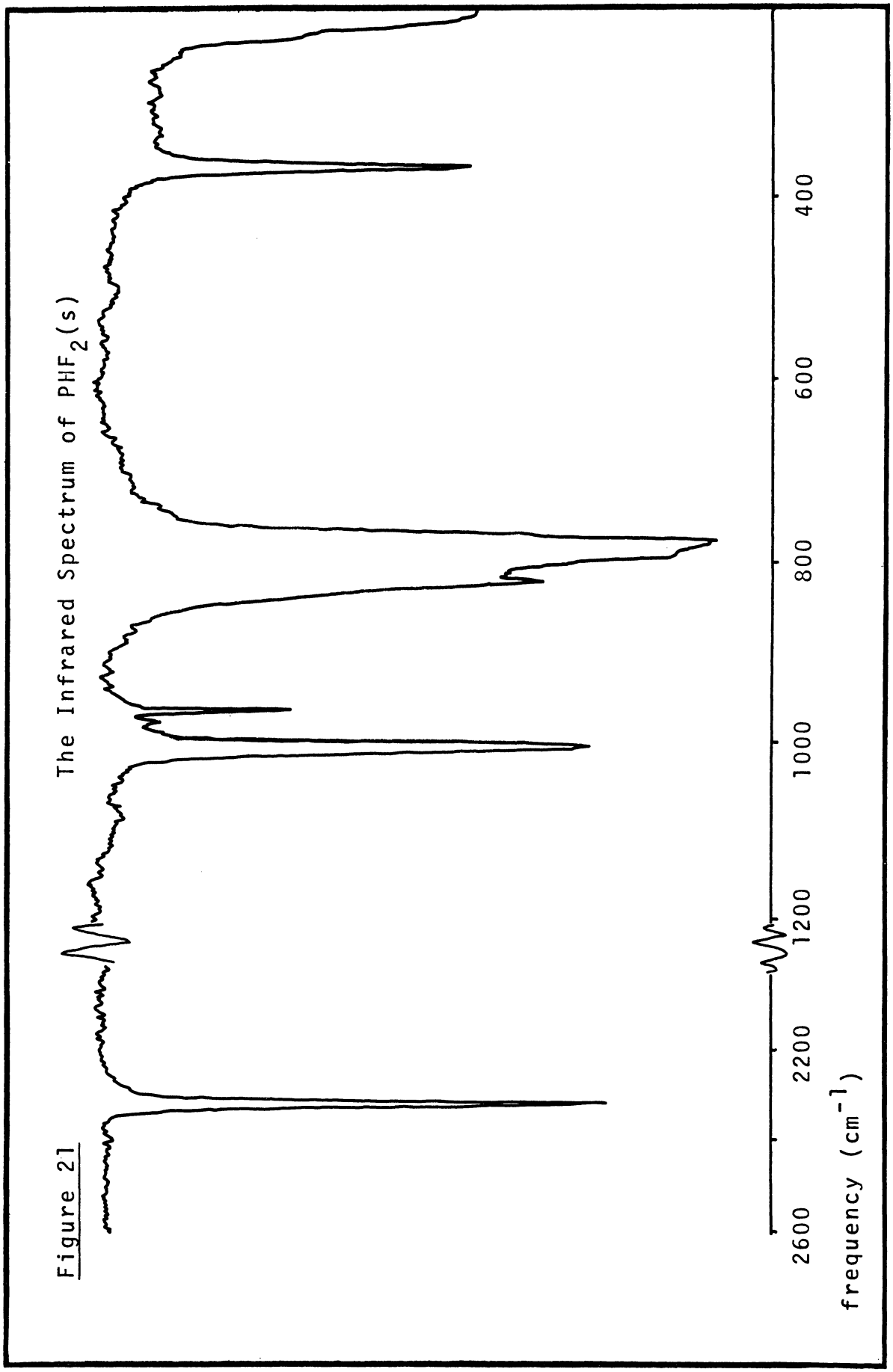
The Infrared Spectrum of PHF_2(s)
2600
2200
1200
1000
800
600
400
frequency (cm^{-1})

Figure 21

frequencies in the solid is probably indicative of interaction through the fluorine atoms resulting in a diminution of the inductive effect of fluorine and a concomitant strengthening of the P-H bond so that the P-H stretching frequency approaches that usually observed in phosphines.

Some physical properties relating to the N-H and P-H bonds of NHF_2 and PHF_2 are similar when compared to those of NH_3 and PH_3. The proton nmr chemical shift (δ = ca. -7.4 ppm)* and N-H stretching (νNH = 3193 cm^{-1})(84) observed for difluoroamine are shifted relative to ammonia [δ = -4.8 ppm(85); ν_sNH = 3336, 3338, ν_{as}NH = 3414 cm^{-1}(86)] in the same manner as the corresponding values for difluorophosphine are shifted relative to phosphine. It will be interesting to observe how the chemistry of the N-H and P-H bonds in difluoroamine and difluorophosphine parallel one another.

III. Some Chemistry of the New Difluorophosphines.

A. General.

The reactions of only two of the newly prepared difluorophosphines have been studied very extensively - they are difluoroiodophosphine and difluorophosphine.

It was suspected that the P-I bond in PF_2I would prove labile enough to be cleaved selectively, and

---

* The nmr data for NHF_2 are very qualitative; however, from the data Kennedy and Colburn(70) it is estimated that δ = approximately the shift of benzene = -7.4 ppm (TMS std.).

therefore, PF_2I would be a useful and reactive intermediate with which one could introduce the difluorophosphino-moiety into new molecules. As mentioned previously, difluorophosphine indeed has been used for the preparation of a number of interesting new ligands. Since the preparative methods involving PF_2I are adequately discussed in previous sections, and since the chemistry of PF_2I was investigated only for its synthetic utility, further discussion is not warranted.

The reactions of the "parent-difluorophosphine", PHF_2, have been investigated in somewhat more detail. Difluorophosphine has been found to undergo reactions which may be classified as 1) Solvolysis, 2) Adduct Formation, and 3) Base Displacement. The latter type-reactions are discussed below and some new species are briefly characterized.

B. Solvolysis of Difluorophosphine.

1) Hydrolysis. The hydrolysis of PHF_2 in 40% NaOH at 100° was found to yield nearly one mole of H_2 for every mole of PHF_2 taken. Initially, it was thought that the equation might be

$$PHF_2 + H_2O \rightarrow PF_2(OH) + H_2,$$

however, P-F bonds are known to be cleaved readily in alkaline solution[35], and no doubt a more likely reaction is

$$PHF_2 + 2NaOH + H_2O \rightarrow P(OH)_3 + H_2 + 2NaF.$$

Although the evolution of hydrogen in basic solution can be characteristic of hydridic M-H linkages as in the silanes[87], it is felt that the P-H bond in difluorophosphine is protonic. If the P-H hydrogen in PHF_2 is hydridic, deuterium should be observed in the hydrogen collected after hydrolysis of PDF_2. When the basic hydrolysis was conducted with a mixture of PHF_2 and PDF_2, a mass-spectral analysis of the liberated hydrogen indicated that no deuterium was present. Thus the hydrolysis of difluorophosphine is felt to proceed with retention of the P-H bond according to the following scheme:

$$PHF_2 + 2NaOH \rightarrow HP(OH)_2 + 2NaF$$

$$\downarrow H_2O$$

$$\overset{O}{HP(OH)_2} + H_2.$$

The latter scheme demonstrates that the phosphorus in PHF_2 is formally in the +1 oxidation state and that the H_2 results from the oxidation of $HP(OH)_2$ by water, not from the attack of H_2O on a hydridic P-H bond.

When excess difluorophosphine is treated with water vapor, a different hydrolysis occurs as indicated by the isolation of SiF_4. This hydrolysis might be

$$PHF_2 + H_2O \rightarrow HP(OH)_2 \cdot 2HF,$$

followed by HF + (glass walls of tube) $\rightarrow SiF_4$. Such a secondary scheme may account for the non-quantitative recovery of H_2 from the basic hydrolysis of PHF_2.

2) Aminolysis. Since F_2PNMe_2 and $FP(NMe_2)_2$ can be prepared from PF_3 and $HNMe_2$ by aminolysis[42], it was felt that analogous reactions with difluorophosphine might proceed as shown

$$2HPF_2 + 3HNMe_2 \rightarrow 2FHPNMe_2 + Me_2NH\cdot 2HF$$

$$HPF_2 + 3HNMe_2 \rightarrow HP(NMe_2)_2 + Me_2NH\cdot 2HF.$$

When equal amounts of $HNMe_2$ and PHF_2 were mixed as gases, a cloud of white solids did form and an unstable, volatile species which may have been $FHPNMe_2$ was isolated. The infrared of the latter species (Figure 22B) is very similar to that of F_2PNMe_2 (Figure 22A) except that bands which can be ascribed to P-H stretching and deformation motions are present near 2240 and 930 cm^{-1}, respectively. Also, disregarding the peaks at 890 and 860 cm^{-1} which are due to PF_3, it can be seen that the peaks in the 900 - 650 cm^{-1} region are shifted somewhat relative to F_2PNMe_2. After removal of the PF_3, the remaining fraction was found to have a vapor density corresponding to a molecular weight of 94 g./mole (theory for $FHPNMe_2$ = 95 g./mole).

Treatment of PHF_2 with larger amounts of dimethylamine ($HNMe_2/PHF_2$ = 2:1, 4:1) led to an even different product, perhaps $HP(NMe_2)_2$. As can be seen from the IR-spectrum shown in Figure 22C, there is no evidence for a P-F bond in the latter species but P-H stretching and deformation motions are evident around 2250 and 930 cm^{-1}. However, the supposed $HP(NMe_2)_2$ decomposed fairly rapidly to $HNMe_2$ and brown, oily solids; the highest

Figure 22 Infrared Spectra

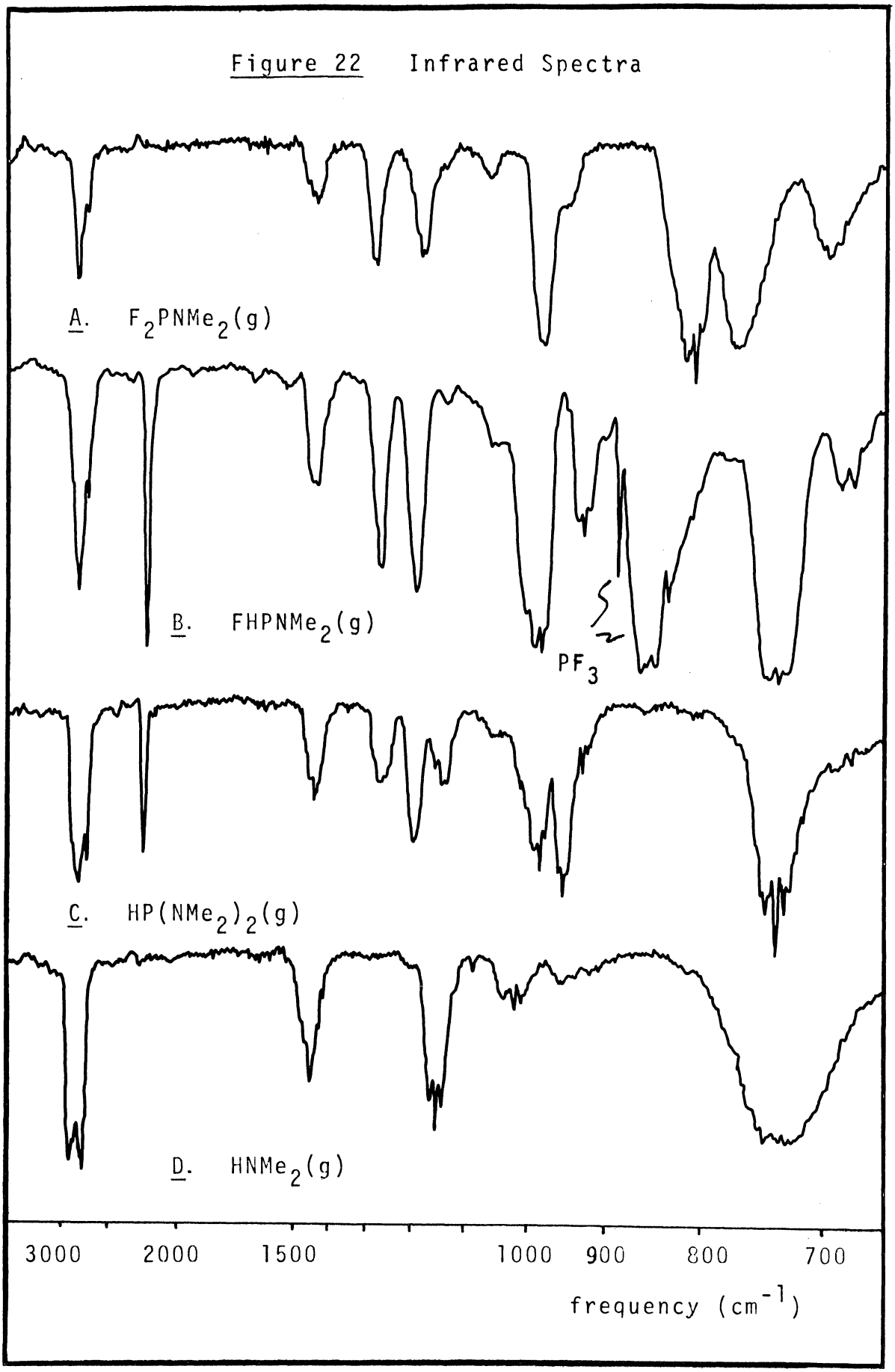

observed molecular weight was 96 g./mole (calcd. for $HP(NMe_2)_2$ = 120 g./mole), but as can be seen by comparing the IR of $HNMe_2$ (Figure 22D) with that for the molecular weight sample (Figure 22C), some dimethylamine was probably present in the $HP(NMe_2)_2$. Since in the case of both $FHPNMe_2$ and $HP(NMe_2)_2$ the supposed species readily decomposed to brown, oily, intractable solids and $HNMe_2$, they were not studied further. The liberation of dimethylamine may indicate that either an intra- or intermolecular hydrogen transfer from the phosphours to the dimethylamino-substituent promotes the decomposition. Since Nöth and Vetter[26] have found $(Me_2N)_2PH \cdot BH_3$ to be reasonably stable, perhaps diborane could be used to remove $FHPNMe_2$ and $HP(NMe_2)_2$, in the form of their respective borane adducts, from the systems mentioned above.

C. PHF_2·Lewis-Acid Adduct Formation.

1) Reaction of HI and PHF_2. In addition to the desired product, an unstable species believed to be $PF_2H \cdot HI$ was isolated during the preparation of difluorophosphine. The latter hydrogen iodide adduct of PHF_2 was characterized by its chemical and physical similarity to an equimolar mixture of HI and PHF_2. A mass-balance of products and reactants was consistent with the formula $PF_2H \cdot HI$ (see Experimental). When allowed to warm to room temperature the adduct apparently split out HF which reacted with the glass in the vacuum system to form SiF_4,

PF_3, and leave yellow, iodine-containing solids behind; the same behavior was noted for an equimolar mixture of PHF_2 and HI. Because of the aforementioned decomposition, it was difficult to obtain a vapor density or to compare the stability of $PF_2H \cdot HI$ with $PH_3 \cdot HI$. However, the infrared spectrum was obtained on a fast scan with the Perkin-Elmer 137 (Figure 23). The spectrum is markedly different from that of difluorophosphine and appears to confirm the presence of a volatile difluorophosphonium iodide "ion-pair", $(PH_2F_2)I$. If the difluorophosphonium ion is assumed to be tetrahedral (C_{2v} symmetry), eight IR-active bands would be expected for this moiety. Only six lines were observed in the spectrum of $PF_2H \cdot HI$, but the PF_2 deformation and rocking motions no doubt occur below the range of the instrument used. In addition to those lines assigned to the difluorophosphonium moiety, a number of very weak bands were noted in the 1500 - 1250 cm^{-1} region. The latter bands may be due to impurities or overtones and combinations, however, this region is characteristic of bridging-hydrogen atom motions which might be observed because of $\rangle P\text{-}H\text{-}I$ type-bonding. Perhaps the latter type of bridge bond would be more evident with a weaker acid like HCl. The observed IR-frequencies of $PF_2H \cdot HI$ and their tentative assignments are listed in Table 16.

Because of its instability, the mass spectrum of $PF_2H \cdot HI$ was difficult to obtain and often only SiF_4 and

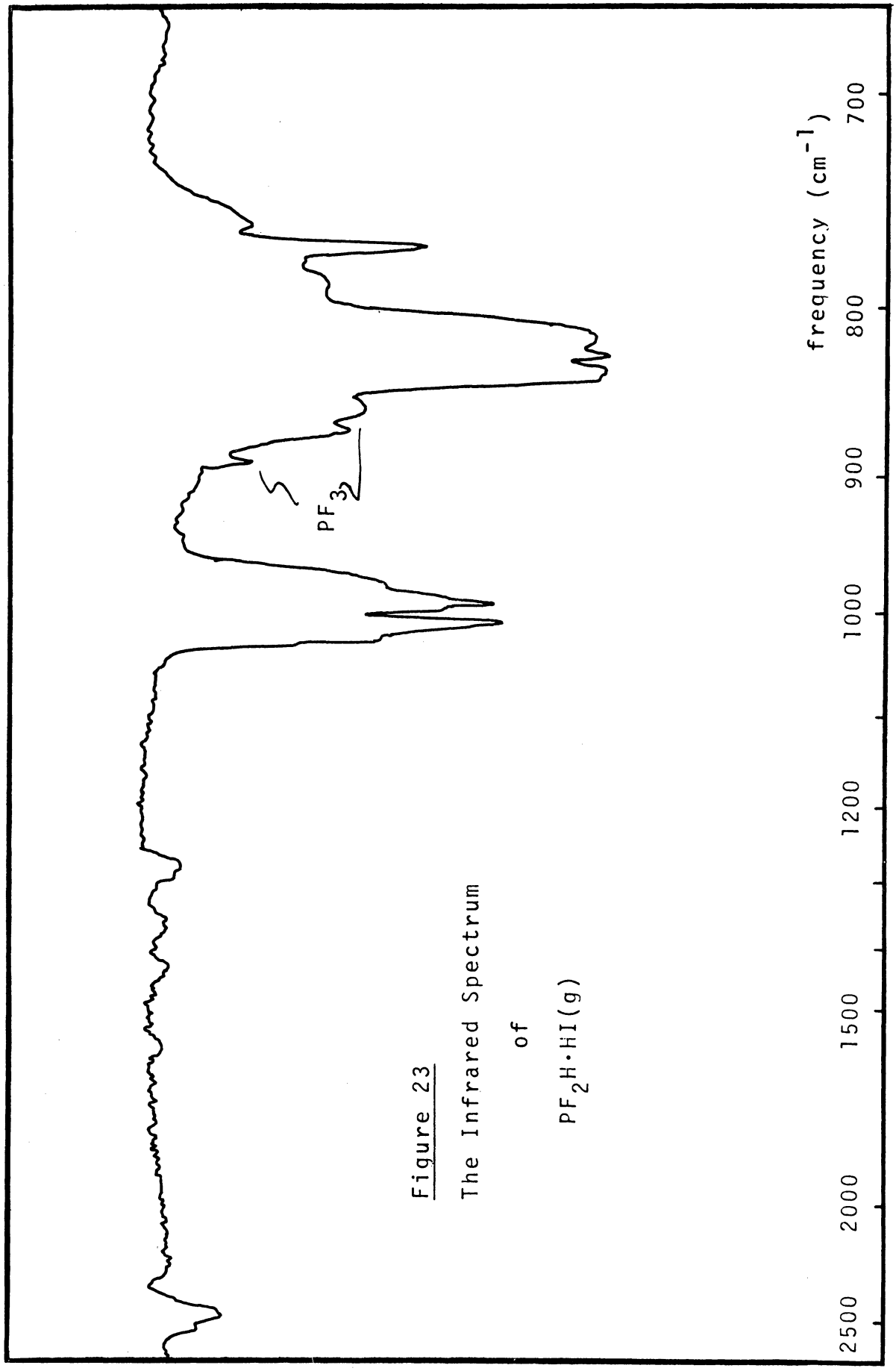

Figure 23

The Infrared Spectrum of $PF_2H \cdot HI(g)$

Table 16

Infrared Spectrum* of $PF_2H \cdot HI$

freq. (cm^{-1}) & intensity	note	tentative assignment
2551 w		$\nu_{as}PH$
2483 w		$\nu_{s}PH$
1450 vw		bridge
1375 vw		hydrogen
1300 vw		motions
1015 vs		$\delta_{s}HPH$
999 vs		ωHPH
980 m	sh	
890 w	PF_3	
865 m	impurity	
835 vvs	R	
825 vvs	Q	$\nu_{s}PF$
815 vvs	P	
785 w	R	
768 vs	Q	$\nu_{as}PF$
755 w	P	

* For an explanation of notion see Appendix A.

PF_3 were observed; however, a number of spectra did show very prominent peaks at m/e = 89, 71, 70, 69, 51, 50, 32, 31, 20, and 19 which may be assigned to PHF_3, PH_2F_2, PHF_2, PF_2, PHF, PF, PH, P, HF, and F unipositive ions, respectively. The m/e = 89 peak may result from the combination of HF and PF_2^+, but another prominent peak found at m/e = 76 cannot be explained unless perhaps it is due to F_4^+, which seems unlikely. The important feature of the mass spectrum, nevertheless, is the presence of peaks consistent with the $PH_2F_2^+$ ion.

2) Reaction of B_2H_6 and PHF_2. A very interesting adduct is formed in 82% yield when diborane and difluorophosphine are mixed as gases at 25°.

$$PHF_2 + \tfrac{1}{2}B_2H_6 \rightarrow PHF_2 \cdot BH_3$$

Pure difluorophosphine borane has been maintained for 22 hr. at 25° and a pressure of ca. 600 mm with no evidence for dissociation or decomposition, in stark contrast to $PH_3 \cdot BH_3$ and $PF_3 \cdot BH_3$ which are both highly dissociated under comparable conditions. The stable new borane adduct may also be prepared by displacement of PH_3 or PF_3 from their respective borane adducts; such base dispacement reactions are discussed completely in Section IV and in the Experimental.

Although classical methods were not used to obtain an elemental analysis, the formula $PHF_2 \cdot BH_3$ is supported unequivocally by other physical methods such as ^{19}F, ^{11}B, and ^1H nmr spectroscopy and mass spectroscopy.

The density of the vapor corresponds well with that expected for the monomer $PF_2H \cdot BH_3$ (Table 17). The mass spectrum (Table 17) displays no appreciable peaks at m/e-values higher than 84 and thus confirms the vapor density molecular weight, however, some features should be noted in the fragmentation pattern. The presence of peaks at m/e = 71, 52 might be due to $PF_2H_2^+$ and PFH_2^+ ions, respectively, which form by recombination of a proton and the appropriate fragment. Such recombination peaks are rather common in high-pressure mass spectroscopy[88] and have also been observed in conventional mass spectroscopy[89]. Peaks are displayed at m/e = 49, 48 which also might be attributed to recombination to form $^{11}BF_2$, $^{10}BF_2$, unipositive ions. The peak at m/e = 30 is better assigned to $^{10}BHF^+$ than to $^{11}BF^+$ since no peak appeared at m/e = 29 (^{10}BF). Other assignments appear straightforward but are not listed in Table 17 because of the multitude of isotopic permutations and combinations.

The vapor pressure data for difluorophosphine borane are compared with the values calculated from the vapor pressure equation (Table 18); the extrapolated boiling point and Trouton constant are also given.

Since the stability of $PF_2H \cdot BH_3$ appeared "anomolous" when compared to $PH_3 \cdot BH_3$ and $PF_3 \cdot BH_3$, it was thought that perhaps it might exhibit an unusual structure. The proton, boron, and fluorine nmr spectra of $PHF_2 \cdot BH_3$ are what might be termed "textbook examples" of first-order nmr spectra

Table 17

Characterization

of

Difluorophosphine Borane

A. Vapor density molecular weight.

obsvd: 83.9 g./mole calcd: 83.8 g./mole

B. Mass spectrum.

m/e	relative peak height	m/e	relative peak height
84	19.7	49	7.8
83	69.8	48	1.9
82	100.0	44	1.0
81	22.9	43	3.2
80	1.8	42	1.9
71	3.7	41	0.3
70	13.7	35	3.2
69	46.1	33	28.6
63	1.6	32	17.9
62	3.0	31	63.2
61	9.4	30	14.2
60	2.1	19	0.6
52	1.0	13	31.5
51	36.7	12	23.4
50	25.9		

Table 18

Physical Constants of $PHF_2 \cdot BH_3$

A. Vapor pressure data.

°C	mm (obsvd)	mm (calcd)
-78.5	5.2	4.9
-63.9	14.3	15.6
-45.6	53.4	54.3
-37.5	88.8	88.6
-36.5	96.4	93.9
-31.9	122.7	121.5
-23.6	191.8	190.4

B. Equation.

$$\log p(\text{mm}) = \frac{-1407}{T} + 7.917$$

C. Trouton constant	b.p. (extrapolated)
23.04 cal./deg. mole	6.2°C

and show unquestionably that difluorophosphine borane is characteristic of the usual BH_3 adduct with a normal P-B bond; the nmr spectra provide no evidence for structures such as

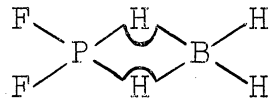

, $[F_2P][BH_4]$, or $[F_2PH_2][BH_2]$.

The proton nmr spectrum of difluorophosphine borane is indicative of two hydrogen environments in the molecule. The basic spectrum consists of a 1:1:1:1 quartet and a doublet of 1:2:1 triplets centered 0.78 and 7.68 ppm downfield from TMS, respectively (Figure 24). The quartet (J_{BH} = 103 cps) is attributed to the borane hydrogen atoms which are split by the ^{11}B nucleus ($I = \frac{3}{2}$). Each member of the borane quartet exhibits further splitting as shown in Figure 25. The spin-spin splitting pattern in the latter figure can be attributed to coupling of the borane-hydrogens with the two equivalent ^{19}F nuclei ($I = \frac{1}{2}$) to give a 1:2:1 triplet (J_{FPBH} = 26.0 cps). Each member of the triplet is split further into a doublet of doublets by interaction of the borane hydrogens with phosphorus ($I = \frac{1}{2}$) and the <u>single</u> phosphine hydrogen; the respective coupling constants are J_{PBH} = 17.5 cps and J_{HPBH} = 4.0 cps.

The doublet of triplets in the proton nmr spectrum of $PHF_2 \cdot BH_3$ (Figure 25) is assigned to the phosphine hydrogen (J_{PH} = 467 cps), the basic phosphine doublet being split into a 1:2:1 triplet by the two equivalent

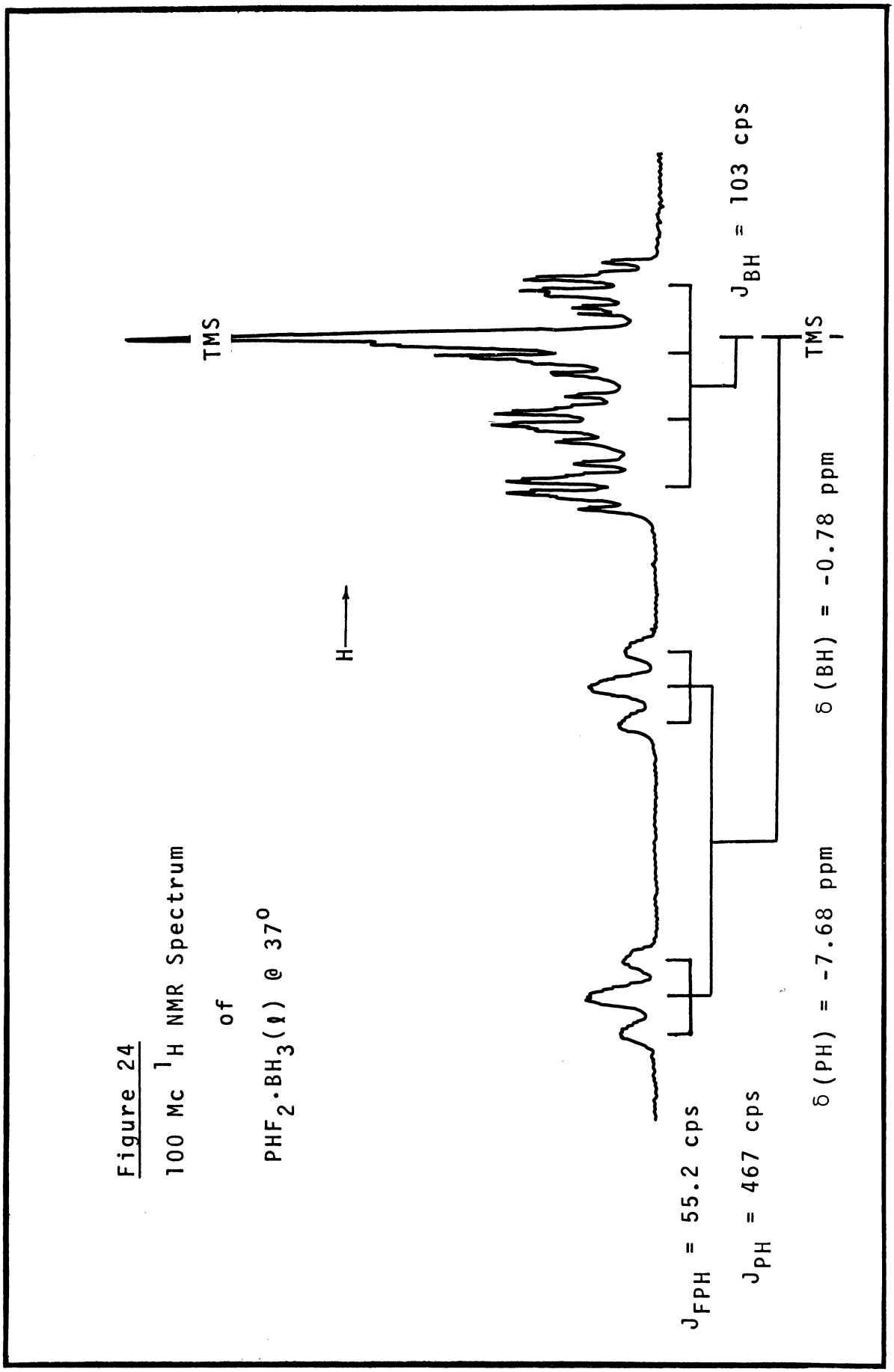

Figure 24

100 Mc ^1H NMR Spectrum

of

$PHF_2 \cdot BH_3$ (ℓ) @ 37°

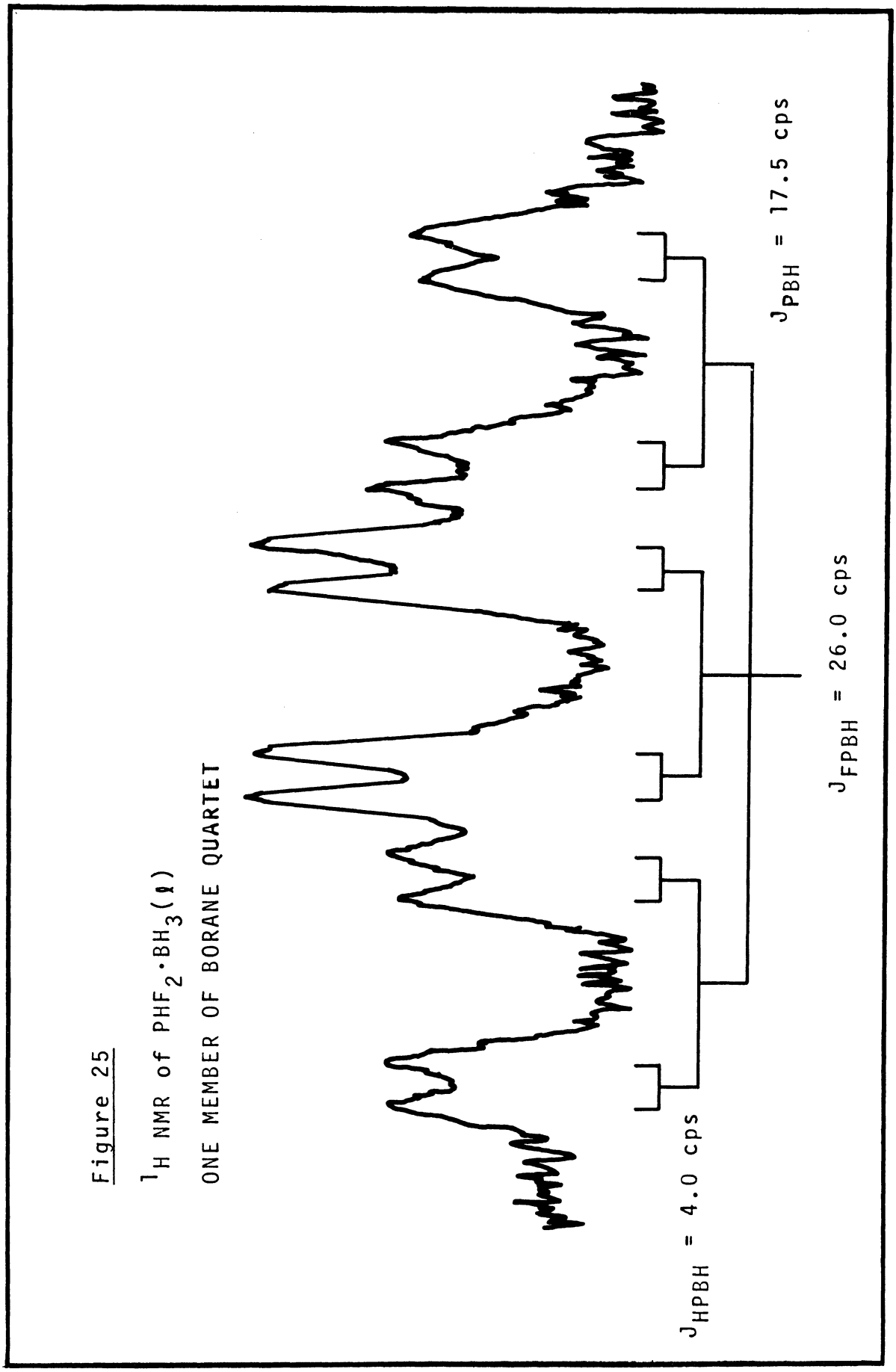

Figure 25

^1H NMR of $PHF_2 \cdot BH_3$ (ℓ)

ONE MEMBER OF BORANE QUARTET

fluorine nuclei (J_{FPH} = 55.2 cps). Careful examination of the 1:2:1 triplet (Figure 26) shows that each component consists of a 1:3:4:4:4:4:4:3:1 ten-line multiplet. This multiplet can be attributed to coupling of the phosphine hydrogen atom with the ^{11}B nucleus to give a 1:1:1:1 quartet (J_{BPH} = 8.0 cps) each component of which is further split into a 1:3:3:1 quartet by spin-spin interaction with the three equivalent borane hydrogens (J_{HPBH} = 4.0 cps); the latter signals overlap to give the observed ten-line multiplet.

The ratio of borane hydrogen to phosphine hydrogen ^1H nmr signals was 3:1 for $PHF_2 \cdot BH_3$.

A 1:3:3:1 quartet of doublets is displayed 60.4 ppm upfield from TMB in the ^{11}B nmr spectrum of $PHF_2 \cdot BH_3$ (Figure 27). The quartet pattern conclusively demonstrates the presence of the BH_3 moiety in the molecule. Other boron hydride fragments might display a 1:1:1:1 quartet in the proton nmr spectrum, but only a borane nucleus bonded to three equivalent hydrogens would be expected to display the observed 1:3:3:1 quartet (J_{HB} = 102 cps) in the ^{11}B spectrum. The doublet splitting of each member of the quartet is attributed to the directly bonded ^{31}P nucleus (J_{PB} = 48.6 cps).

The basic ^{19}F nmr spectrum consists of a doublet centered 21.5 ppm downfield from TFA (Figure 28). The doublet is indicative of spin-spin interaction of the fluorine nuclei with the directly bonded phosphorus

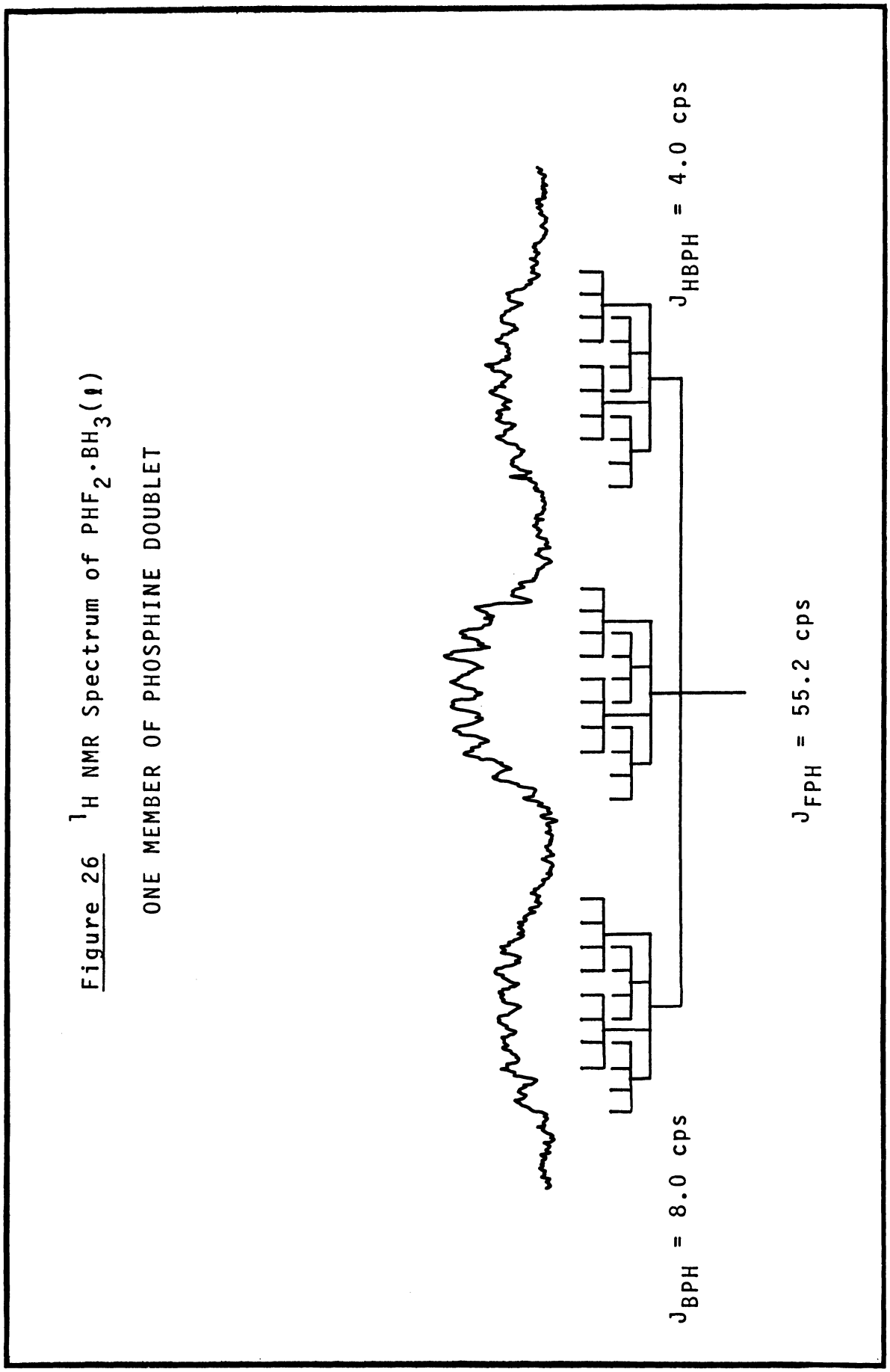

Figure 26 ^1H NMR Spectrum of $PHF_2 \cdot BH_3$ (I)

ONE MEMBER OF PHOSPHINE DOUBLET

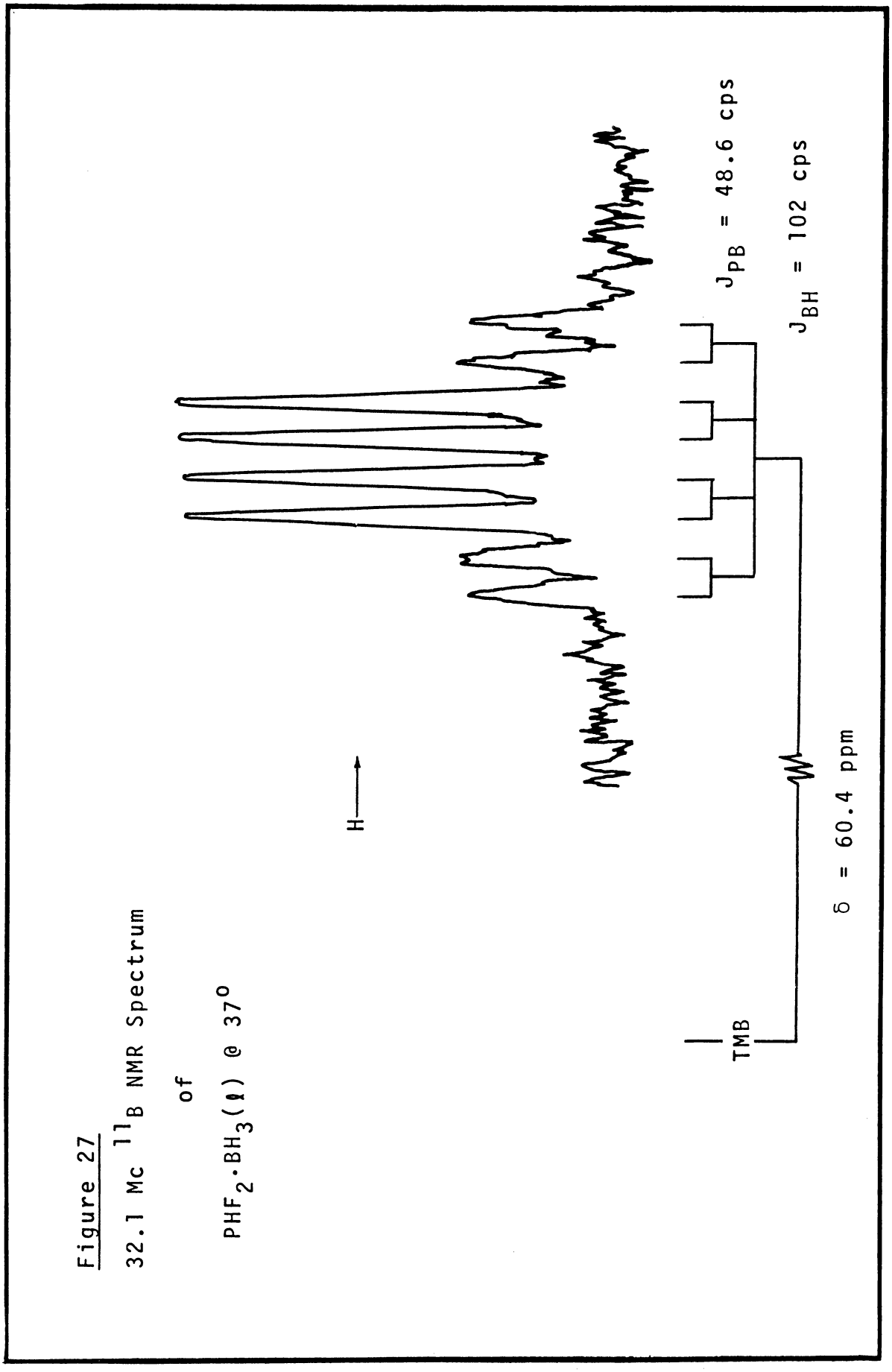

Figure 27

32.1 Mc ^{11}B NMR Spectrum

of

$PHF_2 \cdot BH_3$(ℓ) @ 37°

Figure 28

94.1 Mc ^{19}F NMR Spectrum of $PHF_2 \cdot BH_3$(ℓ) @ 37°

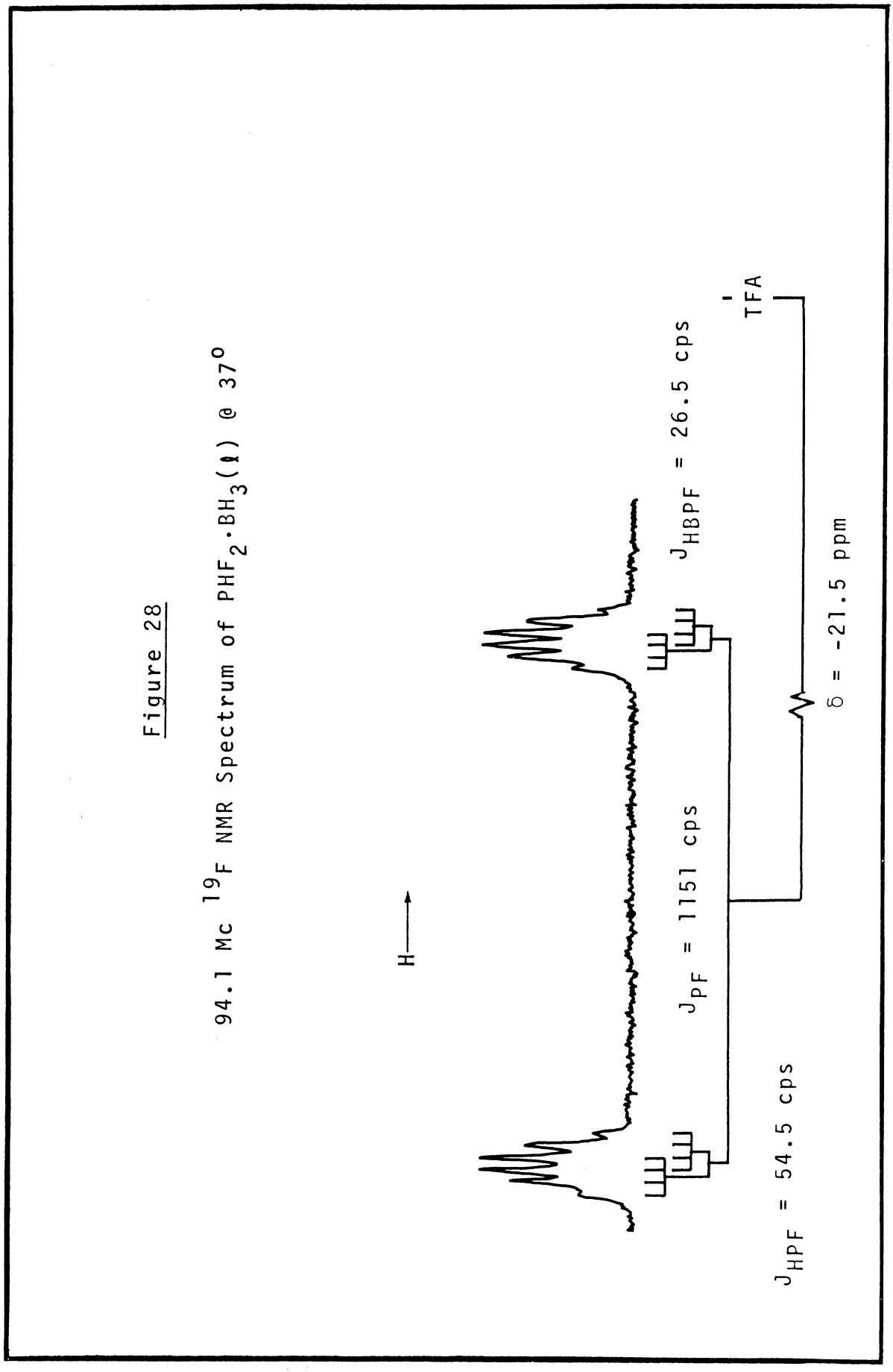

(J_{PF} = 1151 cps). Each member of the doublet consists of a 1:3:4:4:3:1 sextet which can be attributed to the overlap of a doublet of 1:3:3:1 quartets. The latter doublet splitting (J_{HPF} = 54.5 cps) is due to the phosphine hydrogen, and the 1:3:3:1 quartet to the three equivalent borane hydrogens (J_{HBPF} = 26.5 cps).

The coupling constants derived from the proton, boron, and fluorine nmr spectra are compared in Table 19 where it can be seen that they agree within experimental error. Some of these coupling constants are discussed further when the borane adducts of phosphine and trifluorophosphine are compared with difluorophosphine borane (Section IV).

Table 19

Coupling Constants for $PHF_2 \cdot BH_3$

	^1H nmr	^{11}B nmr	^{19}F nmr
J_{BH}	103	102	—
J_{FPBH}	26.0	—	26.5
J_{PBH}	17.5	—	—
J_{HPBH}	4.0	—	—
J_{PB}	—	48.6	—
J_{PF}	—	—	1151
J_{PH}	467	—	—
J_{FPH}	55.2	—	54.5
J_{BPH}	8.0	—	—

In summary, the nmr results show the structure of $PHF_2 \cdot BH_3$ to be

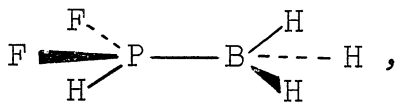

(Figure 29) Structure of $PHF_2 \cdot BH_3$

where free rotation exists about the P-B bond and averages out the molecular environments so that all the nmr spectra are easily interpretable with first-order spin-spin coupling rules; this case is similar to that observed by Shoolery[90] for $Me_2PH \cdot BH_3$.

The structure for $PHF_2 \cdot BH_3$ (Figure 29) deduced from nmr spectroscopy has C_s symmetry and should exhibit 18 IR-active fundamentals - six vibrational frequencies associated with each end of the molecule, considered as a free species with C_s symmetry, and six arising as a consequence of the P-B bond. Therefore, the PHF_2 and BH_3 moieties each contribute four symmetric and two asymmetric motions, while three symmetric and three asymmetric motions are due to the presence of a P-B bond; the eighteen fundamental vibrations and their associated symmetries are summarized in Table 20. Although accurate vibrational assignment is difficult without complimentary Raman data and isotopic substitution, under high resolution a number of bands could be associated with boron by the appearance of a higher frequency shoulder arising from the presence of natural abundance ^{10}B; tentative assignments and vibrational frequencies for gaseous $PHF_2 \cdot BH_3$ are listed in Table 21, and the spectrum is shown in Fig. 30

Table 20

Fundamental Vibrations* for $PHF_2 \cdot BH_3$

	Internal Motions of		Consequence of
	PHF_2	BH_3	P-B bond
A' class	$\nu_s PH$ (ν_5)	$\nu_s BH_3$ (ν_1)	νPB (ν_7)
	$\nu_s PF_2$ (ν_8)	$\nu_{s\text{-}as} BH_3$ (ν_2)	ρBH_3 (ν_{10})
	$\delta_s PH$ (ν_6)	$\delta_s BH_3$ (ν_3)	ρPF_2 (ν_{11})
	$\delta_s FPF$ (ν_9)	$\delta_s HBH$ (ν_4)	
A'' class	$\nu_{as} PF_2$ (ν_{15})	$\nu_{as} BH_3$ (ν_{12})	τPB (ν_{16})
	ωPH (ν_{14})	ωBH (ν_{13})	ωBH_3 (ν_{17})
			ωPF_2 (ν_{18})

* For an explanation of notation see Appendix A.

Table 21

The Infrared Spectrum* of $PHF_2 \cdot BH_3$(g)

freq. (cm^{-1}) & intensity	note	assgn.
2475.5 m	^{10}B	ν_2, ν_{12}
2473.0 m	^{10}B	ν_1
2464.2 vs	^{11}B‡	ν_2, ν_{12}
2462.2 vs	^{11}B	ν_1
2440 m	R	ν_5
2423.7 vs	Q	
2422.3 vs	Q	
2406 m	P	
1120 w		ν_{13}
1035 m	R	ν_6
1031 w		ν_4
1026.9 m	^{10}B	ν_3
1023.2 vs	Q‡	ν_6
1021.8 m	^{11}B	ν_3
1013 m	P	ν_6
978.5 w		ν_{14}
921.1 vs	R	ν_{15}
912.8 vvs	Q	ν_{15}

freq. (cm^{-1}) & intensity	note	assgn.
904.5 vs		ν_8
903.0 vs	P	ν_{15}
820 vw		?
732.3 w	^{10}B	ν_{10}
729.7 w	^{10}B	ν_{17}
728.2 w		?
723.2 s	^{11}B	ν_{10}
720.8 s	^{11}B	ν_{17}
577 w	^{10}B	ν_7
567 w	^{11}B	ν_7
389.2 m		ν_{16}
379.8 m		ν_9
374.7 m		
230 w		ν_{18}
225 w		ν_{11}

* For an explanation of notation see Appendix A and Table 20.

‡ Appeared to be split under high resolution.

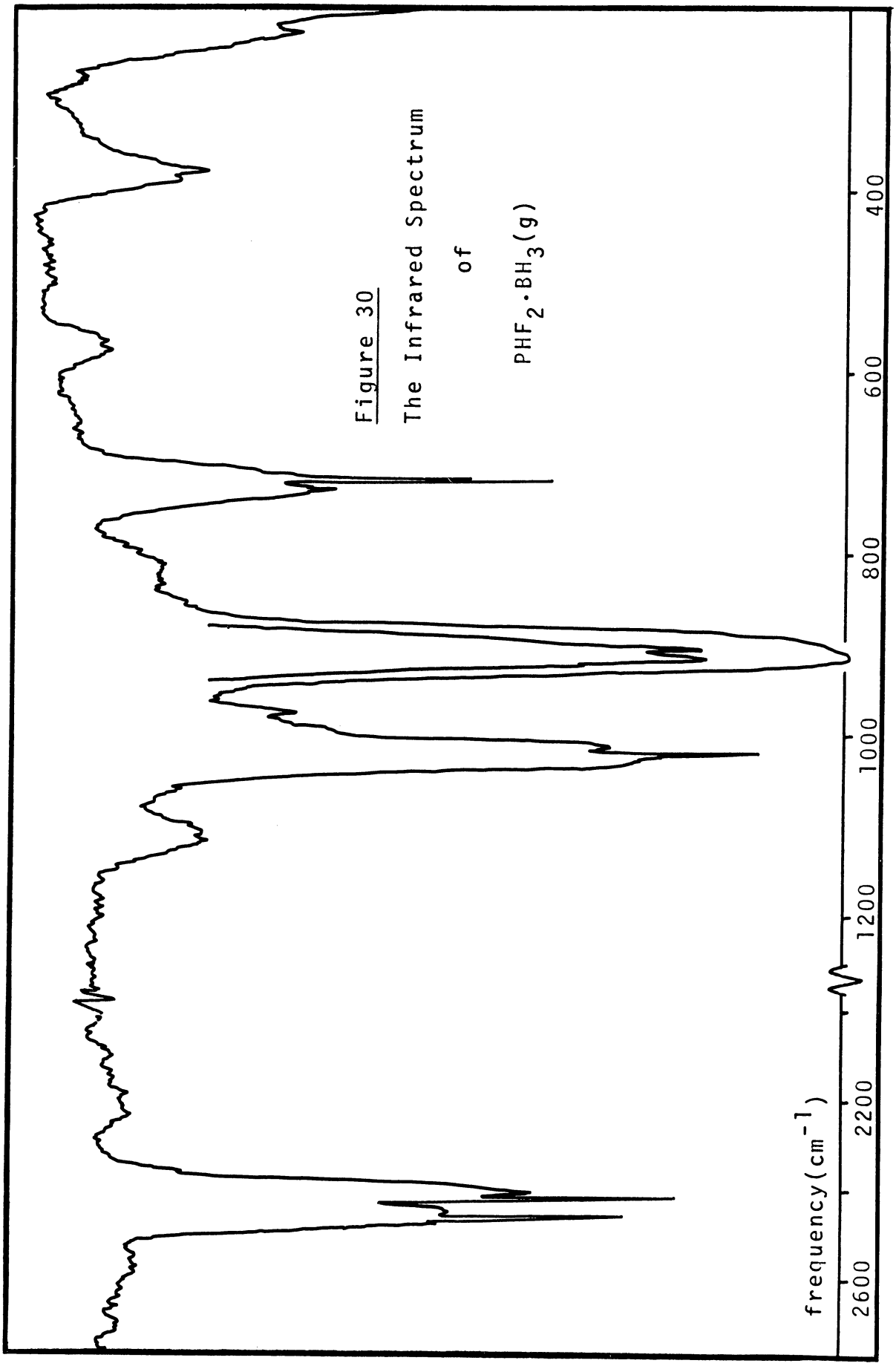

Figure 30

The Infrared Spectrum of $PHF_2 \cdot BH_3$(g)

D. Base Displacement by Difluorophosphine.

1) Displacement of CO from $Ni(CO)_4$. This preliminary study demonstrated that PHF_2 does displace CO from $Ni(CO)_4$ to form $(PHF_2)Ni(CO)_3$.

$$PHF_2 + Ni(CO)_4 \rightarrow (PHF_2)Ni(CO)_3 + CO$$

However, the reaction of nickel tetracarbonyl and difluorophosphine is complicated by side reactions which yield brown, oily, non-volatile substances.

After 3 days reaction time at 0° when the initial $PHF_2/Ni(CO)_4$ ratio was 5:1, an amount of gas equaling the amount of PHF_2 consumed was isolated; after purification by fractional condensation the fraction displayed the infrared spectrum shown in Figure 31. The following discussion shows that the spectrum is consistent with the formula $(PHF_2)Ni(CO)_3$. Because of the small amount of sample isolated further characterization was not possible.

If PHF_2 is assumed to be a point-mass, L, and nickel is considered to be tetrahedral, then the various possible difluorophosphine-substituted nickel carbonyls and their respective symmetries can be deduced as shown in Table 23, which also gives the number of C-O stretching frequencies expected for each degree of substitution. From a comparison of Table 23 with the spectrum (Table 22 and Figure 31), it is immediately apparent that the new species cannot be the tris- or tetrakis-difluorophosphine derivative since the C-O stretching region is too complex. Still the four

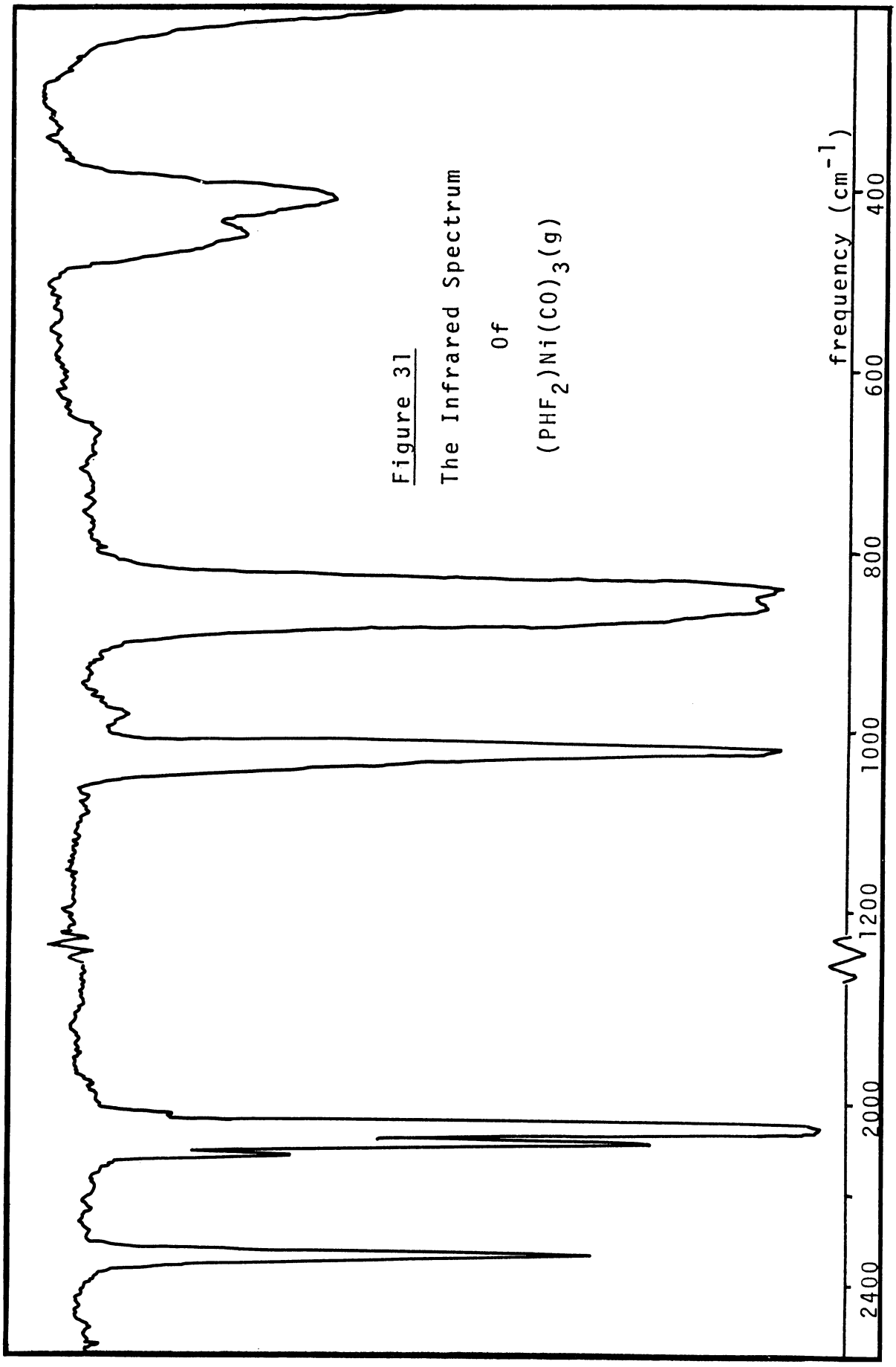

Figure 31

The Infrared Spectrum

Of

$(PHF_2)Ni(CO)_3(g)$

Table 22

The Infrared Spectrum* of $(PHF_2)Ni(CO)_3$

freq. (cm^{-1}) & intensity	tentative assignment
2331.8 vs	νPH
2110.6 m	νCO
2087.2 vs	νCO
2052.0 vvs	νCO
2016 w	2·δPH
1035.9 m 1030 m	overtone or combination
1019.9 vs	δPH
982 w	ωPH
853.3 vvs	νPF
836.0 vvs	νPF
457 m	δNiCO
443 m	δNiCO
421 w	ωNiCO
408 s	δPF_2

* For an explanation of notation see Appendix A.

Table 23

Symmetry and IR-active C-O Stretching for $L_xNi(CO)_{4-x}$, x = 1→4

	C_{3v}	C_{2v}	C_{3v}	T_d
	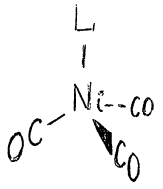	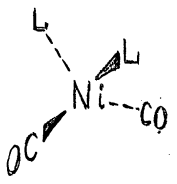	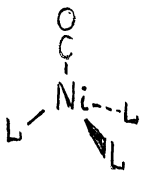	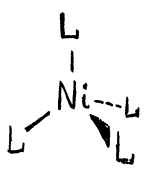
IR-active νCO's	two a_1 & e	two a_1 & b_2	one a_1	none

bands in this region are more than expected for either of the two remaining possibilities; however, if L is not symmetric about the C_3 axis as assumed above in Table 23, and as is the case for PHF_2, the degeneracy of the asymmetric C-O stretch in $LNi(CO)_3$ would be removed and a total of three C-O stretches might be expected. The fourth absorption in the C-O region may be due to an overtone enhanced in intensity by Fermi-resonance[66].

The infrared provides further evidence for the monosubstituted species when the P-H stretching region is also considered. The compound $(PHF_2)_2Ni(CO)_2$ would be expected to show symmetric and asymmetric P-H stretching frequencies. Even under high resolution there was evidence for only one absorption in the P-H region, just as expected for $(PHF_2)Ni(CO)_3$; tentative assignments for the infrared spectrum are listed in Table 22.

When equal amounts of difluorophosphine and nickel tetracarbonyl were mixed at 25°, the displacement of CO appeared to be more extensive as evidenced by the infrared spectra of the reaction products which displayed considerable complexity in the P-H and C-O stretching regions. However, before characterization of the products could be completed the sample was inadvertantly lost. Nevertheless, the experiments mentioned above show that difluorophosphine displaces CO from nickel tetracarbonyl under much milder conditions than those reported for PF_3 to effect the corresponding displacement[22b].

2) Displacement of PH_3 and PF_3. Experiments were conducted in which difluorophosphine was found to displace phosphine and trifluorophosphine from their respective borane adducts, nearly quantitatively.

Typically, after about a day at -78° and an additional day at -45°, difluorophosphine displaced PF_3 from $PF_3 \cdot BH_3$ according to the equation

$$PF_3 \cdot BH_3 + PHF_2 \rightarrow PHF_2 \cdot BH_3 + PF_3.$$

With an excess of trifluorophosphine borane the PHF_2 was completely consumed.

In a similar experiment involving an excess of $PH_3 \cdot BH_3$, after $\frac{1}{2}$ day at 0° the difluorophosphine reacted completely, displacing an equal amount of PH_3 as shown in the equation

$$PH_3 \cdot BH_3 + PHF_2 \rightarrow PHF_2 \cdot BH_3 + PH_3.$$

The latter two base displacements were effected with

a stoichiometric deficiency of PHF_2; yet the difluorophosphine was completely consumed. If the original adducts formed stronger coordinate P-B bonds than PHF_2, under these conditions unreacted difluorophosphine would be present; therefore, PHF_2 is a stronger base than either PH_3 or PF_3. The relative base strengths of PH_3 and PF_3 towards borane are established by experiments and observations discussed in the next section.

IV. Relative Base Strengths of PH_3, PHF_2, and PF_3 Towards BH_3.

A. General.

The relative base strengths of phosphine, difluorophosphine, and trifluorophosphine toward borane would best be measured by the enthalpy change, ΔH, for the dissociation of the adducts in the gas phase into the component donor and acceptor molecules.

$$L \cdot BH_3 \rightleftharpoons L + \tfrac{1}{2}B_2H_6; \quad L = PH_3,\ PHF_2,\ PF_3$$

Such thermodynamic data have been obtained for $PF_3 \cdot BH_3$[102], and conceivably could be for $PHF_2 \cdot BH_3$, if it dissociates at higher temperatures without decomposition; however, $PH_3 \cdot BH_3$ is essentially nonexistent in the vapor, and such a study is precluded in this case. Nevertheless, both base-displacement reactions and the equilibrium constant for adduct dissociation, $K = \frac{[L][B_2H_6]^{\frac{1}{2}}}{[L \cdot BH_3]}$, have been used previously as a measure of relative base strength. The

present study qualitatively relates the results to the equilibrium involved in adduct formation and finds that the relative base strengths towards borane is PHF_2 > PF_3 > PH_3.

So that apparent anomolies in adduct stability cannot be attributed to unusual structural differences, a necessary prerequisite for a study of the relative stability of the coordinate link in a series of Lewis acid-base adducts is the assurance that the adducts be essentially "isostructural". Therefore, before the evidence establishing the relative order of coordinating ability for PF_3, PHF_2, and PH_3 is discussed, the structural similarity of their respective boranes will be shown by nmr spectroscopy.

B. Structures of the PHF_2, PH_3, and PF_3 Borane Adducts.

1) Difluorophosphine Borane. An examination of the nmr spectra of $PHF_2 \cdot BH_3$ as presented in Section III C-2 clearly indicates that the structure is

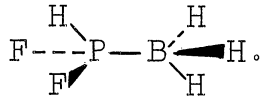

This structure is consistent with the usual borane adduct, and, as will be seen in the following discussion, it is basically no different from the known structures of $PH_3 \cdot BH_3$[91] and $PF_3 \cdot BH_3$[92].

2) Phosphine Borane. In 1940 Gamble and Gilmont prepared "diborane diphosphine" by mixing diborane and phosphine at low temperatures[90]. On the basis of

rudimentary chemical evidence an analogy was drawn to the diammoniate of diborane and a structure analogous to that accepted at that time for $B_2H_6 \cdot 2NH_3$ was proposed, $(PH_4^+)(H_3BPH_2BH_3^-)$. No molecular weight data were available to support the postulated ionic dimer.

Some of the reactions of $(H_2PBH_3)_n$ can be interpreted best in terms of a single monomeric formulation. For example, trimethylamine displaces PH_3 quantitatively to give $H_3BN(CH_3)_3$[93], and a kinetic study of the reaction of B_2H_6 and PH_3 by Brumberger and Marcus[94] suggested the monomeric representation.

Since the original structural postulates were presented, a new model for $B_2H_6 \cdot 2NH_3$ has been accepted[95] in place of the earlier ammonium type of solid, $(NH_4^+)(H_3BNH_2BH_3^-)$ but neither the new diammoniate model nor the monomeric model for $(H_3BPH_3)_n$ rationalized the known reaction with ammonia as easily as did the early dimeric formulation proposed by Gamble and Gilmont:

$$NH_3 + (PH_4^+)(H_3BPH_2BH_3^-) \rightarrow (NH_4^+)(H_3BPH_2BH_3^-) + PH_3.$$

Recently, an x-ray crystallographic study by McGandy[91] showed that $(H_3PBH_3)_n$ is indeed monomeric in the solid. Nevertheless, phosphine borane was investigated further by nmr, infrared, and Raman spectroscopy.

The ^{11}B nmr spectrum of molten H_3BPH_3 at 37° (Figure 32) consists of a 1:3:3:1 quartet of doublets centered 60.8 ppm upfield from TMB. The three magnetically equivalent protons split the boron signal into a quartet

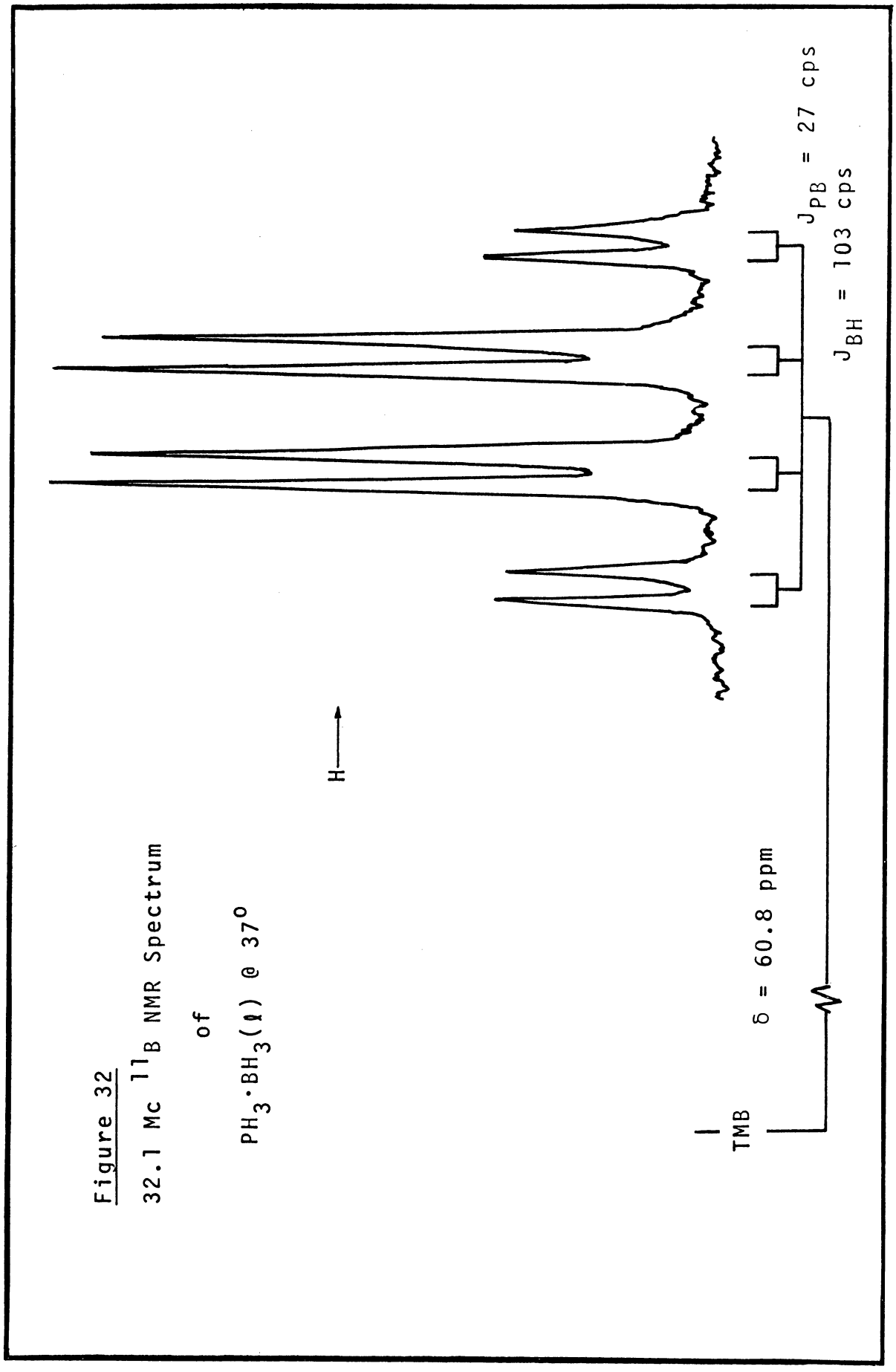

Figure 32

32.1 Mc ^{11}B NMR Spectrum

of

$PH_3 \cdot BH_3$(ℓ) @ 37°

(J_{BH} = 103 cps); then each member of the quartet is split into a doublet by coupling with the phosphorus ($I = \frac{1}{2}$) (J_{BP} = 27 cps). While the 1:3:3:1 quartet of doublets would be expected for both models, H_3BPH_3 and $PH_4(H_3BPH_2BH_3)$, the coupling constant, J_{BH} = 103 cps, compares well with the values (J_{BH} = 100 cps) obtained by Gilje[96] for $CH_3PH_2BH_3$ and the values (J_{BH} = 96 cps, σ = 55.6 ppm upfield from TMB) obtained by Phillips, Miller and Muetterties[97] for $HP(CH_3)_2BH_3$.

The ^1H nmr spectrum of $H_3PBH_3(\ell)$ at 37° (Figure 33) shows only two clear groups of hydrogen signals indicating the presence of two hydrogen atom environments in the molecule. A 1:1:1:1 quartet is found centered 0.53 ppm downfield from TMS while a doublet is displayed 4.31 ppm downfield from TMS. The quartet at 0.53 ppm is attributed to the borane hydrogen atoms split into a 1:1:1:1 quartet by the ^{11}B ($I = \frac{3}{2}$). The value of J_{BH} (104 cps) is in good agreement with the value derived from the ^{11}B spectrum (103 cps) and with that found in $PH_2Me \cdot BH_3$ (100 cps). The doublet at 4.31 ppm due to coupling of phosphorus with hydrogen shows a P-H coupling constant of 372 cps which checks well with the value of 370 cps reported by Gilje[96] for $H_2CH_3PBH_3$. Careful examination of each component of the phosphine doublet reveals a 1:3:3:1 quartet (J_{HPBH} = 8 cps) which would be expected from coupling of the three borane hydrogens with the hydrogens attached to phosphine. Coupling with the borane

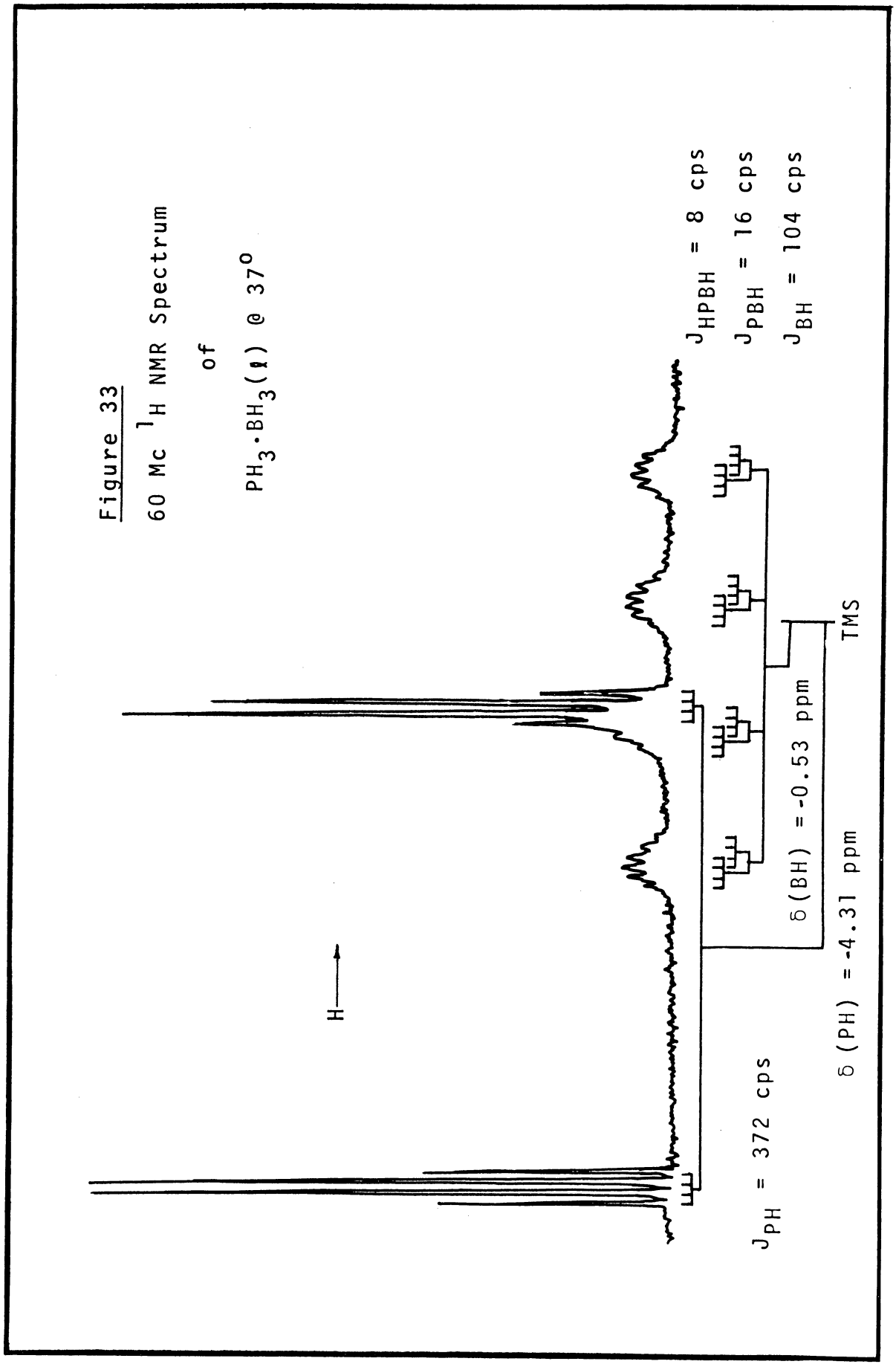
Figure 33
60 Mc ^{1}H NMR Spectrum
of
$PH_3 \cdot BH_3$(ℓ) @ 37°
H
J_{HPBH} = 8 cps
J_{PBH} = 16 cps
J_{BH} = 104 cps
J_{PH} = 372 cps
δ(BH) = -0.53 ppm
δ (PH) = -4.31 ppm
TMS

hydrogens rather than with the boron ($I = \frac{3}{2}$) is indicated by the 1:3:3:1 line intensities in the quartet. Boron coupling would give 1:1:1:1 line intensities. Such H-P-B-H coupling was also observed by Shoolery[90] in an earlier nmr study of Me_2HPBH_3, where the coupling constant J_{HPBH} was listed as 6 cps.

The spin-spin splitting pattern of hydrogens attached to phosphorus is consistent with the H_3BPH_3 model but is not consistent with the formula $(PH_4^+)(H_3BPH_2BH_3^-)$. In the latter representation each member of the P-H doublet should be split into a septet of intensities 1:6:15:30:15:6:1. Even if the outer member of the septet were obscured by low signal intensity, the pattern would be clearly different from the 1:3:3:1 pattern observed.

Under higher resolution each member of the <u>borane quartet</u> was seen to consist of a 1:3:4:4:3:1 six-line multiplet as would be expected for two overlapping 1:3:3:1 quartets. One can identify a doublet arising from spin-spin coupling between the borane hydrogens and the phosphorus nucleus of H_3BPH_3 (J_{PBH} = 16 cps) with each member of the doublet split into overlapping 1:3:3:1 quartets by the three phosphine hydrogens (J_{HPBH} = 8cps).

This spin-spin splitting pattern is completely consistent with the formula H_3BPH_3. It is not consistent with the formula $(PH_4^+)(H_3BPH_2BH_3^-)$ where each component of the P-B-H doublet would be split into a 1:2:1 triplet instead of the quartet by two hydrogens (rather than three)

attached to the phosphorus.

Finally, peak intensities in the proton spectra are in good agreement with predictions of the formula H_3BPH_3. Boron in the sample is about 80% ^{11}B and 20% ^{10}B. The ^{11}B with nuclear spin of $\frac{3}{2}$ gives rise to the quartets observed above. The ^{10}B with a nuclear spin of 3 gives rise to a septet which is not detectable above the background and which is not included in the ^{11}B quartet intensities. Phosphorus with only a single magnetic nucleus does not split the P-H signal beyond the doublet. Thus the compound H_3BPH_3 should show a ratio of H_{boron} to $H_{phosphorus}$ of 0.8 to 1.0 or 0.80. The observed ratio in the spectrum is 0.8.

The foregoing spectra indicate conclusively that molten $(H_3BPH_3)_n$ is the simple acid-base monomer, H_3BPH_3, not the compound $(PH_4^+)(H_3BPH_2BH_3^-)$.

The x-ray study of McGandy[91] first and conclusively showed that phosphine borane is monomeric in the solid state at 25°. The infrared and Raman data presented here (Figures 34-36 and Table 24) are also consistent with the monomeric structure for $PH_3 \cdot BH_3$(s) at -180°. The monomer should display an ethane type configuration with C_{3v} symmetry for which eleven infrared active motions would be expected - four vibrational frequencies associated with each of the $-MH_3$ moieties, considered as free molecules with C_{3v} symmetry, and three arising as a consequence of the P-B bond; a fourth skeletal frequency, the

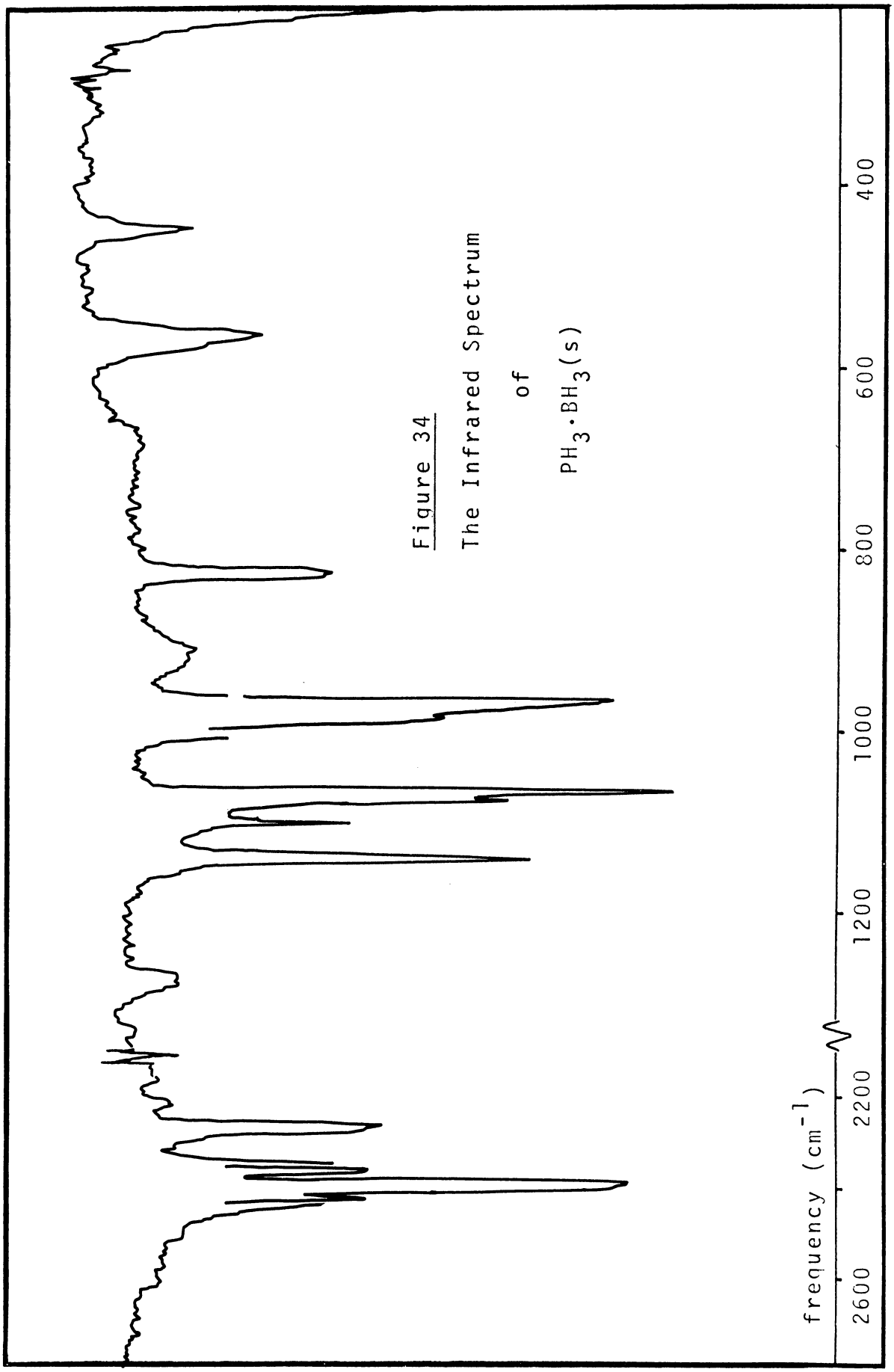

Figure 34

The Infrared Spectrum of $PH_3 \cdot BH_3$(s)

Figure 35

The Raman Spectrum

of

$PH_3 \cdot BH_3(s)$

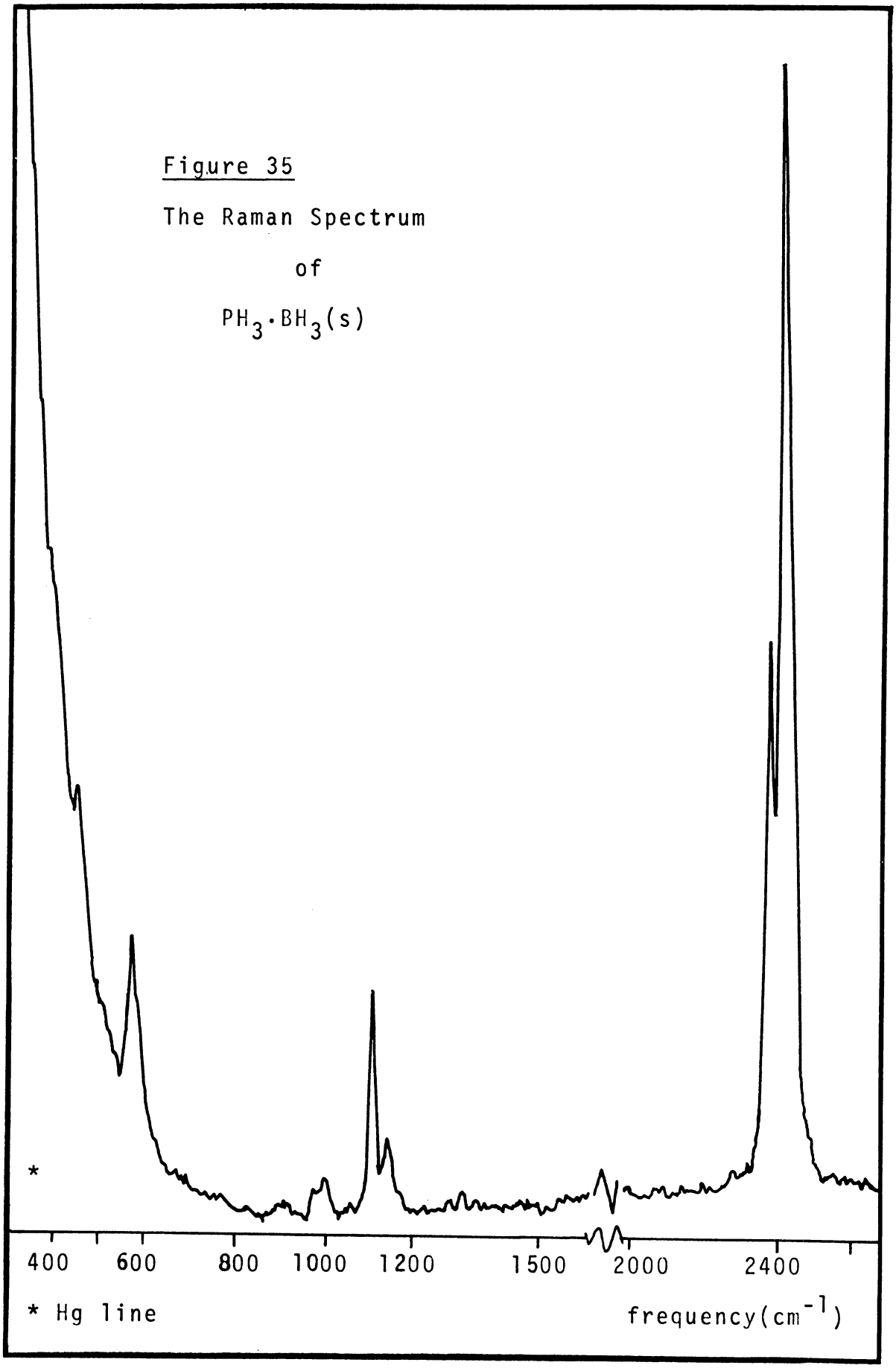

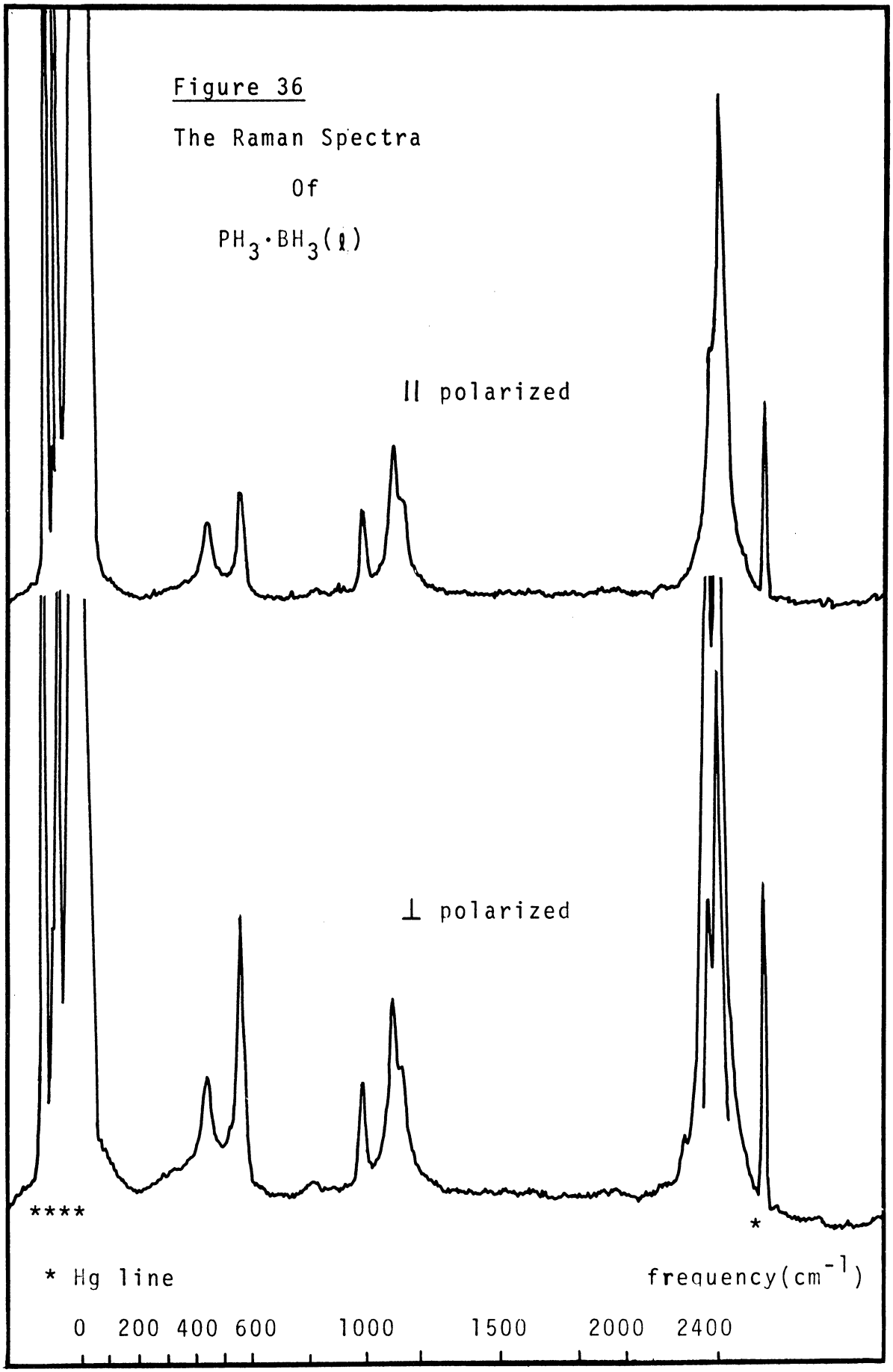
Figure 36
The Raman Spectra
Of
$PH_3 \cdot BH_3$(ℓ)
∥ polarized
⊥ polarized
****
*
* Hg line
frequency(cm^{-1})
0 200 400 600 1000 1500 2000 2400

Table 24

Vibrational Spectra* of $PH_3 \cdot BH_3$

Infrared freq. (cm^{-1}) & intensity (solid -180°)	note	assignment & symmetry	Raman freq. (cm^{-1}) & intensity (solid -180°)	Raman freq. (cm^{-1}), intens. & polarization (liquid 35°)
2421.7 s 2426.0	split in crystal	ν_9, νPH, e	2416 w, sh	†
2399.1 s		ν_7, νBH, e	†	†
2392.0 vs		ν_1, νBH, a_1	2401 vs	2399 vs, p
2361.5 s		ν_3, νPH, a_1	2363 s	2358 s, p
2272.8 w 2263.8 w		$2 \cdot \nu_5$ combination	‡	2262 w, p
1141.1 m		ν_5, δPH_3, a_1	1144 w	1135 m
1103.1 w 1100.8	split in crystal	ν_{11}, δPH_3, e	1102 m	1102 m, dp
1077.5 w 1068.9 m	^{10}B ^{11}B	ν_2, δBH_3, a_1	‡	‡
988.2 s 968.7 vs	^{10}B ^{11}B	ν_8, δBH_3, e	‡	989 m, dp
829.5 w 825.6 w 822.5 w	split in crystal, overlap of ^{11}B and ^{10}B motions.	ν_{10}, ρBH_3, e	‡	817 vw
576.6 vw 563.7 w	^{10}B ^{11}B	ν_4, νPB, a_1	572 m	551 m, p
447.1 w		ν_{12}, ρPH_3, e	451 w	436 m

* For an explanation of notation see Appendix A.
‡ Very weak band observed, but determination of position is difficult.
† Absorption corresponding to this assignment probably masked by nearby peaks.

P-B torsional motion of a_2 symmetry, is inactive. The Raman effect for this model should also display the same eleven fundamentals.

If the structures 1) $[PH_4][H_2P(BH_3)_2]$, as originally proposed by Gamble and Gilmont[93], or 2) $[H_2B(PH_3)_2][BH_4]$, analogous to the structure of the "diammoniate of diborane", were present in the solid, the infrared and Raman spectra of both these structures should differ significantly from those of the C_{3v} monomer. If the $-BH_3$ groups in 1) and the $-PH_3$ groups in 2) are considered as point masses and all angles assumed tetrahedral, each molecule contains ions of T_d and C_{2v} symmetry on the basis of which skeletal frequencies can be predicted. The T_d moieties should display two IR-active motions and four fundamentals in the Raman effect. Likewise, the C_{2v} moieties would be expected to give rise to eight infrared frequencies and nine Raman. Internal motions of the $-MH_3$ groups would increase the complexity of the observed spectrum in the regions of hydrogen frequencies. Thus, it is apparent that the infrared and Raman spectra of either 1) or 2) should differ significantly. In particular, the spectra should display complexity in areas characteristic of P-B and $-MH_3$ motions.

The infrared and Raman spectra of the solid have been found to be similar, relatively simple, consistent with the C_{3v} model, and easily related to the Raman spectrum of the liquid. Accordingly, it is felt that this

evidence complements the crystallographic study[91] which showed unequivocally that solid "diborane diphosphine" is monomeric. The observed infrared and Raman frequencies are listed in Table 24. No evidence for (PH_4^+) or (BH_4^-) is obtained upon comparison of these spectra. Only one P-B motion could be assigned and the spectra are relatively simple.

3) Trifluorophosphine Borane. Taylor and Bissot[98] found that the Raman effect for liquid $PF_3 \cdot BH_3$ at -80° was consistent with the ethane configuration for the molecule (C_{3v} symmetry). A recent microwave study[92] has established the molecular parameters of trifluorophosphine borane. The nmr spectra of $PF_3 \cdot BH_3$ were determined in the present study and also clearly indicate an ethane-type configuration for $PF_3 \cdot BH_3$ in which free rotation about the P-B bond exceeds the nmr time constant, averaging out the magnetic environments of the fluorine and hydrogen nuclei.

The boron nmr spectrum of liquid $PF_3 \cdot BH_3$ at 37° (Figure 37) gives definite evidence for a BH_3 group directly bonded to phosphorus. It consists of a 1:3:3:1 quartet of doublets centered 66.6 ppm upfield from TMB. The basic quartet (J_{BH} = 106 cps) affirms the direct bonding of three hydrogens to the boron, while the doublet splitting (J_{PB} = 39 cps) of each member of the 1:3:3:1 quartet is due to the directly bonded phosphorus nucleus. A close examination of each peak reveals incipient fine

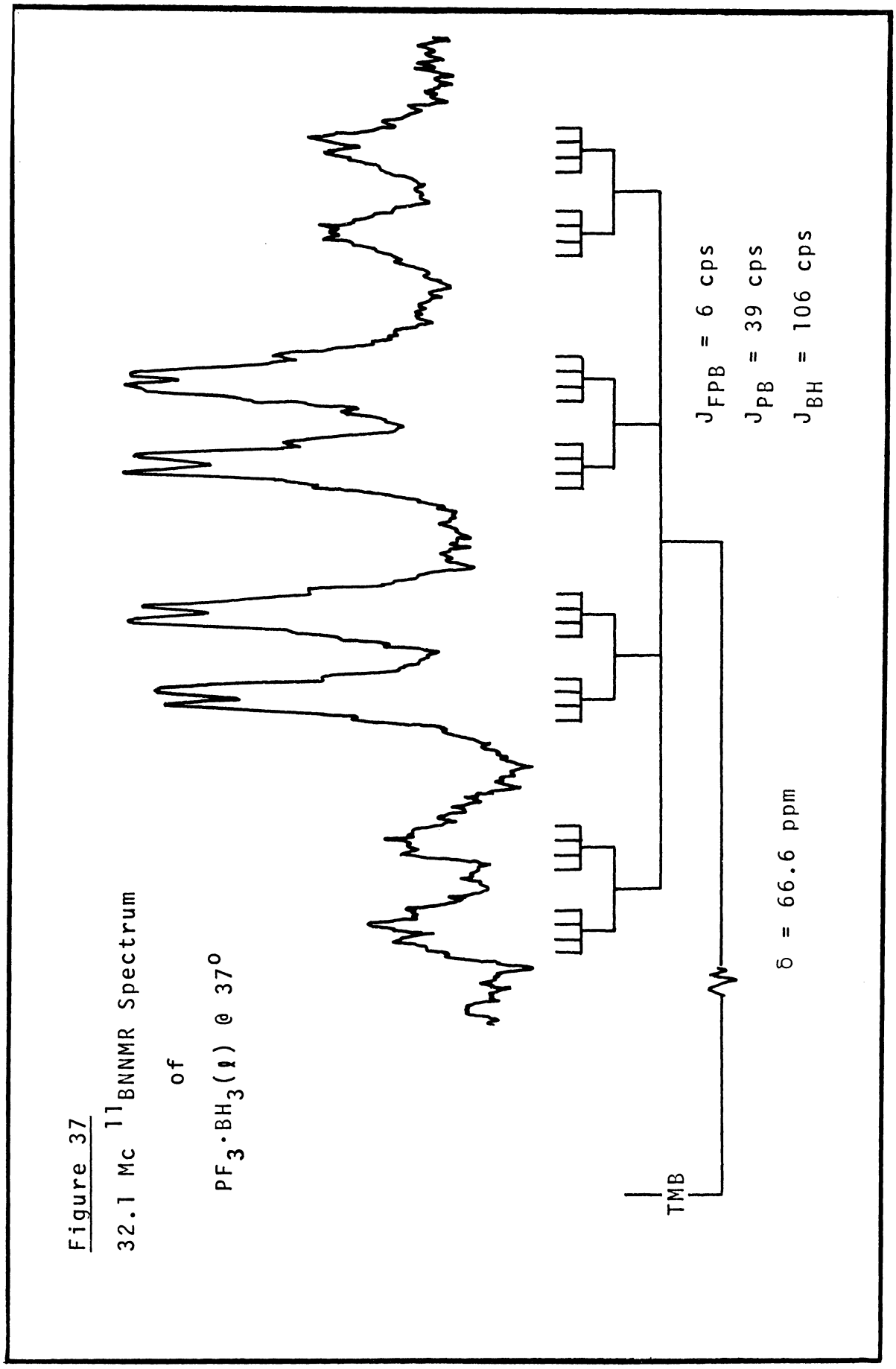

Figure 37

32.1 Mc ^{11}BNMR Spectrum

of

$PF_3 \cdot BH_3$(ℓ) @ 37°

Figure 38

60 Mc ^{1}H NMR Spectrum of $PF_3 \cdot BH_3$(ℓ) @ -40°

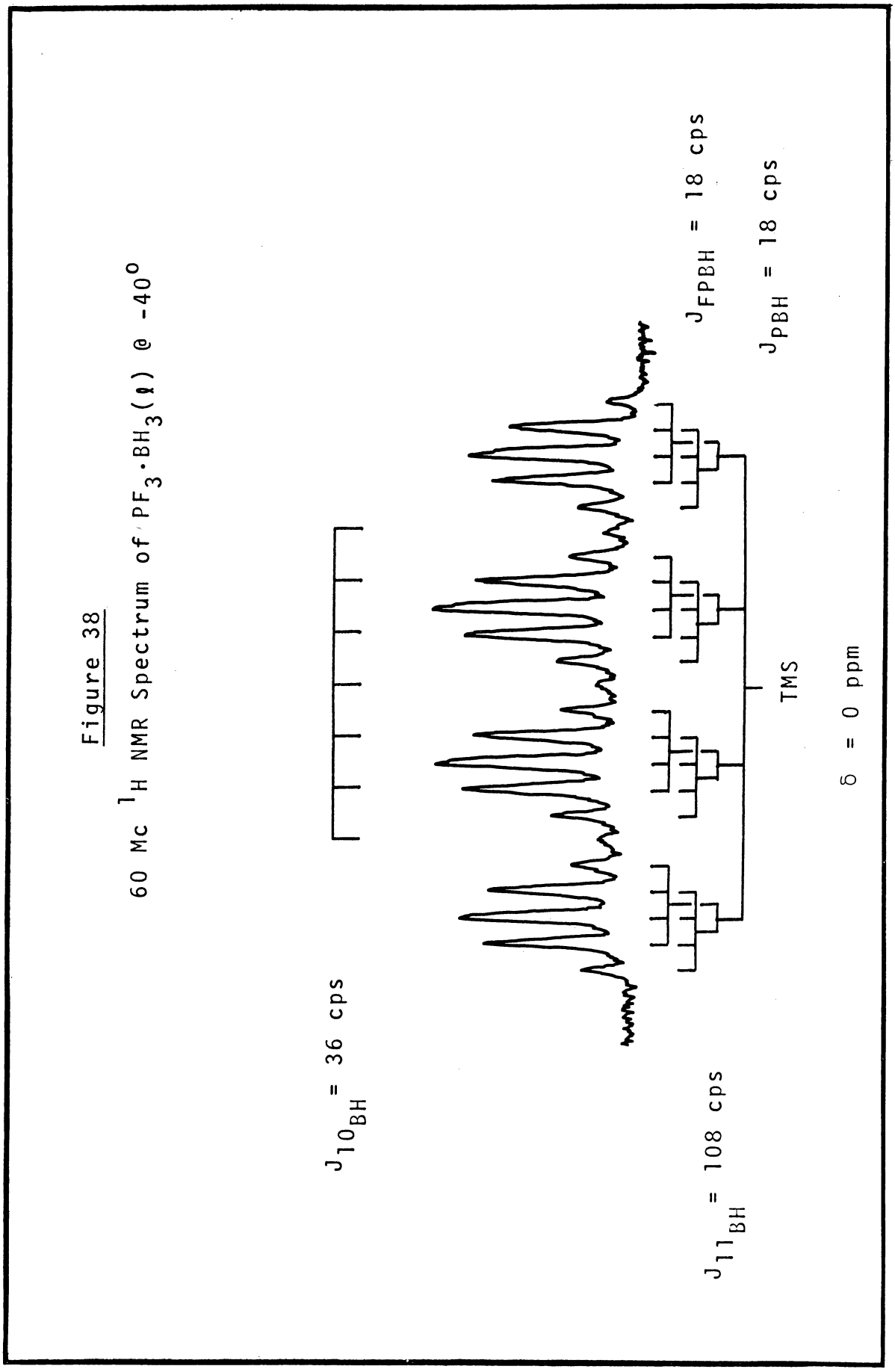

visible members of the septet, the central and outermost members. The spacing between the nuclear energy levels in a magnetic field is directly proportional to the magnetogyric ratio, γ_i, and the perturbing magnetic field[81], in the case of spin-spin splitting the magnetic field within the molecule itself and the γ_i of the perturbing nucleus. Thus, since the only variable altered upon substituting ^{10}B for ^{11}B is γ_i, the $J(^{11}B):J(^{10}B)$ ratio should be equal to the ratio $\gamma(^{11}B):\gamma(^{10}B)$ as is the case.*

$$J(^{11}B)/J(^{10}B) = \frac{108}{36} = 3.000 \text{ and}$$

$$\frac{\gamma(^{11}B)}{\gamma(^{10}B)} = \left[\frac{\mu}{I\hbar}\right]_{^{11}B} \Bigg/ \left[\frac{\mu}{I\hbar}\right]_{^{10}B} = \frac{2.6880}{3/2} \Bigg/ \frac{1.8006}{3} = 2.986$$

The ratio of the ^{11}B-H signal to the ^{10}B-H signal is also in good agreement with the ratio calculated from the natural abundances of ^{11}B and ^{10}B.

The observation of ^{10}B-H spin-spin coupling is usually precluded by the nuclear-quadrupole moment of the ^{10}B nucleus which can interact with fluctuating electric-field gradients to provide a rapid spin relaxation mechanism and consequent broadening of the nmr signal.‡ The sharpening of a signal normally expected to

---

* The expressions were evaluated using the values given in reference 81.

‡ The uncertainty principle $\Delta E \Delta t \approx \hbar$ can be used to estimate the order of magnitude of broadening. Since $\Delta E = h\Delta\nu$, the uncertainity principle implies that the uncertainity in the frequency of absorption is $1/(2\pi\Delta t)$. Thus the line width measured on a frequency scale, owing to spin relaxation, will be inversely proportional to the relaxation time.(81)

be broadened by quadrupole interaction can be attributed to the lack of a field gradient at the nucleus, thus inhibiting the relaxation mechanism as in the case of the highly symmetrical ammonium[99] or borohydride[97] ions. Therefore, the observation of ^{10}B-H spin-spin coupling in $PF_3 \cdot BH_3$ could also be attributed to the lack of an appreciable field gradient at the boron nucleus, or stated differently, a highly symmetrical electron distribution.

A basic doublet attributed to P-F spin-spin coupling (J_{PF} = 1406 cps) is observed centered 19.9 ppm downfield from TFA in the ^{19}F nmr spectrum of $PF_3 \cdot BH_3$ (Figure 39). If the values of J_{FPBH} and J_{FPB} derived from the proton and boron nmr spectra (18 and 6 cps, respectively) are used to determine the expected fine structure pattern for each member of the doublet, a 13-line multiplet with intensity ratios of 1:1:1:4:3:3:6:3:3:4:1:1:1 and spacings of 6 cps is predicted as shown in Figure 40. Although the expected 13-line multiplet could not be resolved, a pattern which shows the prominent features of the expected multiplet was observed, i.e., a strong central maximum and progressively weaker peaks displaced approximately 18 and 36 cps on either side of the center on the outer peaks (Figure 39).

Although the vibrational spectra of trifluorophosphine borane have been investigated rather extensively by Taylor and Bissot[98], and Wyma[100], the spectrum of $PF_3 \cdot BH_3$ vapor has not been reported in detail[102]; intermolecular

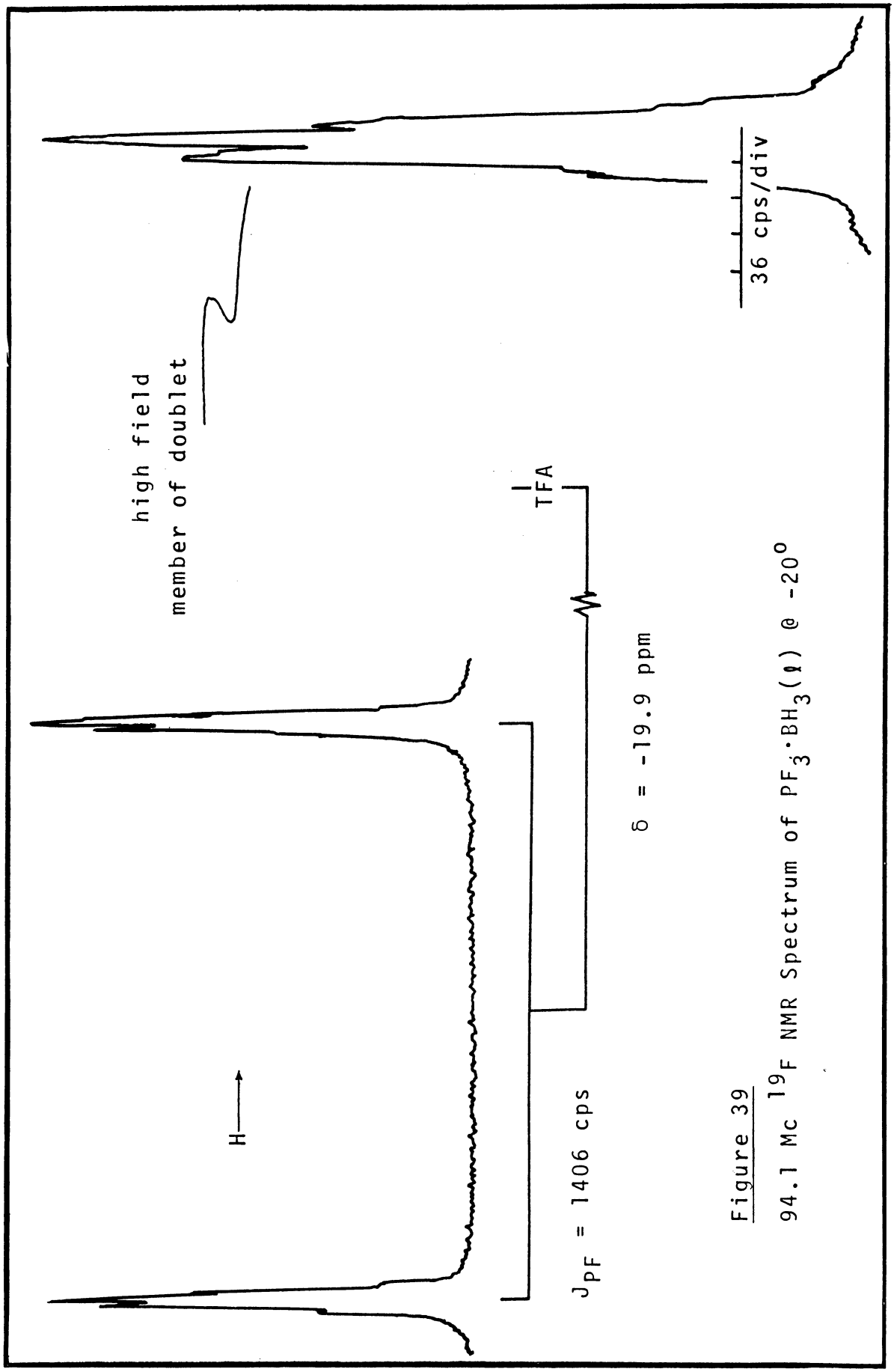

Figure 39

94.1 Mc ^{19}F NMR Spectrum of $PF_3 \cdot BH_3$(ℓ) @ -20°

Figure 40

Expected ^{19}F nmr Pattern for Each Member of P-F Doublet in $PF_3 \cdot BH_3$

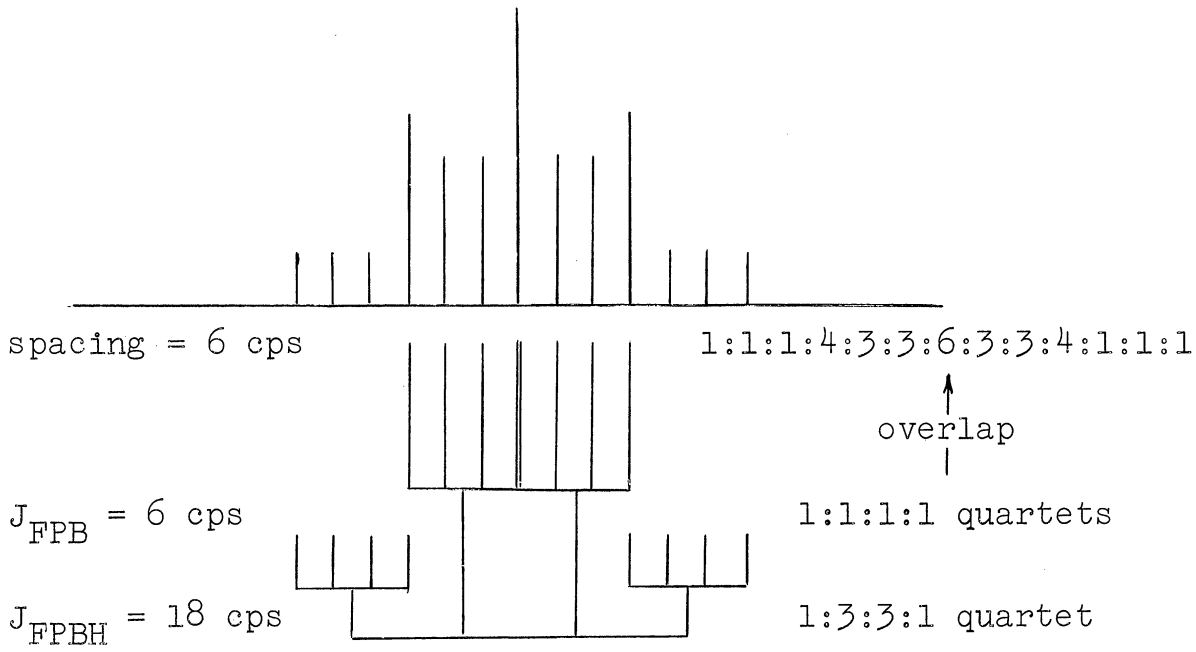

forces such as liquid association or crystalline-lattice forces would not perturb the valence force field in the vapor state. In obtaining the infrared spectrum of $PF_3 \cdot BH_3$ vapor during this study, dissociation was minimized by maintaining the vapor in equilibrium with the liquid which was maintained at about -126°. The spectrum of $PF_3 \cdot BH_3$ vapor (Figure 41 and Table 25) was easily discernable from those spectra due to the small amounts of PF_3 and B_2H_6 which did form. As shown in Table 25, which compares the gas-phase infrared spectrum to the Raman spectrum of $PF_3 \cdot BH_3(\ell)$ at -80° determined by Taylor and Bissot[98], there are considerable shifts in some of the B-H

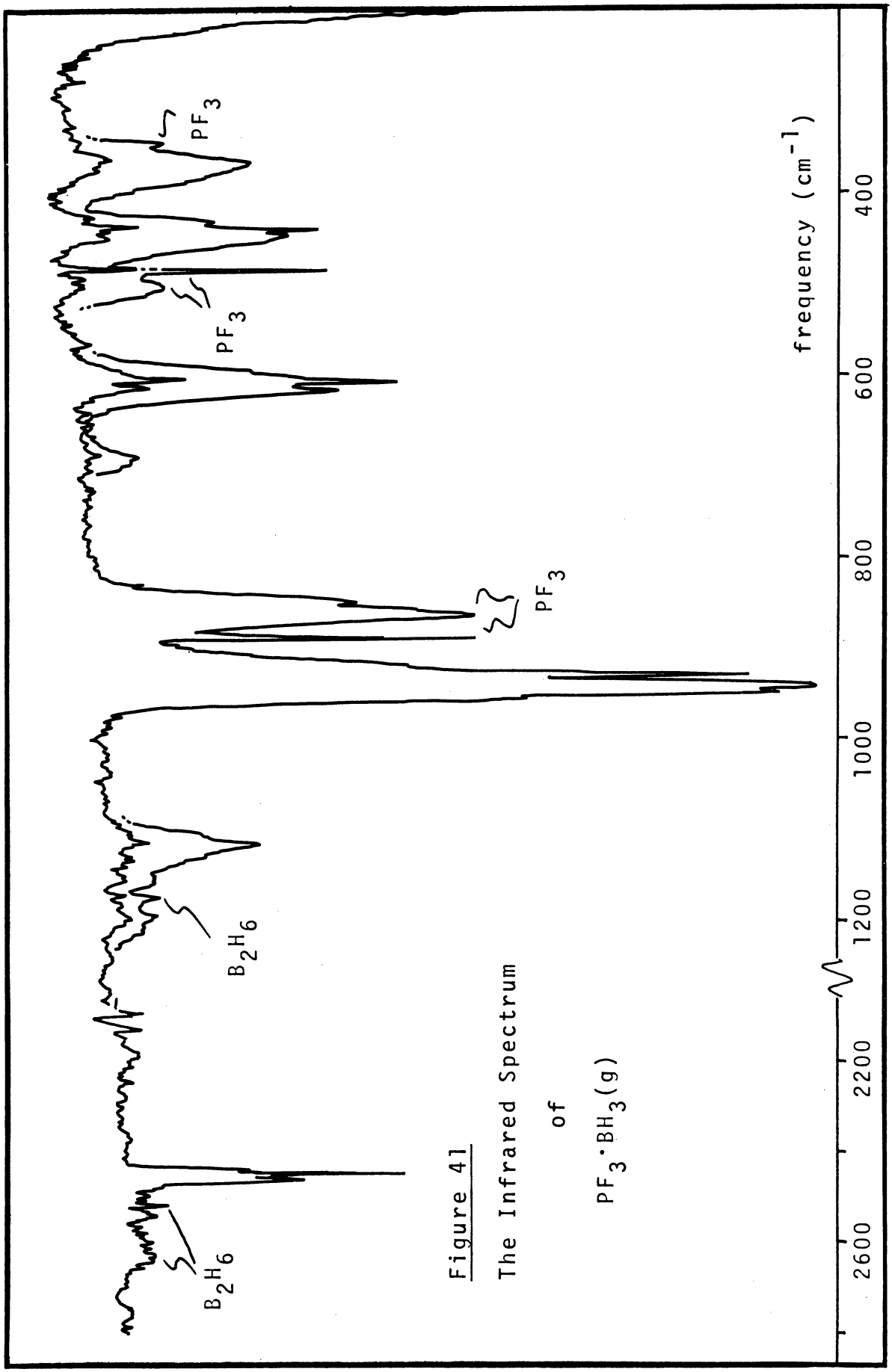

Figure 41

The Infrared Spectrum

of

$PF_3 \cdot BH_3(g)$

Table 25

Vibrational Spectra* of $PF_3 \cdot BH_3$

Infrared (g) freq. (cm^{-1}) & intensity	note	assignment & symmetry	Raman‡ (ℓ) freq. (cm^{-1}), intens. & polarization
2464.5 m	^{10}B	νBH, e	
2462.7 m		νBH, a_1	
2453.1 s	^{11}B	νBH, e	2455 vs, dp
2451.3 s		νBH, a_1	2385 vs, p
1131.7 w	R		
1116.6 w	Q	δBH_3, e	1117 s, dp
1105.4 w	P		
——		δBH_3, a_1	1077 w, p
958.9 vs	R		
951.3 vvs	Q	νPF, e	957 m, dp
943.4 vvs	R,P		
931.3 vvs	Q	νPF, a_1	944 m, p?
922 vs,sh	P		
693 vw		ρBH_3, e	697 vw
619.1 w	^{10}B	νPB	607 s, p
609.5 m	^{11}B		
452.2 w	R		
448.4 w	Q?		
441.8 m	Q	δPF_3, a_1	441 m, p
433.0 w	P		
370.2 w,br		δPF_3, e	370 vw
		ρPF_3, e	197 m, dp

* For an explanation of notation see Appendix A.

‡ The spectrum of Taylor and Bissot[98], with the exception of many overtone and combination bands.

vibrational frequencies. The PF_3 rocking frequency fell below the range of the Beckman IR-12, and the symmetric BH_3 deformation assigned to the absorption at 1077 cm^{-1} in Raman could not be observed in the infrared of the gas - perhaps it has shifted to higher frequency and is one of the lines observed around 1120 cm^{-1}. It also appears that the symmetric PF_3 deformation Q-branch at 441.8 cm^{-1} in the infrared (441 cm^{-1} in the Raman) shows another Q-branch, probably due to a ^{10}B isotopic shift, at 448.4 cm^{-1}.

C. Phosphine Borane and Trifluorophosphine Borane Systems.

Difluorophosphine is a markedly stronger base towards BH_3 than either PF_3 or PH_3 as demonstrated by the base displacement reactions described in Section III D-2. In order to determine whether phosphine or trifluorophosphine is a stronger base towards borane, the base displacement reactions described below were investigated.

1) Phosphine and Trifluorophosphine Borane. When $PF_3 \cdot BH_3$ was treated with twofold excess of PH_3 at -35° to 0°, after about one day 87% of the PF_3 had been displaced according to the equation

$$PH_3 + PF_3 \cdot BH_3 \rightarrow PF_3 + PH_3 \cdot BH_3.$$

However, other experiments showed that under nearly identical conditions when equal amounts of $PF_3 \cdot BH_3$, PH_3 and PF_3 were taken, the displacement only proceeded 48% to completion. Thus, there appears to be an equilibrium

situation among the following processes.

$$PF_3 \cdot BH_3(g) \rightleftharpoons PF_3(g) + \tfrac{1}{2}B_2H_6(g)$$

$$PH_3(g) + \tfrac{1}{2}B_2H_6(g) \rightleftharpoons PH_3 \cdot BH_3(s)$$

From the various experiments a value was obtained for the equilibrium constant for the displacement (p in atm.)

$$K(0°) = \frac{[p(PF_3)]}{[p(PH_3)][p(PF_3 \cdot BH_3)]} \approx 1.7 \text{ to } 2.2 \times 10^{-5}$$

The fact that PF_3 is displaced to any appreciable extent is felt to be a consequence of an unusually high lattice energy for $PH_3 \cdot BH_3(s)$ which drives the equilibrium in the favor of its formation. Therefore, the displacement reaction is not a true measure of the P-B bond strength in the above case. Evidence which indicated the weakness of the P-B coordinate link in $PH_3 \cdot BH_3$ is cited below.

2) Observations Concerning $PH_3 \cdot BH_3$ and $PF_3 \cdot BH_3$. Gamble and Gilmont[93] did not mention the volatility of $PH_3 \cdot BH_3$, however, Schlesinger and Burg[101] noted that the compound could be sublimed almost undecomposed in a high-vacuum; vapor density measurements are precluded by the rapid decomposition of $PH_3 \cdot BH_3$ vapor. The present study confirmed the latter observations and found that when the sublimate condenses into a cold tube, it does so before mercury, i.e., the black mercury ring appears in regions of the tube which are colder than those where the white ring of $PH_3 \cdot BH_3$ forms, implying that the vapor pressure of $PH_3 \cdot BH_3$ at 25° is lower than that of mercury. The low vapor pressure of $PH_3 \cdot BH_3$ is also indicated by

the fact that the vapors comprising the dissociation pressure of $PH_3 \cdot BH_3(s)$ are entirely composed of PH_3 and B_2H_6, at least with the usual means of detection such as vapor density and infrared spectroscopy. Therefore, $PH_3 \cdot BH_3$ apparently exists for appreciable lengths of time only in the molten (viz. nmr spectra) and solid states. This leads to the postulate that the P-B bond is very weak and that the driving force leading to the formation of $PH_3 \cdot BH_3$ in the condensed states is an unusually large "lattice energy". Perhaps this "lattice energy" is due to $(H^+)---(H^-)$ "hydrogen-bonding" between the acidic phosphine hydrogens and the hydridic borane hydrogens.

In the original study[93] of $PH_3 \cdot BH_3$ the data shown in Table 26 were given for the equilibrium dissociation pressures of the solid. The dissociation occurs according to the equation

$$PH_3 \cdot BH_3(s) \rightleftharpoons PH_3(g) + \tfrac{1}{2} B_2H_6(g),$$

Table 26

Equilibrium Data for $PH_3 \cdot BH_3$

°C	Dissociation pressure[93] (mm)	K*
25	1400	.96200
0	200	.05190
-11	71	.01100
-21	11	.00067

* p in atm.

and therefore, the equilibrium constant (p in atm.)

$$K = [p(PH_3)][p(B_2H_6)]^{\frac{1}{2}}$$

for the dissociation can be obtained by using the law of partial pressures to solve for the equilibrium pressures of PH_3 and B_2H_6 [viz. $p(B_2H_6) = \frac{1}{3}$ p(total), etc.]. The equilibrium constants calculated from the data of Gamble and Gilmont[93] are tabulated in Table 26 and log K is plotted vs. 1/°K in Figure 42. The slope of this plot corresponds to a ΔH of approximately 18 kcal/mole for the dissociation*

$$PH_3 \cdot BH_3(s) \rightleftharpoons PH_3(g) + \tfrac{1}{2}B_2H_6(g).$$

Recently Burg and Fu[102] reported the heat of dissociation for $PF_3 \cdot BH_3$,

$$PF_3 \cdot BH_3(g) \rightleftharpoons PF_3(g) + \tfrac{1}{2}B_2H_6(g),$$

to be ΔH = 11.87 kcal/mole. In order to compare the latter value with that for $PH_3 \cdot BH_3(s)$ as a measure of the P-B bond strength, it is necessary to subtract the heat of sublimation for

$$PH_3 \cdot BH_3(s) \rightleftharpoons PH_3 \cdot BH_3(g)$$

from the heat of dissociation for $PH_3 \cdot BH_3$. Although the

---

* The data of Gamble and Gilmont[93] are felt to be accurate since the value for the equilibrium constant at 0° given by Brumberger and Marcus[94] (1.14×10^6 mm^3 or 0.05090 $atm.^{\frac{3}{2}}$) corresponds well with the value derived from the data of G. & G. (0.05190 $atm.^{\frac{3}{2}}$). Since there is only a small amount of data, however, the calculation is indeed rather crude but does give an estimate of the energetics involved in P-B bond formation for $PH_3 \cdot BH_3$.

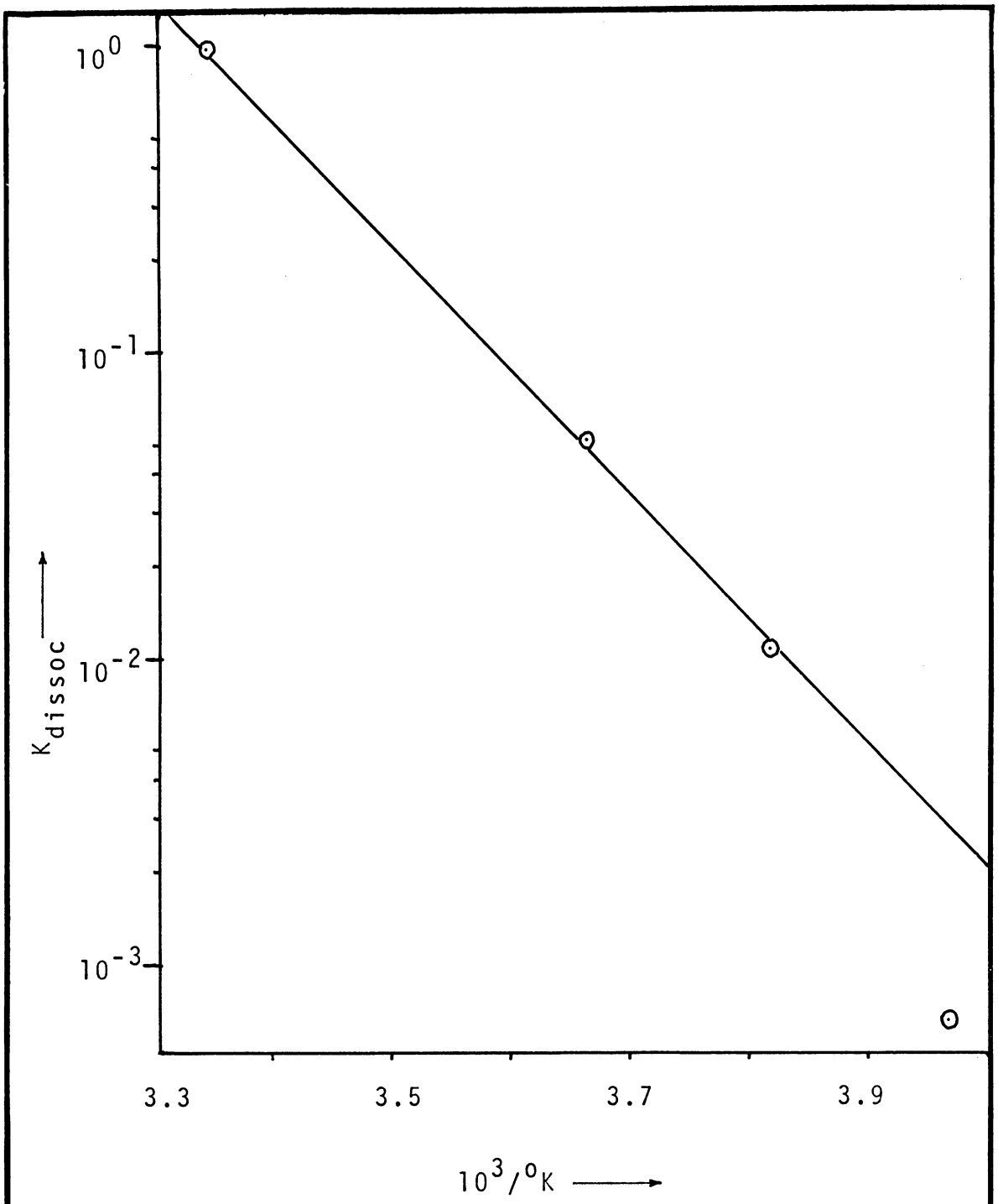

Figure 42

Plot of log K_{dissoc} vs. $1/^oK$

for $PH_3 \cdot BH_3(s) \rightleftharpoons PH_3(g) + 1/2\ B_2H_6(g)$

heat of sublimation for phosphine borane is not known*, it is expected to be substantially greater than the 6.5 kcal/mole difference between the ΔH of dissociation for $PF_3 \cdot BH_3(g)$ and $PH_3 \cdot BH_3(s)$. In other words, compensating for the heat of sublimation of $PH_3 \cdot BH_3(s)$, the thermodynamic data show that the P-B link in $PF_3 \cdot BH_3$ is stronger than in $PH_3 \cdot BH_3$. The observations mentioned above, as well as the existence of $PF_3 \cdot BH_3$ in the vapor and the non-existence of $PH_3 \cdot BH_3$ in the vapor, imply that the coordinate bond in $PH_3 \cdot BH_3$ is weaker than that in $PF_3 \cdot BH_3$; this conclusion, considered along with the displacement of PF_3 and PH_3 from their respective boranes by PHF_2, to give gaseous $PHF_2 \cdot BH_3$, shows that the relative base strength toward borane decreases in the order $PHF_2 > PF_3 > PH_3$; a consideration of the equilibrium involved in adduct formation leads to the same order as is indicated below.

Since no diborane of difluorophosphine can be detected in equilibrium with $PHF_2 \cdot BH_3$ at 25°, it can be said that the dissociation constant (pressure in atm.)

$$K\,(PHF_2 \cdot BH_3) = \frac{[p(PHF_2)][p(B_2H_6)]^{\frac{1}{2}}}{[p(PHF_2 \cdot BH_3)]} \ll 1,$$

another good indication of a strong P-B bond.

---

* Gmelin[103] does list a value for the heat of sublimation of $PH_3 \cdot BH_3$ (15 kcal/mole), however, a personal communication with Dr. R. A. Marcus, the reference cited in Gmelin, indicated that he had not determined the value nor knew of any such determination.

The dissociation constant (pressure in atm.)

$$K\ (PF_3 \cdot BH_3) = \frac{[p(PF_3)][p(B_2H_6)]^{\frac{1}{2}}}{[p(PF_3 \cdot BH_3)]}$$

was estimated earlier to be nominally 1 at 25°. Estimation of this constant during the course of this study yielded comparable values which Burg and Fu[102] recently confirmed.

Although it was not possible to observe the dissociation constant of $PH_3 \cdot BH_3$ directly, it is estimated that

$$K\ (PH_3 \cdot BH_3) = \frac{[p(PH_3)][p(B_2H_6)]^{\frac{1}{2}}}{[p(PH_3 \cdot BH_3)]} >> 1$$

at 25°. Observations show that the vapor pressure of $PH_3 \cdot BH_3$ is very low at 25°, approximately that of mercury ($\sim 10^{-3}$ mm); since the corresponding dissociation pressure of $PH_3 \cdot BH_3$ is rather large (1400 mm)[93], a very large dissociation constant is indicated. The coordinate bond in $PH_3 \cdot BH_3$ must be very weak.

The qualitative arguments advanced above show that the dissociation constants increase in the order $K\ (PHF_2 \cdot BH_3) < K\ (PF_3 \cdot BH_3) < K\ (PH_3 \cdot BH_3)$ which corresponds to an ordering of donor ability towards borane of $PHF_2 > PF_3 > PH_3$.

D. Conclusions.

The previous discussion has established the relative base strength of PHF_2, PF_3, and PH_3 towards BH_3.

It follows that one would expect the P-B stretching frequencies in these borane adducts to increase directly

with the stability of the P-B bond; however, since the vibrational assignments for these molecules are still tentative, and since the extent of coupling would be undetermined without a complete normal-coordinate analysis, no discussion along these lines will be attempted here.*

An examination of the nmr data (Table 27) obtained for the series $H_3B \cdot PH_xF_{3-x}$ (x = 0,1,3) shows a striking correlation between J_{PB} and the strength of the P-B bond established here [J_{PB}(cps): 49 ($PHF_2 \cdot BH_3$) > 39 ($PF_3 \cdot BH_3$) > 27 ($PH_3 \cdot BH_3$)]. A trend in J_{PB} is also evident for the series $PH_xMe_{3-x} \cdot BH_3$ (x = 0,1-3) [J_{PB}(cps): 64 ($PMe_3 \cdot BH_3$)[104] > 50 ($PHMe_2 \cdot BH_3$)[97] > 43 ($PH_2Me \cdot BH_3$)[105] > 27 ($PH_3 \cdot BH_3$)]; this trend follows the generally accepted order of adduct stability. However, the correlation of J_{PB} with P-B bond strength does not necessarily hold from one acid series to another since J_{PB}(cps) = 174 ($PMe_3 \cdot BF_3$)[104] > 64 ($PMe_3 \cdot BH_3$)[104], where Graham and Stone[7] have shown by displacement that with PMe_3, borane forms a stronger P-B coordinate link than boron trifluoride. Intuitively, it would seem that such a convenient "handle" as the magnitude of the P-B coupling constant should be related to bond order and thus the strength of the coordinate link. However, the terms which contribute to the observed

---

* A vibrational analysis of $PF_3 \cdot BH_3$ has nearly been completed by Dr. R. C. Taylor, University of Michigan. The results give a P-B force constant of about 2.38×10^5 dynes/cm for $PF_3 \cdot BH_3$. A simple diatomic molecule approximation of the P-B force constant in $PH_3 \cdot BH_3$ indicates that it is approximately 1.8×10^5 dynes/cm.

Table 27

NMR Data* for

	$PF_3 \cdot BH_3$ (cps)	$PHF_2 \cdot BH_3$ (cps)	$PH_3 \cdot BH_3$ (cps)
J_{BH}	107	103	104
J_{PF}	1406	1151	—
J_{PH}	—	467	372
J_{PB}	39	49	27
J_{HBPH}	—	4	8
J_{FPBH}	18	26	—
J_{FPH}	—	55	—
J_{PBH}	18	17	16
J_{BPF}	6	—	—
^1H nmr (TMS std)	(ppm)	(ppm)	(ppm)
δ(BH)	0	-0.78	-0.53
δ(PH)	—	-7.68	-4.31
^{19}F nmr (TFA std)			
δ(PF)	-19.9	-21.5	—
^{11}B nmr (TMB std)			
δ(B)	66.6	60.4	60.8

* For an explanation of notation see Appendix A.

value are manifold, can vary in sign, and involve the entire electronic configuration of the molecule[81]; therefore, it is still to be determined whether this correspondence of J_{PB} to P-B bond strength can be justified on other than empirical bases. Similar reasoning leads to the conclusion that no meaningful correlations can be forwarded for the coupling constants which operate over a number of bonds; however, J_{PF}, J_{PH}, and J_{BH} have been related by some investigators to molecular stereochemistry (or orbital hybridization).

As also observed by Heitsch[101] in a more extensive nmr study of boron-containing acid-base adducts, there appears to be no correlation between the ^{11}B chemical shift and adduct stability (Table 27). Phosphorus chemical shifts on the other hand have provided some interesting correlations which will be discussed in the next section in relationship to the nature of the P-B coordinate link.

V. The Nature of the P-B Bond.

Since phosphine and trifluorophosphine form borane adducts which are highly dissociated at 25°, the stability of difluorophosphine borane appears anomolous. At least a two parameter model is necessary to rationalize the presence of the unexpected maximum in base strength at PHF_2 rather than the expected monotonous increase in base strength upon progression from PH_3 to PHF_2 to PF_3. The

qualitative arguments which might expain the anomolous base strength of PHF_2 are legion and unfortunately appear to be just beyond the realm of predictive utility. It must be emphasized that more tenable predictions and theories will result only after more quantitative work has been completed in this field. Nevertheless, some models will be discussed.

One model which might be used to explain the unusual base strength of PHF_2 towards borane might be presented as follows.

Some authors[7,9,11,17-19] maintain that in compounds of borane with phosphines, an H_3 group orbital of π-symmetry can overlap with a vacant $d\pi$-orbital on the phosphorus ligand. Thus, they believe that the P-B coordinate link might have a $d\pi$-$p\pi$ component supplementing the classical σ-bond and thereby enhancing the stability of the adduct. This description of "back-bonding" is parallel to the picture of methyl hyperconjugation except that methyl hyperconjugation leads to an increase in charge separation, whereas π-bonding from the borane group would reduce the charge separation existing in the dative σ-bond. Thus, the existence of "unusual" compounds such as $OC{\cdot}BH_3$ and $F_3P{\cdot}BH_3$ has been attributed to supplementary π-bonding[16-18]. In general, fluorine bonded to phosphorus should increase its ability to π-bond through a removal of negative charge from the phosphorus with a concommitant lowering of the $3d\pi$-electron energy levels

and greater overlap with substituent π-orbitals[106]; therefore, difluorophosphine should show less π-bonding propensity than trifluorophosphine, while certainly such bonding would be minimal for phosphine. Thus, on the basis of the aforementioned π-bonding arguments alone there is no a priori reason to suspect that $PHF_2 \cdot BH_3$ would be more stable than $PF_3 \cdot BH_3$. The stability of difluorophosphine borane relative to $PF_3 \cdot BH_3$ must then be due to a substantial increase in the σ-bond strength. The σ-bond contribution is supposedly essentially non-existent in $PF_3 \cdot BH_3$ and very small in $PH_3 \cdot BH_3$ but increases just enough in $PHF_2 \cdot BH_3$ to effect a synergistic balancing of σ- and π-contributions to adduct stability. The progression of these contributions might be pictured as shown in Figure 43, however, it is emphasized that this curve was arrived at after the fact and a priori considerations based on a combination of σ- and π-bonding probably would not have arrived at this conclusion.

On the basis of bond lengths and heats of formation VanWazer[107] suggested that many four-coordinate phosphorus compounds form multiple bonds which help to reduce the positive charge on the central phosphorus atom. However, if such a reduction in charge separation is necessary for adduct stability, in the fluorophosphine boranes reduction of the positive charge through multiple bonding from the borane group seems far less reasonable to this author than reduction by fluorine which has

Figure 43

Hypothetical Sigma- and Pi-Bonding Contributions to Adduct Stability

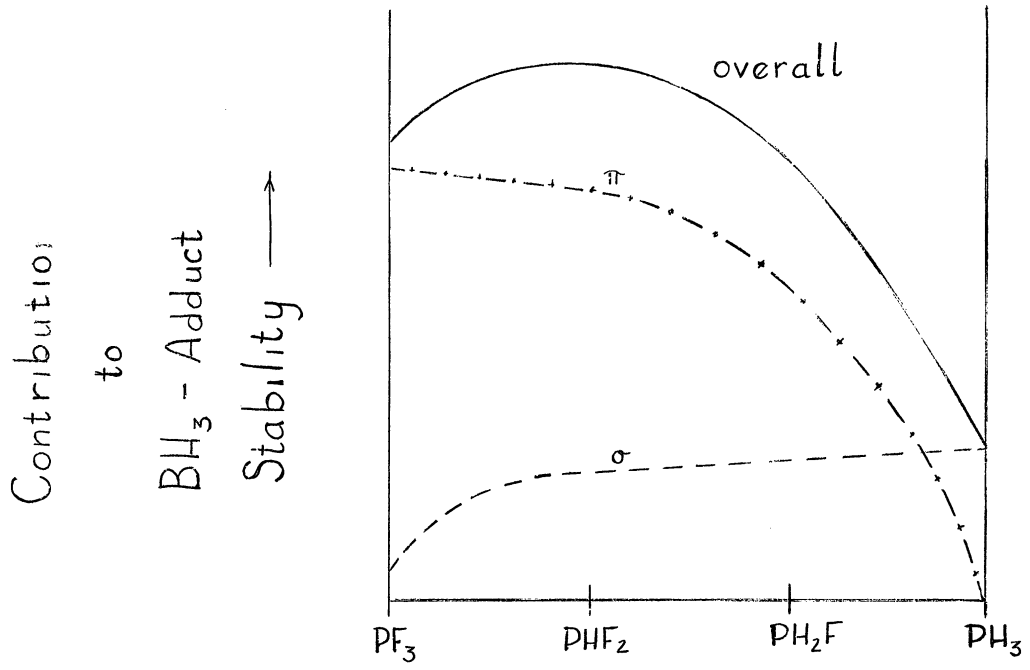

non-bonded electrons available for back-donation. In fact, some authors[106,108] feel that even with the tri-coordinate phosphorus in PF_3 there is considerable degree of multiple bonding which arises in order to compensate for the drift of negative charge through the σ-system to the highly electronegative fluorine atoms. Theoretically, the degree of multiple bonding should increase upon addition of a fourth substituent since the dative bond formation implies an increase in the formal positive charge on phosphorus. If indeed back-coordination is essential for adduct stability, the inability of BH_3 to back-coordinate would also help to explain why $PH_3 \cdot BH_3$ is unstable, for since there are no non-bonded electron pairs in coordinated

PH_3, certainly it cannot be expected to reduce the separation of charge through back-donation (Figure 44). On the other hand in the fluorophosphine boranes the fluorine atoms have non-bonded electron pairs available for multiple bonding (Figure 44).

Figure 44

A Possible Back-Donation Mechanism

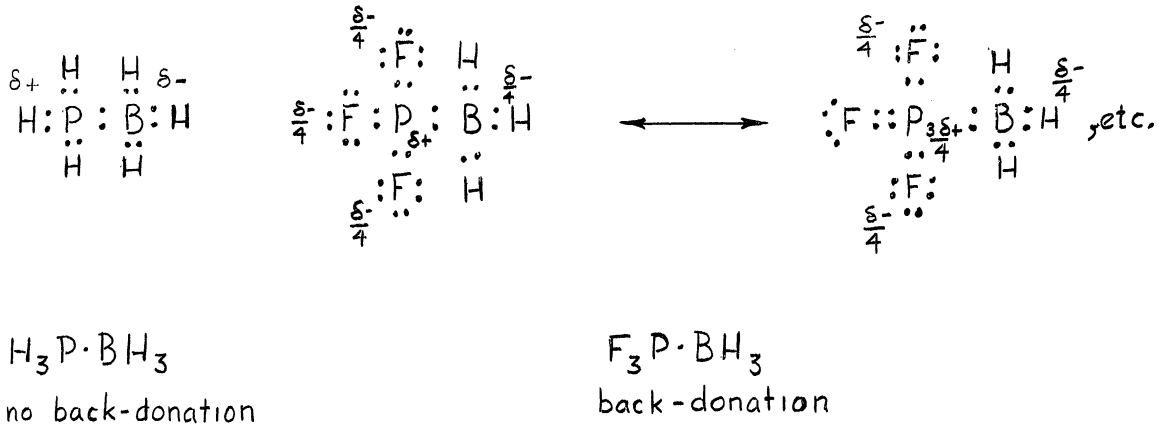

$H_3P \cdot BH_3$
no back-donation

$F_3P \cdot BH_3$
back-donation

The "back-bonding" hypothesis has also been forwarded to explain the "reverse order" of coordination[7,17-19] shown by the borane group (P>N, S>O); however, this "reverse order" has recently been shown to be a function of the strength of the reference Lewis-acid[20]. Thus, the coordinating ability of phosphines and other similar polarizable ligands like sulfides is strongly dependent on the field strength of the reference acid, i.e. the acid of high field strength forms a stronger coordinate link with the more polarizable ligand.

If a model that neglects π-bonding contributions is used, the observed base strength towards borane, $PHF_2 > PF_3 > PH_3$, can be related to the polarizability of the electron pair on phosphorus. The arguments are similar to those forwarded by Weaver and Parry[109] to explain the base strengths of the alkyl amines and the alkyl phosphines. The lone electron-pair on phosphine has a high degree of "s-character" and is tightly held by the three closely bonded protons; thus, the pair has a relatively low polarizability and is not available for the formation of a strong coordinate bond. Since fluorine is bonded at a greater distance than hydrogen and is larger than hydrogen, the substitution of fluorine for hydrogen should have a loosening effect on the lone-pair, albeit the effect would be smaller than for the isoelectronic methyl group because of the electronegativity of the fluorines and the relatively small change in bond distance (for PF_3, P-F = 1.55 Å[52]; PH_3, P-H = 1.42 Å[78]). The electronegative fluorines would also be expected to distort the loosened P-F bonding electrons as well as the phosphorus lone-pair, thus shifting negative charge away from the phosphorus and reducing its σ-bond base strength. In order to fit the observed trend this model requires that the loosening due to the removal of one hydrogen is large and that the tightening by the fluorines becomes effective only in the case of PF_3. The two opposing effects can be pictured as shown in Figure 45. In line with this

Figure 45

Hypothetical Contributions of Fluorine and Hydrogen to Phosphorus Lone-Pair Polarizability

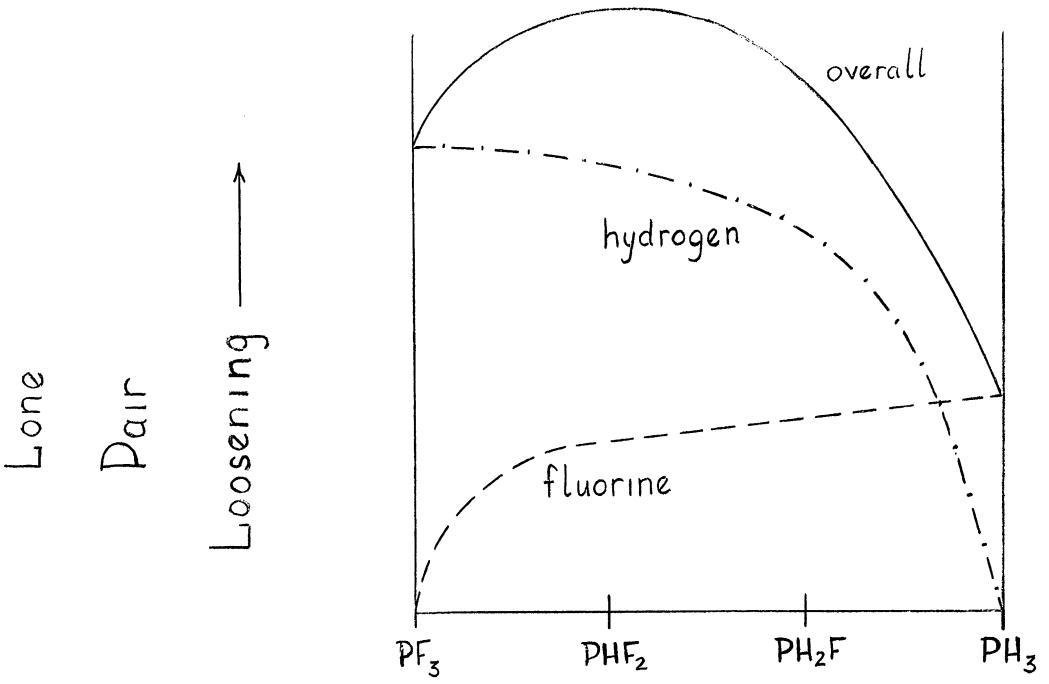

model Weaver and Parry[109] have attributed the increasing base strength in the series PH_3 through PMe_3 to a loosening effect on the electron pair as protons are replaced by methyl groups. The series PH_3 through PF_3 differs importantly in that fluorine is more electronegative than a methyl group. Again the latter trends (Figure 45) are presented after the fact and probably such a marked loosening of the phosphorus lone-pair would not have been anticipated upon replacement of a fluorine in PF_3 with a hydrogen. A mechanism which might cause a loosening effect when one F is replaced by an H is presented below.

An interaction between the protonic hydrogen and the non-bonded electron pairs of the fluorine atoms might

account for the anomolous base strength of difluorophosphine towards borane. Such an interaction can be pictured as reducing the effective positive charge of the hydrogen and thus permitting a distortion of the P-H bonding electrons towards phosphorus and a loosening of the phosphorus lone-pair electrons. In phosphine no such interaction is possible and the protons are very effective in contracting the lone-pair and rendering it essentially unavailable for dative bond formation. Extrapolation of this model to the as yet unknown fluorophosphine, PH_2F, would predict a species with greater base strength than PH_3, probably comparable to that of PF_3, but not as great as PHF_2 since one fluorine could not as effectively attenuate the positive charges of two protons. Although there is no unequivocal evidence for such an H---F interaction in difluorophosphine, the P-H stretching frequency is low (2240.5 vs 2327, 2421 cm^{-1} for PH_3[83]) which in itself is indicative of a reduction in the electron density of the P-H bond; a preliminary vibrational analysis of PHF_2 implies that an appreciable interaction between P-H and P-F motions may exist. An accurate determination of the molecular parameters for PHF_2 will provide an interesting test of the latter model; the proposed interaction would be expected to give rise to short H---F distances, and an F-P-F angle more acute than those in PF_3. The H-P-F angle would probably approximate 90° but the size of the fluorines should preclude H-P-F

angles much smaller than the H-P-H angles in PH_3.

Previously, the correlation of J_{PB} with the strength of the coordinate bond in the methyl phosphine boranes and the fluorophosphine boranes was noted (Table 27). The ^{31}P chemical shifts for the series PH_xF_{3-x} (x = 0,1,3) (Table 28) tend toward lower field with increasing base strength if BH_3 is used as the reference acid; a similar trend is also evident for the methyl phosphines PH_xMe_{3-x} (x = 0,1,2,3) (Table 28). There appears to be general agreement[110-115] that ^{31}P shifts are related to the electrostatic potential produced at the nucleus by the electrons. Such potential is a result of diamagnetic shielding which may be: 1) enhanced by multiple bonding, 2) attenuated by a "second-order paramagnetic term" due to electronic asymmetry around the nucleus, or 3) decreased due to the ionic nature of the bonds induced by electronegative substituents. The trend in the methyl phosphines is probably related primarily to a reduction of the electrostatic potential at the nucleus resulting from replacement of the hydrogens by the larger methyl groups. Such substitution gives rise to a transition from a tight, highly-screening environment around phosphorus to a more diffuse electronic environment providing less shielding. On the other hand, the factors contributing to the ^{31}P chemical shifts of PF_3 and PHF_2 are felt to be more numerous and complex. Since, in direct contradiction to predictions based on electronegativity alone, the PF_3

Table 28

NMR Data* for

	PHF_2	$PHF_2 \cdot BH_3$	PF_3	$PF_3 \cdot BH_3$	PH_3	$PH_3 \cdot BH_3$
^{31}P nmr (OPA std)						
δ(ppm)	-224	-171	-105†	-107	246†	113
Δ (ppm)‡	+53		-2		-133	
^{19}F nmr (TFA std)						
δ (ppm)	42.2	-21.5	-42.3†	-19.9	—	—
J_{PF} (cps)	1134	1151	1441[51]	1406	—	—
J_{PH} (cps)	182.4	467	—	—	182.2[65a]	372

	PMe[112]	$PHMe_2$[112]	PH_2Me[112]	PH_3
^{31}P nmr (OPA std)				
δ (ppm)	62	98.5	163.5	246†

* For an explanation of notation see Appendix A.
† Determined during this study, however, spectra not shown.
‡ $\Delta \equiv (\delta^{P-B} - \delta^{P})$ where δ^{P} = chem. shift of free ligand, and δ^{P-B} = chem. shift of borane adduct.

signal appears at higher field than any of the other phosphorus trihalides, a significant shielding of the phosphorus nucleus due to multiple bonding has been proposed.[110] Since hydrogen is less electronegative than fluorine, replacement of a fluorine with hydrogen in going from PF_3 to PHF_2 would be expected to give a P-substituent bond with less ionic character. The replacement of hydrogen by fluorine should also decrease the degree of multiple bonding due to a concommitant raising of the phosphorus 3d-electron energy levels. Therefore, in comparison with PF_3, it would be difficult to rationalize the low field shift of PHF_2 on the basis of ionic and multiple-bonding differences unless one of these effects is much larger than the other. The latter should enhance the phosphorus shielding while the former decreases it. The low field resonance of difluorophosphine might best be attributed to a marked attenuation of the diamagnetic shielding by the "second-order paramagnetic contribution" which is significant in this case because of the electronic asymmetry around phosphorus.

It is tempting to try to relate the phosphorus chemical shifts mentioned above (Table 28) to the polarizability of the phosphorus lone-pair and therefore the relative base strength within both series towards borane. The comparison seems tenable in the case of the methyl phosphines but may be fortuitous in the case of PHF_2, PF_3 and PH_3 in the light of the many variables which can

affect the chemical shift. Additional data are needed to test the correlation.

When a phosphine ligand forms a coordinate bond with a Lewis-acid like borane, there usually appears to be significant decrease in the shielding of the phosphorus due to the attraction of the lone-pair electrons by the acid - what might be termed a rehybridization of the phosphorus bonding orbitals or a loosening of the lone-pair electrons occurs. Therefore, a shift in the phosphorus resonance of the coordinated phosphine to lower field relative to the free ligand would be expected, i.e., the quantity defined as $\Delta \equiv [\delta^{P-B} - \delta^{P}]$ (where δ^{P} = chem. shift of free phosphine-ligand and δ^{P-B} = chem. shift of borane adduct) would be negative. Meriwether and Leto[114] found this to be true for the great majority of nickel-carbonyl-phosphine complexes they studied. No such data could be found for other phosphine complexes, but it is interesting to anticipate the results in the case of the methyl phosphine boranes. Weaver and Parry[109] contend that the lone-pair in PH_3 is tight and relatively hard to polarize while for PMe_3 the polarizability is greater and the lone-pair more diffuse. However, the arguments of Weaver and Parry[109] do not describe the change in the phosphorus lone-pair upon coordinate bond formation. Since coordination of BH_3 to PH_3 requires a considerable "drawing-out" of the lone-pair, the phosphorus deshielding effect should be large, i.e., a large negative Δ.

Similarly, increasingly smaller changes in deshielding are anticipated upon progression through PH_2Me to $PHMe_2$ and PMe_3 because of the greater ease (Smaller lone-pair perturbation) with which the P-B dative bond formation occurs. Thus, the negative Δ-values are predicted to become increasingly smaller in going from $PH_3 \cdot BH_3$ to $PMe_3 \cdot BH_3$.

During the present work the ^{31}P nmr spectra (Figure 46) and the quantity Δ were determined for $PH_3 \cdot BH_3$, $PF_3 \cdot BH_3$, and $PHF_2 \cdot BH_3$. The Δ-values do not show a regular decrease in negative value with increasing P-B bond strength as predicted above for the methyl phosphine series. However, the large negative Δ-value for $PH_3 \cdot BH_3$ (Δ = -133 ppm) is indicative of the large change in hybridization and loosening of the lone-pair required for coordination in the case of PH_3; this change from $\sim p^3$ to $\sim sp^3$ is also implied upon comparison of the P-H coupling constants of PH_3 and $PH_3 \cdot BH_3$ (Table 28), the increase in J_{PH} indicating more "s-character" in the bonding-orbitals. Since the lone-pair in PF_3 is probably slightly more diffuse that in PH_3, and since it must protrude somewhat, smaller changes in hybridization would be anticipated on coordination to BH_3. The small negative Δ-value for $PF_3 \cdot BH_3$ (Δ = -2 ppm) indeed implies a slight change which is substantiated by the similarity in the P-F coupling constants for PF_3 and $PF_3 \cdot BH_3$ (Table 28). The positive Δ-value for $PHF_2 \cdot BH_3$ (Δ = 53 ppm) is somewhat surprising. It might be attributed by some to a

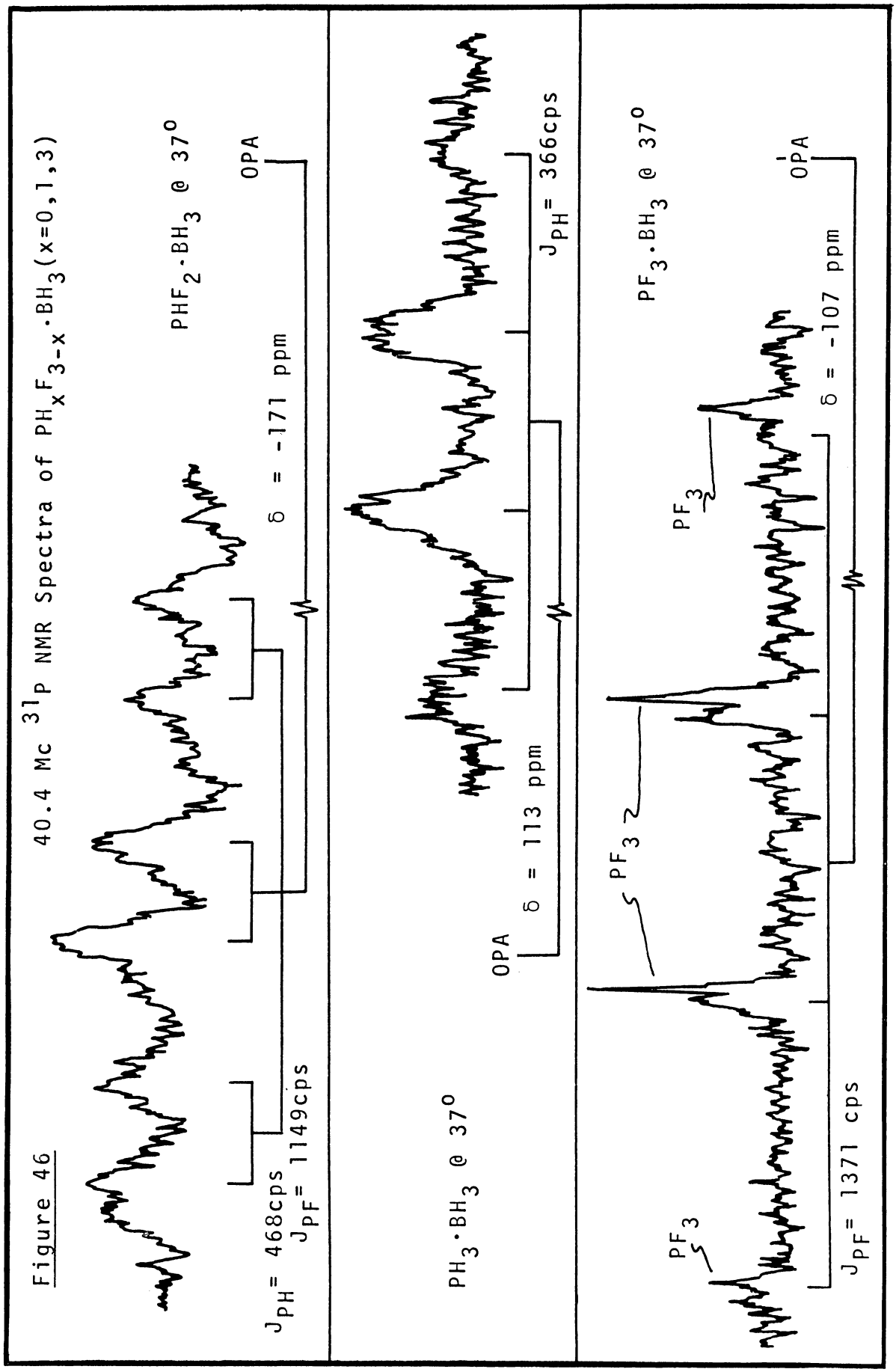
Figure 46
40.4 Mc ^{31}P NMR Spectra of $PH_xF_{3-x}\cdot BH_3$ (x=0,1,3)
$PHF_2\cdot BH_3$ @ 37°
OPA
δ = -171 ppm
J_{PH}= 468cps
J_{PF}= 1149cps
$PH_3\cdot BH_3$ @ 37°
OPA
δ = 113 ppm
J_{PH}= 366cps
$PF_3\cdot BH_3$ @ 37°
PF_3
PF_3
OPA
δ = -107 ppm
J_{PF}= 1371 cps

compensation of the phosphorus deshielding through back-donation from the BH_3. Alternatively, the electronic symmetry about a four-coordinate phosphorus should be greater than about a three-coordinate one. Hence the positive Δ-value for $PHF_2 \cdot BH_3$ could be attributed to the existence of a relatively small paramagnetic contribution to the phosphorus chemical shift in $PHF_2 \cdot BH_3$ as opposed to a large paramagnetic contribution for difluorophosphine itself. Upon coordination, a large change in the electron environment of the phosphorus in PHF_2 is also implied by comparison of the ^{19}F chemical shifts for the free and coordinated PHF_2 ligand (Table 28). Extrapolating from the theory of Saika and Slichter[116] for ^{19}F chemical shifts, this shift of the fluorine signal to lower field upon coordination of PHF_2 points to a change to more covalent P-F bonds in the borane adduct. The fluorine environments must be similar in both $PHF_2 \cdot BH_3$ and $PF_3 \cdot BH_3$, judging from the closeness of their chemical shifts (Table 28). There is also other evidence of a change in hybridization upon coordination of PHF_2 to BH_3 since the P-H coupling constant changes from 183 to 467 cps, indicative of more "s-character" in the P-H bond after coordination.

VI. Summary.

The new mixed phosphorus halide, PF_2I, was characterized and used as a reactive starting material in two new synthetic routes to difluorophosphine ligands via metathetic and coupling reactions. The new species, PF_2CN, F_2POPF_2, P_2F_4, and PHF_2, were characterized and some of the chemistry of PHF_2 investigated. Difluorophosphine was found to form an interesting borane adduct $PHF_2 \cdot BH_3$ which is more stable than either $PH_3 \cdot BH_3$ or $PF_3 \cdot BH_3$. Further study showed that the relative base strength towards borane decreases in the order $PHF_2 > PF_3 > PH_3$. Rationale for the order was presented. Spectroscopic studies which yielded infrared, Raman, and ^{1}H, ^{19}F, ^{11}B, and ^{31}P nmr data for many of the compounds were also completed and discussed in relationship to structure and bonding.

Experimental

I. General Procedures.

The compounds investigated were handled in a high-vacuum system. High-vacuum techniques such as pressure volume measurements, vapor density determinations, etc. are adequately discussed elsewhere[117, 118]. All stopcocks and standard-taper joints were greased with Apiezon-N. In order to minimize the contact of reactive materials with mercury, manometers were isolated from the system with stopcocks. Non-volatile materials were handled in an atmosphere of dry nitrogen.

II. Starting Materials.

Dimethylaminodifluorophosphine was made in a manner similar to that described by Schmutzler[29] by the fluorination of dimethylaminodichlorophosphine with NaF in a suspension of tetramethylene sulfone.

Hydrogen Iodide was prepared as outlined in the literature[119] by the reaction of iodine and 1,2,3,4-tetrahydronaphthalene.

Dimethylamine was obtained from Matheson Co., Inc. and passed through a -78° U-tube before use.

Diborane was kindly supplied by Callery Chemical Co.; it was purified by fractional condensation.

Phosphine was prepared by the pyrolysis of phosphorus acid[120] at 200-250°.

Phosphine Borane was formed at -105° from the combination of liquid diborane and phosphine[93]. When the desired amount of product had formed the excess reactants were pumped from the tube which was maintained at -78°.

Trifluorophosphine was obtained from the Ozark Mahoning Co. and purified by passing it through a -160° trap before use.

Trifluorophosphine Borane of high purity was donated by R. J. Wyma of Dr. R. C. Taylor's research group.

Nickel Tetracarbonyl did not require further purification as obtained from the Matheson Co., Inc.

In general, volatile materials were checked for purity before use by vapor pressure, molecular weight, and/or infrared spectroscopy.

Cuprous Oxide (Baker & Adamson reagent grade) and Cuprous Cyanide (Baker & Adamson technical grade) were used without further purification.

Mercury was triply distilled in Dr. R. C. Taylor's laboratories.

III. Preparation and Reactions of PF_2I.

A. Preparation.

In a typical experiment difluoroiodophosphine, PF_2I, was prepared by separately condensing 12.76-mmoles of F_2PNMe_2 and 25.52-mmoles of HI into a 1000 cc reaction bulb equipped with a stopcock. The bulb was then allowed

to warm slowly to 25°. Reaction was indicated by the formation of clouds of pale red-yellow solids. The bulb was allowed to stand at 25° for 15 min. after the clouds had settled and then the volatile products were separated by fractional condensation (-126°, -196°). The desired difluoroiodophosphine (11.96-mmoles) was retained at-126° while PF_3 (0.25-mmole) passed through the -126° trap and was held at -196°. It is important to use exact stoichiometric amounts of HI and F_2PNMe_2 if pure PF_2I is desired since it is difficult to separate PF_2I and F_2PNMe_2, and since excess HI appears to promote the decomposition of PF_2I in the liquid state.

A 244.6 mg. sample of PF_2I was hydrolyzed in 25 ml. of 40% NaOH and the solution analyzed for P, F, and I by Huffman Laboratories, Inc., Wheatridge, Colo.; results are given in the Discussion.

B. Reaction of PF_2I and Cu_2O - Synthesis of F_2POPF_2.

A 40 cc reaction tube equipped with a stopcock was charged with ~0.5 g. Cu_2O (3.5-mmoles), attached to the vacuum system, evacuated, and PF_2I (1.07-mmoles) condensed into the tube. The contents of the tube were allowed to warm to 25° and cooled to -196° several times. Reaction was evidenced by the formation of tan solids. Finally, the volatile products were removed from the vessel by pumping through a series of traps held at -112, -145, and -196°. It was necessary to heat the tube to ~150° with a hot-air gun to remove the last trace of products. Retained

at -112° was 0.05-mmole of an unidentified material; PF_3 (0.04-mmole) was stopped at -196°. The desired F_2POPF_2 (0.39-mmole) corresponding to 73% yield based on the amount of PF_2I taken was removed from the -145° trap. The x-ray powder photograph of the solids remaining in the tube was consistent with a mixture of CuI and Cu_2O. The preparation was also carried out on a considerably larger scale with somewhat smaller yields.

C. Reaction of PF_2I and CuCN - Synthesis of PF_2CN.

A reaction tube (70 cc) was charged with ~1 g. (11-mmoles) of CuCN by shaking the powder through a piece of polyethylene tubing which had been inserted into the vessel through the 4 mm vacuum stopcock. The tube was placed on the vacuum system and 1.39-mmoles of PF_2I were condensed onto the powder. After repeatedly warming to 25° and cooling to -196° the volatile products were removed from the tube and separated by fractional condensation (-95, -126, -196°). It was necessary to heat the reaction vessel to ~150° with a hot-air gun to remove the last trace of product. The -196° trap contained 0.31-mmole of PF_3 while an undetermined amount of unreacted PF_2I was held at -126°. Cyanodofluorophosphine (0.44-mmole) was retained at -95° which corresponds to a 32% yield based on the PF_2I taken.

D. Reaction of PF_2I and Mercury - Synthesis of P_2F_4.

Difluoriodophosphine (2.39-mmoles) was condensed into a 1000 cc bulb equipped with a stopcock and containing 2 cc of mercury. The bulb and contents were slowly warmed to 25°, removed from the vacuum system, and shaken. A discoloration of the mercury and formation of yellow and gray solids indicated reaction. After 4 hr. of shaking, the bulb was attached to the system and the volatile contents removed by pumping through U-tubes maintained at -112, -126, and -196°. The -196° fraction was 0.10-mmole of PF_3 while 0.30-mmole of unreacted PF_2I (contained undetermined amount of F_2PNMe_2) was retained at -112°. The desired P_2F_4 (0.97-mmole) slowly passed through the -112° trap and was held at -126°. This corresponds to a 93% yield based on the amount of PF_2I which reacted.

Another experiment was conducted in which the initial PF_2I pressure was higher. Difluoroiodophosphine (0.84-mmole) was shaken with mercury in a 35 cc reaction tube. After 21 hrs. the volatiles were investigated and found to consist entirely of PF_3 (0.52-mmole). Perhaps the additional reaction time in the latter experiment precluded the observation of P_2F_4, or the PF_2I disproportionated under influence of mercury at the higher pressure.

E. Reaction of PF_2I, HI and Mercury - Synthesis of PHF_2.

A 2 cc sample of mercury was placed in a 70 cc reaction tube which was equipped with a stopcock and

standard taper joint. The tube was evacuated and 3.36-mmoles of PF_2I and 3.36-mmoles of HI were condensed into the tube at -196°. After warming to 25° the tube was shaken for 1.5 hr. The tube was then opened to the Toepler system through two -196° traps and 0.17-mmole of H_2 (identified by gas density) was recovered. The products condensable at -196° were passed through traps at -140, -160, and -196°. A 0.72-mmole sample of PF_3 was trapped at -196° and a 0.47-mmole sample of an unstable compound assumed to be $PHF_2 \cdot HI$ was retained at -140°. This latter compound decomposed upon warming to room temperature to yield PF_3, SiF_4, and yellow solids which contained iodine. A 1.85-mmole sample of the desired PHF_2 was retained in the trap at -160°. Another run using 1.52-mmoles of each reagent gave 0.84-mmole of PHF_2, 0.30-mmole of PF_3, 0.10-mmole of H_2, and 0.18-mmole of the unstable species retained at -140° as products. A satisfactory mass balance is obtained for each run if one assumed that PF_3 was formed by $3PF_2I \rightarrow 2PF_3 + PI_3$ and that the unstable material stopped at -140° was $PHF_2 \cdot HI$. Run 1: mmoles in: P, 3.36; F, 6.72; H, 3.36; mmoles out: P, 3.40; F, 6.80; H, 3.13. Run 2: mmoles in: P, 1.52; F, 3.04; H, 1.52; mmoles out: P, 1.47; F, 2.94; H, 1.40.

The x-ray powder pattern of the gray solids formed during the reaction was consistent with that of Hg_2I_2.

A sample of difluorophosphine (0.81-mmole) was

pyrolyzed over chunks of uranium metal. The hydrogen evolved (0.41-mmole) was identified by gas density.

IV. Reactions of PHF_2.

A. Hydrolysis of PHF_2.

Difluorophosphine (0.49-mmole) was condensed into a tube containing 10 ml. of 40% NaOH and then the tube was sealed off and held at 100° for 2 hrs. After opening the tube 0.44-mmole of H_2 was recovered in the Toepler system. In a similar experiment involving PDF_2 the hydrogen evolved on hydrolysis was found to contain no deuterium by mass spectroscopic analysis.

In a separate experiment, water vapor (0.32-mmole) was allowed to mix with PHF_2 vapor (0.43-mmole) at 25° in a 500 cc bulb. The only volatile recovered after 15 min. of reaction was silicon tetrafluoride (0.17-mmole).

B. Aminolysis of PHF_2.

The reaction vessel consisted of two bulbs (50 and 500 cc) separated by a stopcock so that the reactants could be introduced into each bulb separately and then mixed as gases by opening the stopcock. In one experiment 0.36-mmole of PHF_2 was condensed into the 50 cc bulb and 0.36-mmole of $HNMe_2$ was introduced into the 500 cc bulb. Upon mixing the gaseous reactants at 25°, white clouds formed which turned pale yellow-brown upon settling. After 10 min. the volatile products were fractionated

(-145, -196°); a trace amount of PF_3 was isolated at -196° and an unstable species thought to be $FHPNMe_2$ (0.16-mmole) remained at -145°. A preliminary characterization of the latter species is presented in the Discussion Section.

In two other experiments the $HNMe_2/PHF_2$ ratio was increased and the major product produced appeared to be $HP(NMe_2)_2$ as shown in the Discussion Section. In one case 1.08-mmoles of PHF_2 were mixed with 1.95-mmoles of $HNMe_2$ in the same manner as described in the previous experiment. Again a trace amount of PF_3 was separated by passage through a -135° into a -196° trap. Stopped at -135° was 0.93-mmole of an unstable mixture which was difficult to cleanly free of excess dimethylamine; however, a rough separation could be obtained by fractional condensation at -95 and -135°, the supposed $HP(NMe_2)_2$ being retained at -95°. Similar results were obtained when 0.55-mmole of PHF_2 was mixed with 2.08-mmoles of $HNMe_2$. Because of the instability of the species further experiments were not undertaken.

C. Reaction of PHF_2 and B_2H_6.

Diborane (1.94-mmoles) and difluorophosphine (1.92-mmoles) were condensed into a 150 cc vessel attached to a manometer and allowed to warm to 25°. After 4 hr., when the pressure in the vessel had become constant at about $\frac{3}{4}$ its calculated initial value, the products were separated by fractional condensation (-135, -196°). Retained in the

-135° trap was $PHF_2 \cdot BH_3$ (1.57-mmoles). A mixture of B_2H_6 and PF_3 (1.35-mmoles) was stopped at -196°. The amount of PF_3 was estimated to be about 0.20-mmole from the infrared spectrum of the mixture. A small amount of yellow solid and a trace of noncondensable gas were also formed during the reaction.

D. Reaction of PHF_2 and $Ni(CO)_4$.

Nickel tetracarbonyl (0.43-mmole) and difluorophosphine (2.00-mmoles) were separately condensed into a 40 cc reaction tube equipped with a stopcock. The reactants were warmed to and held at -23° for 3 hrs. The rate of evolution of noncondensable gas increased after warming the tube to 0° where it was maintained for 17 additional hours, and finally after 18 hrs. at 25° the evolution of CO had ceased and the products were recovered by fractional condensation (-112, -196°). Carbon monoxide (0.32-mmole identified by gas density) was collected in the Toepler system while 1.86-mmoles of unreacted PHF_2 were retained at -196°. A difluorophosphine derivative of $Ni(CO)_4$ thought to be $(PHF_2)Ni(CO)_3$ was recovered from the -112° fraction (0.15-mmole). Characterization of the latter species is mentioned in the Discussion.

The ratio of reactants was varied in another experiment in which 2.05-mmoles of $Ni(CO)_4$ and 1.86-mmoles of PHF_2 were allowed to react at 25° for 2 hrs. in a 40 cc tube. Carbon monoxide (1.34-mmoles) was displaced in this time. Fractionation (-112, -195°) showed that all the PHF_2

had reacted. An undetermined mixture of difluorophosphine substituted nickel carbonyls was retained at -112° (the sample was inadvertantly lost). Passing the -112° trap was an appreciable amount of SiF_4 (ca. 0.5-mmole). In this and in the previous experiment, appreciable amounts of black, non-volatile oils remained behind. Thus, it is felt that side-reactions also occurred.

V. Base Displacement Reactions.

A. PHF_2 and $PF_3 \cdot BH_3$.

In a typical experiment, 0.59-mmole of PHF_2 was condensed into a 40 cc tube with 0.83-mmole of $PF_3 \cdot BH_3$. The tube was maintained at -78° for 25.5 hrs. after which time 0.34-mmoles of PF_3 was isolated (57% yield). Everything was condensed back into the tube and the reaction allowed to proceed for 24.5 additional hours at -45° before the products were finally separated by fractional condensation (-126, -160, -196°). Trifluorophosphine (0.58 —mmole) passed through the -160° trap, while $PF_3 \cdot BH_3$ (0.22-mmole) was retained at -160°. Difluorophosphine borane (0.57-mmole, 97% yield) was retained at -126°. The best separation was effected when distillation through the -126° U-tube was rapid. Upon prolonged standing at -126°, $PHF_2 \cdot BH_3$ slowly passes to colder regions.

B. PHF_2 and $PH_3 \cdot BH_3$.

Phosphine borane (1.93-mmoles) and difluorophosphine

(0.91-mmole) were condensed into a 43 cc reaction tube. The tube was maintained at -23° for 5.5 hrs. after which time the products were recovered; it was found that displacement had not proceeded to an appreciable extent. Everything was condensed back into the tube and maintained at 0° for 12 additional hrs. The tube was then cooled to -78° and the volatiles removed through U-tubes held at -126, -160, and -196°. A very small amount of H_2 (0.02-mmole) passed through the -196° trap which held a 0.96-mmole mixture of PH_3 and PF_3 plus a trace of B_2H_6. This mixture weighed 34.4 mg. which indicates that it contained ca. 0.04-mmole PF_3 and ca. 0.91-mmole PH_3. All of the PHF_2 had been consumed as indicated by the fact that nothing was retained at -160°. The -126° trap held 0.84-mmole of $PHF_2 \cdot BH_3$. The solids left in the reaction tube were composed of a small amount of a non-volatile yellow species and 0.97-mmole of $PH_3 \cdot BH_3$. The latter decomposed on warming to room temperature to give a mixture (1.46-mmoles) of B_2H_6 and PH_3.

When the displacement of PH_3 from $PH_3 \cdot BH_3$ by PHF_2 was attempted at lower temperatures and/or higher pressures, it was complicated by an increased amount of disproportionation as indicated by the formation of appreciable amounts of PF_3 and non-volatile yellow solids. Under these conditions the displaced PH_3 appeared to react with free PHF_2 to give an unstable species which has not been characterized completely but which does display

spectral characteristics similar to those attributed to $PHF_2 \cdot HI$.

C. PH_3 and $PF_3 \cdot BH_3$.

Trifluorophosphine borane (1.00-mmole) was condensed into a 43 cc reaction tube equipped with a stopcock. Phosphine (1.82-mmoles) was also added to the tube which was then warmed to -78° for 4 hrs., however, the reaction proceeded only slowly at this temperature. After an additional 10 hrs. at -35°, separation of the products showed that 0.56-mmole of PF_3 had been displaced. All the products and reactants were returned to the tube which was then maintained at 0° for 16 additional hrs. Finally, the products were separated (-112, -160, -196°). A mixture (1.91-mmoles) of PF_3 and PH_3 (trace of B_2H_6) which weighed 109.4 mg. passed the -160° trap. Retained at -160° was 0.13-mmole of $PF_3 \cdot BH_3$. The -112° trap contained a white solid characteristic of $PH_3 \cdot BH_3$. A mass balance of products and reactants indicates that 87% of the PF_3 was displaced under these conditions according to the equation

$$PF_3 \cdot BH_3 + PH_3 \rightarrow PF_3 + PH_3 \cdot BH_3.$$

A similar experiment was conducted, but trifluorophosphine was added to the system in order to test its effect on the extent of displacement. Equal amounts (0.99-mmole) of $PF_3 \cdot BH_3$, PH_3 and PF_3 were held at -35° for 10 hrs.; separation of the products and reactants

indicated that 27% of the PF_3 was displaced. Everything was returned to the reaction tube and maintained at 0° for an additional 20 hrs. Separation yielded 2.17-mmoles of a mixture (weight 153.9 mg.) of PF_3 and PH_3 (trace of B_2H_6), plus 0.51-mmole of $PF_3 \cdot BH_3$. Thus only 48% of the PF_3 was displaced under these conditions.

Appendix A

Spectroscopic Notation and Procedures

Infrared Spectra. Unless otherwise noted the spectra were obtained with a Beckman IR-12 which operates in the 4000 - 200 cm^{-1} range. The precise vibrational frequencies listed in the Tables were determined by recording each band under high dispersion. A gas cell with a 75 mm path length and CsI windows which were held in place against O-ring seals by atmospheric pressure was used for volatile substances. The infrared spectra of solids were observed at ca. -180° in transmission through a thin film sublimed onto the CsI window of a cold cell similar to that described by Wagner and Hornig[121].

Raman Spectra. Pure liquids were distilled into 2 mm i.d. capillary tubes fitted with flat ends suitable for transmission of the scattered light; the $PH_3 \cdot BH_3(\ell)$ sample was prepared *in situ* as the solid (m.p. 33°) and warmed to 35° for the Raman spectrum; the unreacted diborane and phosphine were removed before the capillary tube was sealed. For solid $PH_3 \cdot BH_3$ the sample was also prepared as just described in a 5 mm o.d. pyrex tube and transferred to a cell designed especially for the determination of the Raman effect of solids at -180°. The spectra were graciously determined by C. F. Farran; further description

of experimental details and equipment design may be found in his thesis[122]. The Raman spectra displayed in this text are microdensitometer traces of the photographic plates.

Notation for Vibrational Spectra. The following abbreviations and symbols are used in the Tables: ν, stretching; δ, deformation; ω, wagging; ρ, rocking; τ, torsional; as, asymmetric; s, symmetric; p, polarized; dp, depolarized. For intensities and band shapes: br, broad; sh, shoulder; v, very; s, strong; m, medium; w, weak. P, Q, and R refer to band shapes reminicent of typical P, Q, and R branches arising from vibrational-rotation interaction.

NMR Spectra. The spectra were determined on Varian Associates NMR Spectrometers. Most of the ^{1}H nmr spectra were obtained on the A-60. The spectra of other nuclei were determined by coupling the HR-100 with the appropriate radiofrequency unit i.e., ^{11}B (32.1 Mc), ^{19}F (94.1 Mc), and ^{31}P (40.4 Mc). In a few cases where the chemical shifts of non-equivalent hydrogens overlapped, the hydrogen spectra were obtained at 100 Mc so that the signals were separated sufficiently for easy interpretation. Conditions such as sample temperature and radiofrequency are included with the individual spectra. Samples were prepared by condensing the pure substances into 5 mm o.d. semi-micro nmr tubes (NMR Specialities, Inc., New Kensington, Pa.)

and sealing the tube under vacuum. However, in the case of $PH_3 \cdot BH_3$ the solid was prepared in situ from stoichiometric amounts of PH_3 and B_2H_6; it melted at 33° without evidence of significant decomposition.

Signal separations were measured by calibrating the sweep with side bands of a known frequency except in the case of the proton spectra determined on the A-60 where the sweep is internally calibrated. Chemical shifts were obtained by tube interchange.

NMR Notation. Coupling constants, J, are expressed in cycles per second, cps; their assignment is indicated by the appropriate subscript, i.e., J_{PBH} refers to the interaction between phosphorus and hydrogen nuclear spins across two bonds, the P-B and the B-H bonds. Chemical shifts, δ, were calculated according to the equation(81)

$$\delta = \frac{H_{sample} - H_{reference}}{H_{reference}}$$

and are reported in parts per million, ppm. Thus, relative to the appropriate standard, low field shifts are negative and high field shifts are positive. The following abbreviations are used for chemical shift standards: TMS = tetramethylsilane, ^1H nmr; TFA = trifluoroacetic acid, ^{19}F nmr; TMB = trimethylborate, ^{11}B nmr; OPA = 85% orthophosphoric acid, ^{31}P nmr.

Mass Spectra. A Consolidated Electrodynamics Model 21-103 B Mass Spectrometer operating at 70 eV was used

to obtain the spectra. Unstable samples were maintained at -196° until just before injection into the spectrometer. In general the spectra were not determined below m/e ≈ 12 - 14. For the spectra given in the tables all peak heights were adjusted relative to the most intense peak which was taken as 100.

EPR Spectra. The spectra were graciously determined by Dr. J. Gendell on his Varian Instrument. The signals observed for P_2F_4 were fairly broad, 6 - 60 gauss. Samples were contained in 3 mm o.d. quartz or pyrex tubes.

Appendix B

Band Shape Analysis For Difluorophosphine

Assuming the following molecular parameters

$PF = 1.52\ \text{Å}$ $\quad\quad$ $\angle FPF = 90°$

$PH = 1.52\ \text{Å}$ $\quad\quad$ $\angle FPH = 100°$

the principal moments of inertia for PHF_2 were calculated with the aid of a computer program kindly supplied by C. F. Farran; the calculated values are given below in g. $cm^2 x 10^{40}$:

I_A	I_B	I_C
22.79	45.95	64.66

The principal axes fall roughly as shown in Figure 47.

Figure 47

Principal Axes of PHF_2

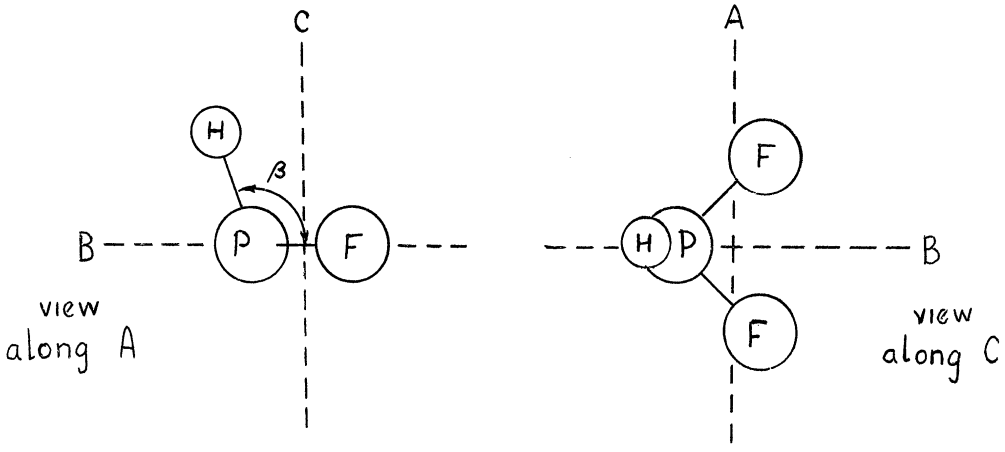

The moments of inertia are essentially independent of β, the FPH angle, and are not changed markedly by alternation of the FPF angle between 90 and 110°. Thus, difluorophosphine appears to be an asymmetric top ($I_A \neq I_B \neq I_C$). Three types of band outlines, or hybrid combinations of these, are observed for asymmetric top molecules; they are classified as A, B, and C types depending along which principal axis the vibration occurs[66,123,124]. In Figure 48 the expected band outlines for ν_sPH and δ_sFPF are summarized with respect to type (A, B, or C) for both the planar and pyramidal geometries of PHF_2. The band

Figure 48

Band Shape and Type for

	ν_sPH	δ_sFPF
planar PHF_2	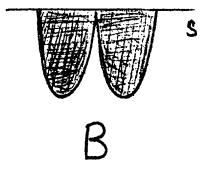	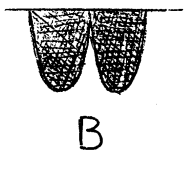
pyramidal PHF_2	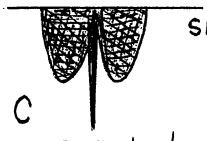	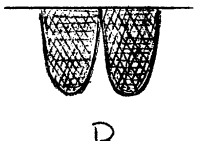
observed	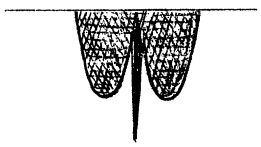	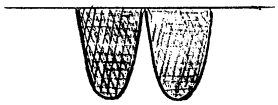

shapes actually observed in the infrared spectrum of gaseous PHF_2 (Figures 20 & 48) are consistent with the pyramidal geometry. If PHF_2 were planar, the P-H stretching motion would not be expected to show a strong central maximum typical of a Q-branch. The other fundamental vibrations of PHF_2 give rise to bands which overlap, complicating such straightforward analysis as presented above.

Appendix C

The C-N Stretching Vibration in PF_2CN

Using the following molecular parameters

PF = 1.52 Å	∠ FPF = 95°
PC = 1.78 Å	∠ FPC = 93°
CN = 1.15 Å	∠ PCN = 180°

the principal moments of inertia for PF_2CN were calculated on the computer. The values are given below in g. $cm^2 x 10^{40}$ along with the respective rotational constants in cm^{-1}.

I_A	I_B	I_C
64.17	146.58	177.87

A	B	C
0.44	0.19	0.16

The C-N stretching frequency for PF_2CN (Figure 49) displays an interesting series of lines spaced 2.3 cm^{-1} which were at first attributed to vibration-rotation interaction, however, this spacing is too large to be consistent with the moments of inertia listed above for pyramidal PF_2CN. In fact, additional calculations show that the spacing is too great to be attributed to the planar or any other reasonable structure for PF_2CN. Irrespective of a planar or pyramidal configuration for PF_2CN, the calculations also indicated that the molecule

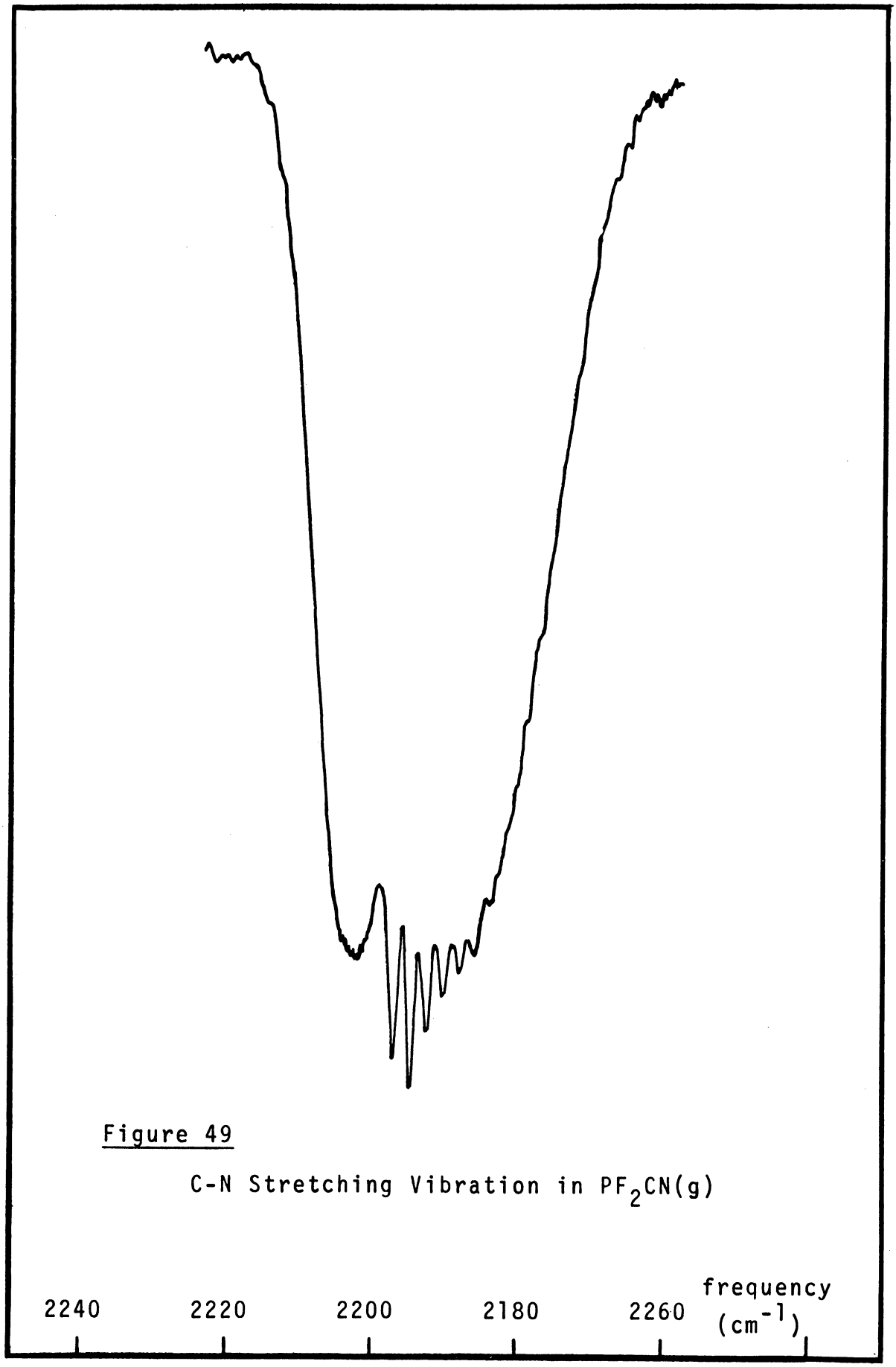

Figure 49

C-N Stretching Vibration in $PF_2CN(g)$

is probably an asymmetric top with the C-N stretch occurring along the axis of least moment of inertia (A axis). Therefore, the C-N stretch should show a strong central Q-branch (A-type band for asymmetric top[66,123,124]). The band observed in the C-N region appears to be the superposition of a typical PQR-structure and several additional Q-branches to the low frequency side of the main Q-branch. The additional Q-branches are probably due to "hot" bands[124] which arise when an appreciable number of molecules exist in a vibrationally excited state. Such a vibrationally excited state may be populated by a low frequency vibration. By roughly fitting the intensities of the "hot" bands (each successive "hot" Q-branch was estimated to have 0.42 the absorbance of the previous) to a Boltzmann distribution the energy of the low frequency vibration responsible for the "hot" bands was estimated as 180 cm^{-1}.

Appendix D

Analysis of $X_2AA'X'_2$ Systems

Harris[125] has recently derived expressions for the line positions and relative intensities in the X spectrum of an $X_nAA'X'_n$ nuclear magnetic system when $J_X = 0$ (J_X is the coupling between nuclei of X and X' types). The expressions are valid only for nuclei of spin $\frac{1}{2}$. Analysis of the ^{19}F nmr spectrum of F_2POPF_2 was possible using the expressions of Harris; the calculations are outlined below. Unfortunately, expressions applicable to the ^{31}P nmr spectrum of F_2POPF_2 were not outlined by Harris. Lack of time precluded the application of the less explicit expressions of Lynden-Bell[65b] which do apply to the ^{31}P nmr spectrum.

According to Harris for an $X_nAA'X'_n$ system there <u>may</u> be a total of $(2n + 1)$ pairs of lines symmetrically placed about ν_X, where ν_X is the unperturbed resonance frequency of X and X'. For F_2POPF_2, $2n + 1 = 5$, and three pairs of lines were observed in the fluorine nmr (Figures 9 and 50); the calculations outlined below show that one of the remaining pair has zero intensity and the other remaining pair was unresolved under other lines.

If the expressions of Harris are valid in the case of F_2PPF_2, up to five pairs of lines would also be expected in the ^{19}F nmr spectrum. In fact, at least

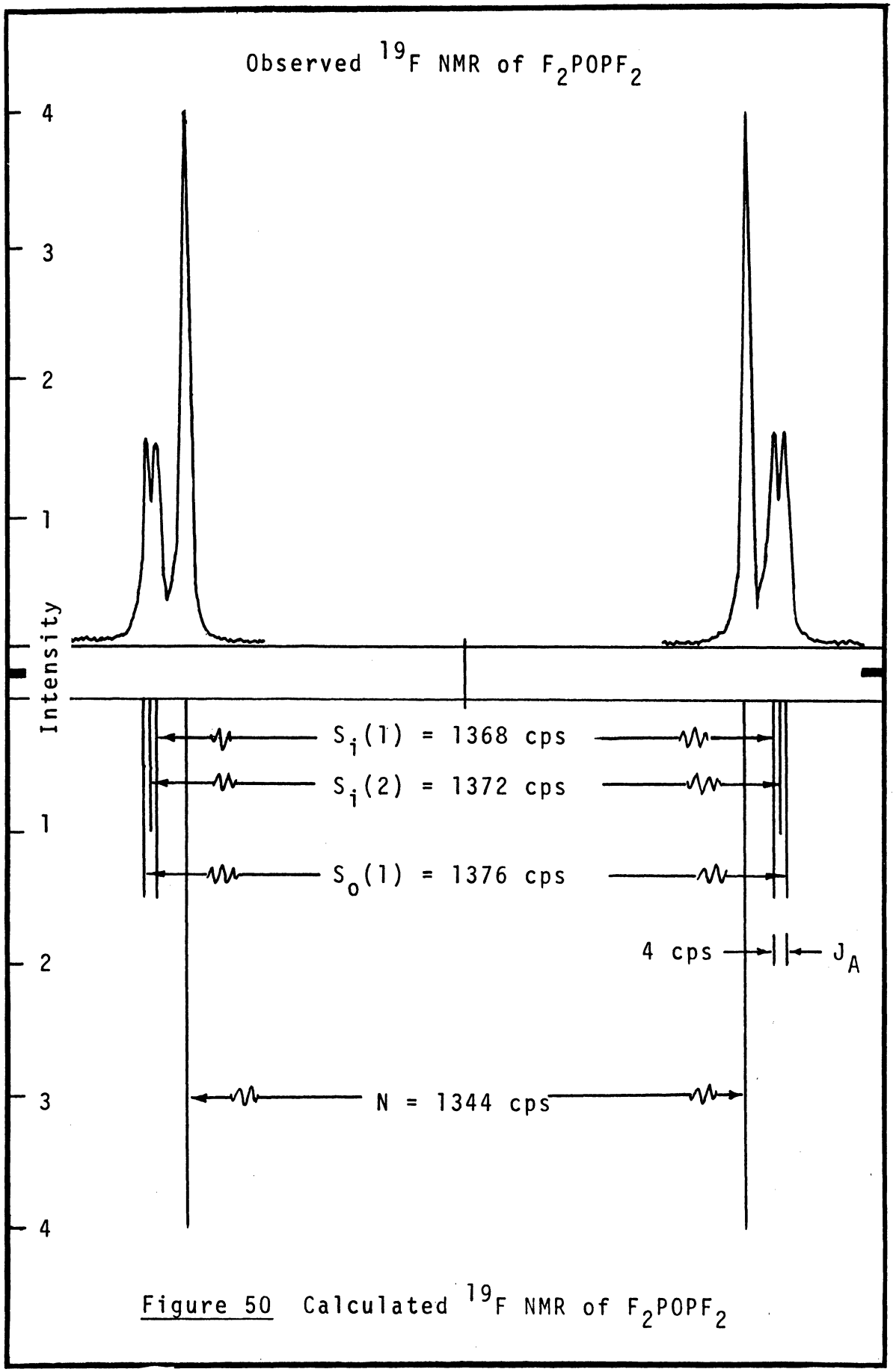

Figure 50 Calculated ^{19}F NMR of F_2POPF_2

13-pairs of lines were observed for F_2PPF_2 (Figure 11). Therefore, it is apparent that the assumption of $J_X = 0$ is invalid for F_2PPF_2 and the expressions derived by Harris[125] will not work in this case. Again lack of time prevented the application of other expressions which do not make the assumption that $J_X = 0$. Undoubtedly, the ^{31}P and ^{19}F nmr spectra of F_2PPF_2 are amenable to analysis in terms of an $X_2AA'X'_2$ nuclear spin system.

The expressions used in the following are given by Harris. For $F_2POP'F'_2$ it was noted that the innermost doublet (Figure 50) contained half of the total intensity and thus it was assigned the doublet separation $N = |J_{PF} + J_{P'OPF}| = 1344$ cps, where $J_{PF} = J_{P'F'}$ and $J_{P'OPF} = J_{POP'F'}$. The doublet of separation N was then mentally discarded from the spectrum. The smaller separation between one member of the inner pair and one member of the outer pair of the remaining lines, 4 cps, then gave J_A (Figure 50), where $J_A = J_{PP'}$. The distance between the inner pair, $S_i(1)$ (Figure 50), of the four lines is given by

$$S_i(1) = [L^2 - J_A{}^2]^{\frac{1}{2}} - |J_A| = 1368 \text{ cps}.$$

Since $|J_A| = 4$, then

$$L^2 = (1368 + 4)^2 + (4)^2$$

$$L = 1372 \text{ cps}$$

where L is the parameter $|J_{PF} - J_{P'OPF}|$. Thus, the parameters N, L, and J_A have been obtained from the observed spectrum and will now be used to construct the corresponding theoretical spectrum for an $X_2AA'X'_2$ system.

The most intense doublet in the spectrum has the separation N and one-half of the total intensity [that is, relative intensity $2^{(2n - 1)} = 8$]. The other $2n = 4$ pairs of lines share the remaining intensity, however, some of the lines may have zero intensity. In the left hand column below the separations of the two pairs of inner and two pairs of outer lines are calculated using the expressions of Harris[125]. The corresponding line intensities are calculated in the right hand column. The calculations are a function of χ which designates the transition involved; $\chi = 1, 2$ for $n = 2$. The limiting intensities of the lines also vary with χ and are given by

$$\frac{1}{n} \sum_{r=\chi}^{n} r({}^{n}C_{r})({}^{n}C_{r-\chi})$$

where ${}^{n}C_{r}$ is the appropriate binomial coefficient. Thus the limiting intensities for $\chi = 1, 2$ are given by:

for $\chi = 1$

$$\text{sum} = \tfrac{1}{2}\{({}^{2}C_{1} \cdot {}^{2}C_{0}) + (2 \cdot {}^{2}C_{2} \cdot {}^{2}C_{1})\}$$

$$= \tfrac{1}{2}(2 \cdot 1 + 2 \cdot 1 \cdot 2) = 3$$

for $\chi = 2$

$$\text{sum} = \tfrac{1}{2}\{2 \cdot {}^{2}C_{2} \cdot {}^{2}C_{0}\} = 1$$

It is also necessary to weight each limiting intensity as a function of g, where

$$g = \frac{[\chi(\chi - 1)L^2 + J_A{}^2]}{\{[\chi^2 L^2 + J_A{}^2][(\chi - 1)^2 L^2 + J_A{}^2]\}^{\frac{1}{2}}}.$$

Thus for $\chi = 1$, $g \approx 0$, and for $\chi = 2$, $g \approx 1$. In the calculations below, line separations are designated by $S_o(\chi)$ or $S_i(\chi)$, and intensities by $Z_o(\chi)$ or $Z_i(\chi)$. The subscripts o and i refer to outer and inner, respectively.

Separations	Intensities
$S_o(1) = \{L^2 + J_A{}^2\}^{\frac{1}{2}} + J_A$	$Z_o(1) = \frac{1}{2}(1 - g)\{{}^{\text{lim.}}_{\text{intens.}}\}$
$= \{(1372)^2 + 4^2\}^{\frac{1}{2}} + 4$	$= \frac{1}{2}(1 - 0)\{3\}$
$= 1376$ cps	$= \frac{3}{2}$
$S_o(2) = \{2^2L^2 + J_A{}^2\}^{\frac{1}{2}}$	$Z_o(2) = \frac{1}{2}(1 - g)\{{}^{\text{lim.}}_{\text{intens.}}\}$
$+ \{L^2 + J_A{}^2\}^{\frac{1}{2}}$	$= \frac{1}{2}(1 - 1)\{1\}$
$= 2 \cdot 1372 + 1372$	$= 0$
$= 4116$ cps	
$S_i(1) = \{L^2 + J_A{}^2\}^{\frac{1}{2}} - J_A$	$Z_i(1) = \frac{1}{2}(1 + g)\{{}^{\text{lim.}}_{\text{intens.}}\}$
$= 1372 - 4$	$= \frac{1}{2}(1 + 0)\{3\}$
$= 1368$ cps	$= \frac{3}{2}$
$S_i(2) = \{2^2L^2 + J_A{}^2\}^{\frac{1}{2}}$	$Z_i(2) = \frac{1}{2}(1 + g)\{{}^{\text{lim.}}_{\text{intens.}}\}$
$- \{L^2 + J_A{}^2\}^{\frac{1}{2}}$	$= \frac{1}{2}(1 + 1)\{1\}$
$= 2 \cdot 1372 - 1372$	$= 1$
$= 1372$ cps	

The calculated spectrum is shown as the mirror image of the observed spectrum in Figure 50. From a comparison of the calculated and observed spectra, it is apparent that the doublet of separation $S_i(2)$ remained unresolved in the observed spectrum but did contribute its intensity to the $S_i(1)$ and $S_o(1)$ doublets. Therefore, each member of the doublet of doublets has one-half the integrated intensity of each component of the central doublet. From the parameters L, N, and J_A, the following coupling constants were obtained for $F_2POP'F'_2$

$$J_{PF} = 1358 \text{ cps}$$

$$J_{P'OPF} = -14 \text{ cps}$$

$$J_{PP'} = 4 \text{ cps}$$

$$J_{FPOP'F'} = 0$$

where J_{PF} and $J_{P'OPF}$ are only relative in sign and rigorously cannot be distinguished; however, J_{PF} certainly must be the larger. Also the sign of $J_{PP'}$ is undetermined.

References

1) J. Chatt, Nature, 165, 637 (1950).

2) J. Chatt and A. A. Williams, J. Chem. Soc., 3061 (1951).

3) L. Pauling "Nature of Chem. Bond", 1st ed., Cornell Univ. Press, Ithaca, N.Y. (1939).

4) H. S. Booth and J. H. Walkup, J. Am. Chem. Soc., 65, 2334 (1943).

5) R. W. Parry and T. C. Bissot, J. Am. Chem. Soc., 78, 1524 (1956).

6) A. B. Burg and H. I. Schlesinger, J. Am. Chem. Soc., 59, 780 (1937).

7) W. A. G. Graham and F. G. A. Stone, J. Inorg. Nucl. Chem., 3, 164 (1956).

8) S. H. Bauer, J. Am. Chem. Soc., 59, 1804 (1937).

9a) A. B. Burg, Record Chem. Progress (Kresge-Hooker Sci. Library), 15, 159 (1954).

9b) W. Gordy, H. Ring, and A. B. Burg, Phys. Rev., 78, 512 (1950).

10) G. Wilkinson, J. Am. Chem. Soc., 73, 5501 (1951).

11) S. Ahrland, J. Chatt, and N. R. Davis, Quart Rev., 12, 265 (1958).

12) C. A. Coulson, Quart. Rev., 1, 144 (1947).

13a) E. R. Alton, Jr., Doctoral Dissertation, Univ. of Mich. (1960).

13b) E. R. Alton, Jr., Dissert. Abstr., 21, 3620 (1961).

14) F. G. A. Stone, Adv. Inorg. Chem. Radiochem., 2, 301 (1960).

15) R. W. Parry and R. N. Keller, "Chemistry of the Coordination Compounds", J. C. Bailar, Jr., ed., Reinhold, New York (1956) p. 119.

16) T. D. Coyle and F. G. A. Stone, Prog. Boron Chem., 1, 137 (1964).

17) F. G. A. Stone, Chem. Revs., 58, 101, (1958).

18) T. D. Coyle, H. D. Kaesz, and F. G. A. Stone, J. Am. Chem. Soc., 81, 2989 (1959).

19) A. B. Burg, J. Chem. Ed., 37, 482 (1960).

20) D. E. Young, G. E. McAchran, and S. G. Shore, Inorg. Chem., 5, to be published (1966).

21) F. Seel, K. Ballreich, and R. Schmutzler, Chem. Ber., 94, 1173 (1961).

22a) R. J. Clark, Inorg. Chem., 3, 1395 (1964).

22b) R. J. Clark and E. O. Brimm, ibid., 4, 651 (1965).

22c) R. J. Clark and P. I. Hobermann, ibid., 4, 1771 (1965).

23a) Th. Kruck, Chem. Ber., 97, 2018 (1964).

23b) Th. Kruck, Angew. Chem., 76, 593, 787, 892 (1964).

24) L. A. Woodward and J. R. Hall, Spectrochim. Acta, 16, 654 (1960).

25) R. Schmutzler, Adv. Fluorine Chem., 5, 31 (1965).

26) H. Nöth and H. J. Vetter, Chem. Ber., 96, 1298 (1963).

27) J. F. Nixon, J. Chem. Soc., 2469 (1964).

28) See reference 29, footnote 3.

29) R. Schmutzler, Inorg. Chem., 3, 415 (1964).

30) D. R. Martin and P. J. Pizzolato, J. Am. Chem. Soc., 72, 4584 (1950).

31) D. R. Martin, W. D. Cooper, D. R. Spessard, and H. S. Booth, ibid., 74, 809 (1952).

32) V. N. Kulakova, Yu. M. Zinov'ev, and L. Z. Soborovskii, Zh. Obshch. Khim., 29, 3957 (1959); C. A., 54, 20846a (1960).

33) R. Schmutzler, Inorg. Chem., 3, 410 (1964).

34) R. N. Sterlin, R. D. Yatsenko, L. N. Pinkina, and I. L. Knunyants, Izv. Akad, Nauk SSSR, Otdel, Khim. Nauk, 1991 (1960); C. A., 55, 13297d (1961).

35) R. Schmutzler, Chem. Ber., 96, 2435 (1963).

36) J. F. Nixon, Chem. Ind., 1555 (1963).

37) W. VanDoorne, Doctoral Dissertation, Univ. of Mich., (1965).

38) H. S. Booth and A. R. Bozarth, J. Am. Chem. Soc., 61, 2927 (1939).

39) H. S. Booth and S. G. Frary, ibid., 61, 2934 (1939).

40) R. R. Holmes and W. P. Gallagher, Inorg. Chem., 2, 433 (1963).

41) H. H. Anderson, J. Am. Chem. Soc., 69, 2495 (1947).

42a) Sr. M. A. Fleming, Doctoral Dissertation, Univ. of Mich., (1963).

42b) Sr. M. A. Fleming, Dissert. Abstr., 24, 1385 (1963).

43) A. Moyé, unpublished results, Univ. of Mich., (1961).

44) R. G. Cavell, J. Chem. Soc., 1992 (1964).

45) W. Mahler, private communication, E. I. duPont de Nemours & Co., Wilmington, Del. (1966).

46) G. M. Kosolapoff,"Organophosphorus Compounds", Wiley, New York (1950).

47) J. R. VanWazer, "Phosphorus and its Compounds", v. 1, Interscience, New York (1958).

48) A. B. Burg and W. Mahler, J. Am. Chem. Soc., 79, 4242 (1957).

49) F. W. Bennett, H. J. Emeléus and R. N. Haszeldine, J. Chem. Soc., 1565 (1953).

50) G. Bokerman and R. W. Rudolph, unpublished results, Univ. of Mich., (1965).

51) E. L. Muetterties and W. D. Phillips, Adv. Inorg. Chem. Radiochem., 4, 231 (1962).

52) P. W. Allen and L. E. Sutton, Acta Cryst., 3, 46 (1950).

53) Gmelin, Handb. anorg. Chem., 8 Auf., Weinheim, Bergstr. (1965) Bd. Phosphor, tl. C., syst. n. 16, p. 621.

54) H. H. Anderson, J. Am. Chem. Soc., 69, 2495 (1947); ibid., 67, 2176 (1945).

55) M. L. Dewaulle and M. F. Francois, J. Chim. Phys., 46, 87 (1949).

56a) J. Goubeau, H. Haeberle, and H. Ulmer, Z. anorg. allg. Chem., 311, 110 (1961).

56b) F. Miller, S. G. Frankis, and O. Sala, Spectrochim. Acta, 21, 775 (1965).

57) L. J. Bellamy, "The Infra-red Spectra of Complex Molecules", Wiley, New York (1958).

58) U. Wannagat and J. Rademachers, Z. anorg. allg. Chem., 289, 66 (1957).

59) E. A. Robinson, Can. J. Chem., 40, 1725 (1962).

60) D. E. C. Corbridge, J. Appl. Chem., 6, 456 (1956).

61) J. E. Griffiths and A. B. Burg, J. Am. Chem. Soc., 84, 3442 (1962).

62) A. Finch, Can. J. Chem., 37, 1793 (1959).

63) G. S. Harris and D. S. Payne, Quart. Rev., 15, 173 (1961).

64) L. A. Ross, Diss. Abstr., 23, 1920 (1962).

65a) R. M. Lynden-Bell, Trans. Farad. Soc., 57, 888 (1961).

65b) R. M. Lynden-Bell, Mol. Phys., 6, 601 (1963).

66) G. Herzberg, "Infrared and Raman Spectra of Polyatomic Molecules", Van Nostrand Co., Princeton, N. J. (1945).

67) C. B. Colburn and F. A. Johnson, J. Chem. Phys., 33, 1869 (1960).

68) F. A. Johnson and C. B. Colburn, J. Am. Chem. Soc., 83, 3043 (1961).

69) J. B. Farmer, M. C. L. Gerry, and C. A. McDowell, Mol. Phys., 8, 253 (1964).

70) A. Kennedy and C. B. Colburn, J. Am. Chem. Soc., 81, 2906 (1959).

71) W. Marckwald and M. Wille, Chem. Ber., 56, 1319 (1923).

72) R. M. Chapin, J. Am. Chem. Soc., 51, 2112 (1929).

73) P. Royen and K. Hill, Z. anorg. allg. Chem., 229, 112 (1936).

74) E. Wiberg and G. Muller-Schiedmayer, Chem. Ber., 92, 2372 (1959).

75) B. Blaser and K. H. Worms, Ang. Chem., 73, 76 (1961).

76) B. Blaser, II Int. Symp. Fluorine Chem., Estes Park, Colo. (1962) Abstr. p. 444.

77) Zh. M. Ivanova and A. V. Kirsanov, Zh. Obshch. Khim., 31, 3991 (1961); C. A. 57, 8605h (1962).

78) M. H. Sirvetz and R. E. Weston, J. Chem. Phys., 21, 898 (1953).

79) E. D. Morris, Jr. and C. E. Nordman, to be published.

80) H. S. Gutowsky, D. W. McCall, and C. P. Slichter, J. Chem. Phys., 21, 279 (1953).

81) J. A. Pople, W. G. Schneider, and H. J. Berstein, "High-Resolution Nuclear Magnetic Resonance", McGraw Hill, New York (1959).

82) W. G. Schneider and J. A. Pople, J. Chem. Phys., 28, 601 (1958).

83) E. Lee and C. K. Wu, Trans. Faraday Soc., 35, 1366 (1939).

84) J. J. Comeford, D. E. Mann, L. J. Schoen, and D. R. Lide, Jr., J. Chem. Phys., 38, 461 (1963).

85) H. S. Gutowsky and S. Fujiwara, J. Chem. Phys., 22, 1782 (1954).

86) H. Y. Sheng, E. F. Barker, and D. M. Dennison, Phys. Rev., 60, 786 (1941).

87) D. T. Hurd, "Chemistry of the Hydrides", Wiley, New York (1952).

88) S. Wexler and N. Jesse, J. Am. Chem. Soc., 84, 3425 (1962).

89) I. Shapiro, et al., Adv. Chem. Series, 32, 133 (1961).

90) J. N. Shoolery, Disc. Faraday Soc., 19, 215 (1955).

91) E. L. McGandy, Dissert. Abstr., 22, 754 (1961).

92) R. L. Kuckowski and D. R. Lide, Jr., Abstr. Symp. Mol. Structure and Spectroscopy, Ohio State Univ., Columbus (June, 1965) p. 78.

93) E. L. Gamble and P. Gilmont, J. Am. Chem. Soc., 62, 717 (1940).

94) H. Brumberger and R. A. Marcus, J. Chem. Phys., 24, 741 (1956).

95) D. R. Schultz and R. W. Parry, J. Am. Chem. Soc., 80, 4 (1958); S. G. Shore and R. W. Parry, ibid., 80, 8, 12 (1958); R. C. Taylor, D. R. Schultz and A. R. Emery, ibid., 80, 27 (1958); C. E. Nordman and C. R. Peters, ibid., 81, 3551 (1959).

96a) J. Gilje, Doctoral Dissertation, Univ. of Mich. (1965).

96b) J. Gilje, Dissert. Abstr., 26, 2458 (1965).

97) W. D. Phillips, H. C. Miller, and E. L. Muetterties, J. Am. Chem. Soc., 81, 4496 (1959).

98) R. C. Taylor and T. C. Bissot, J. Chem. Phys., 25, 780 (1956).

99) R. A. Ogg and J. D. Ray, J. Chem. Phys., 26, 1339 (1957).

100a) R. J. Wyma, Doctoral Dissertation, Univ. of Mich., (1964).

100b) R. J. Wyma, Dissert. Abstr., 25, 6991 (1965).

101) H. I. Schlesinger and A. B. Burg, Chem. Rev., 31, 1 (1942).

102) A. B. Burg and Yuan-Chin Fu, J. Am. Chem. Soc., 88, 1147 (1966).

103) Gmelin, Handb. anorg. Chem., 8Auf., Weinheim. Bergstr. (1965) Bd. Phosphor, tl. C., syst. no. 16, p. 612.

104) C. W. Heitsch, Inorg. Chem., 4, 1019 (1965).

105) K. W. Morse, unpublished results, Univ. of Mich.

106) H. H. Jaffe, J. Inorg. Nucl. Chem., 4, 372 (1957).

107) J. R. VanWazer, J. Am. Chem. Soc., 78, 5709 (1956).

108) P. Kisliuk, J. Chem. Phys., 22, 86 (1954).

109) J. R. Weaver and R. W. Parry, Inorg. Chem., 5, in press (1966).

110) H. S. Gutowsky and D. W. McCall, J. Chem. Phys., 22, 162 (1954).

111) N. Muller, P. C. Lauterbur, and J. Goldenson, J. Am. Chem. Soc., 78, 3557 (1956).

112) J. R. VanWazer, C. F. Callis, J. N. Shoolery, and R. C. Jones, J. Am. Chem. Soc., 78, 5715 (1956).

113) J. R. Parks, J. Am Chem. Soc., 79, 757 (1957).

114) L. S. Meriwether and J. R. Leto, J. Am. Chem. Soc., 83, 3192 (1961).

115) J. F. Nixon and R. Schmutzler, Spectrochim. Acta, 20, 1835 (1964).

116) A. Saika and C. P. Slichter, J. Chem. Phys., 22, 26 (1954).

117) R. S. Sanderson, "Vacuum Manipulation of Volatile Compounds", Wiley, New York (1948).

118) W. L. Jolly, "Synthetic Inorganic Chem.", Prentice-Hall, Englewood Cliff, N. J. (1960).

119) C. J. Hoffman and E. A. Heintz, Inorg. Syn., 7, 180 (1963).

120) D. Gokhale and W. L. Jolly, Inorg. Syn., 8, in press.

121) E. L. Wagner and D. F. Hornig, J. Chem. Phys., 18, 296 (1950).

122) C. F. Farran, Doctoral Dissertation, Univ. of Mich. (1966).

123) R. M. Badger and L. R. Zumwalt, J. Chem. Phys., 6, 711 (1938).

124) M. Davies, "Infrared Spectroscopy and Molecular Structure", Elsevier, New York (1963).

125) R. K. Harris, Can. J. Chem., 42, 2275 (1964).